



National Library
of Canada

Bibliothèque nationale
du Canada

Canadian Theses Service

Service des thèses canadiennes

Ottawa, Canada
K1A 0N4

NOTICE

The quality of this microform is heavily dependent upon the quality of the original thesis submitted for microfilming. Every effort has been made to ensure the highest quality of reproduction possible.

If pages are missing, contact the university which granted the degree.

Some pages may have indistinct print especially if the original pages were typed with a poor typewriter ribbon or if the university sent us an inferior photocopy.

Reproduction in full or in part of this microform is governed by the Canadian Copyright Act, R.S.C. 1970, c. C-30, and subsequent amendments.

AVIS

La qualité de cette microforme dépend grandement de la qualité de la thèse soumise au microfilmage. Nous avons tout fait pour assurer une qualité supérieure de reproduction.

S'il manque des pages, veuillez communiquer avec l'université qui a conféré le grade.

La qualité d'impression de certaines pages peut laisser à désirer, surtout si les pages originales ont été dactylographiées à l'aide d'un ruban usé ou si l'université nous a fait parvenir une photocopie de qualité inférieure.

La reproduction, même partielle, de cette microforme est soumise à la Loi canadienne sur le droit d'auteur, SRC 1970, c. C-30, et ses amendements subséquents.

UNIVERSITY OF ALBERTA

A FINITE ELEMENT ANALYSIS OF A SANDWICH COMPOSITE CHASSIS

BY

CURT J. STOUT

A THESIS

SUBMITTED TO THE FACULTY OF GRADUATE STUDIES AND RESEARCH IN

PARTIAL FULFILLMENT OF THE REQUIREMENTS FOR THE DEGREE OF

MASTER OF SCIENCE

DEPARTMENT OF MECHANICAL ENGINEERING

EDMONTON, ALBERTA

SPRING 1991



National Library
of Canada

Bibliothèque nationale
du Canada

Canadian Theses Service Service des thèses canadiennes

Ottawa, Canada
K1A 0N4

The author has granted an irrevocable non-exclusive licence allowing the National Library of Canada to reproduce, loan, distribute or sell copies of his/her thesis by any means and in any form or format, making this thesis available to interested persons.

The author retains ownership of the copyright in his/her thesis. Neither the thesis nor substantial extracts from it may be printed or otherwise reproduced without his/her permission.

L'auteur a accordé une licence irrévocable et non exclusive permettant à la Bibliothèque nationale du Canada de reproduire, prêter, distribuer ou vendre des copies de sa thèse de quelque manière et sous quelque forme que ce soit pour mettre des exemplaires de cette thèse à la disposition des personnes intéressées.

L'auteur conserve la propriété du droit d'auteur qui protège sa thèse. Ni la thèse ni des extraits substantiels de celle-ci ne doivent être imprimés ou autrement reproduits sans son autorisation.

ISBN 0-315-66600-5

UNIVERSITY OF ALBERTA
RELEASE FORM

NAME OF AUTHOR: CURT J. STOUT

TITLE OF THESIS: A FINITE ELEMENT ANALYSIS OF A SANDWICH
COMPOSITE CHASSIS

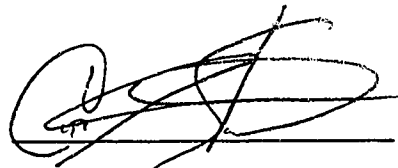
DEGREE: MASTER OF SCIENCE

YEAR THIS DEGREE GRANTED: SPRING 1991

PERMISSION IS HEREBY GRANTED TO THE UNIVERSITY OF ALBERTA
LIBRARY TO REPRODUCE SINGLE COPIES OF THIS THESIS AND TO LEND OR
SELL SUCH COPIES FOR PRIVATE SCHOLARLY OR SCIENTIFIC RESEARCH
PURPOSES ONLY.

THE AUTHOR RESERVES OTHER PUBLICATION RIGHTS, AND NEITHER
THE THESIS NOR EXTENSIVE EXTRACTS FROM IT MAY BE PRINTED OR
OTHERWISE REPRODUCED WITHOUT THE AUTHOR'S WRITTEN PERMISSION.

(SIGNED)



PERMANENT ADDRESS

10720 - 60 A AVENUE

EDMONTON, ALBERTA

T6H 1K7

DATED 22 APRIL 1991

*'Twas brillig, and the slithy toves
Did gyre and gimble in the wabe;
All mimsy were the borogroves,
And the mome raths outgrabe.*

Lewis Carroll

UNIVERSITY OF ALBERTA

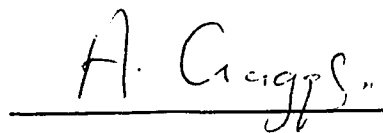
FACULTY OF GRADUATE STUDIES AND RESEARCH

THE UNDERSIGNED CERTIFY THAT THEY HAVE READ, AND RECOMMEND TO
THE FACULTY OF GRADUATE STUDIES AND RESEARCH FOR ACCEPTANCE,
A THESIS ENTITLED

A FINITE ELEMENT ANALYSIS OF A SANDWICH COMPOSITE CHASSIS

SUBMITTED BY **CURT J. STOUT**

IN PARTIAL FULFILLMENT OF THE REQUIREMENTS FOR THE DEGREE OF
MASTER OF SCIENCE



D. A. Craggs
Supervisor



Dr. D.J. Marsden
Supervisor



Dr. B.M. Patchett

DATED 19 APRIL 1991

I would like to dedicate this work to my wife Catherine,
A woman with whom I love, laugh, and live.

ABSTRACT

The purpose of this investigation was two-fold. The first objective concerned the selection and verification of a finite element suitable for modelling sandwich panel deflections in structures having stiff facings and a flexible core. The second objective dealt with the practical application of the selected element to the analysis of an aluminum-foam sandwich monocoque chassis. Of particular interest was the aggregate chassis stiffness for each of three load cases: torsion, vertical beaming, and lateral beaming.

The selected quadrilateral layered shell element exhibited acceptable convergence behaviour when used to represent plate bending having a significant shear deflection component. This element was relatively insensitive to thickness aspect ratio variations in a range from 0.2 to 2.0. The element performed well in modelling torsion of a sandwich cylinder. Some locking behaviour was observed for particular element layer configurations.

The results of the finite element analysis of the sandwich monocoque indicated that the model retains its torsional stiffness through the open cockpit section. This is a result of specific design parameters such as minimizing the cockpit opening dimensions and maintaining a large section height throughout this area. Vertical and lateral beaming stiffness values are very nearly identical and are adequate for the expected loads. The model performs well in comparison with other structures of a similar type.

ACKNOWLEDGEMENT

I would like to express my appreciation and thanks to Dr. Craggs and Dr. Marsden for their supervision and assistance during this project. I would also thank Dr. Faulkner, past Department Chairman, for his assistance and patience in the early stages of this project.

TABLE OF CONTENTS

Chapter 1	Introduction	1
1.1	Historical Development Of The Automobile Chassis	1
1.2	Chassis Structure And Analysis Techniques	3
1.2.1	Frame And Body Shell Structures	3
1.2.2	Composite Sandwich Structures	5
1.3	Sandwich Monocoque Finite Element Analysis	9
Chapter 2	Element Theory And Verification	11
2.1	Element Theory	12
2.1.1	Composite Quadrilateral Shell Element, SHELL4L	12
2.1.2	8-Node Layered Solid Element, STIF46	13
2.1.3	Shell-Solid Combined Element, SHELL4-SOLID	15
2.1.4	Layered Shell Element, STIF99	16
2.2	Plate Bending Verification	17

2.2.1	Analytical Model	18
2.2.2	Mesh Sensitivity Finite Element Model	21
2.2.3	Mesh Sensitivity Results	24
2.2.4	Aspect Ratio (t/L) Sensitivity Finite Element Model	29
2.2.5	Aspect Ratio (t/L) Sensitivity Results	32
2.2.6	SHELL4-SOLID Hybrid Analysis	41
2.2.7	STIF99 Analysis	43
2.3	Cylinder Torsion Analysis	46
2.3.1	Description Of Physical Model	46
2.3.2	Description Of Analytical Solution	47
2.3.3	Finite Element Model	47
2.3.4	Finite Element Results	49
2.4	Comments On Element/Program Anomalies	49
2.4.1	SHELL4L Shear Locking	49
2.4.2	Coordinate System Errors	51

Chapter 3 Vehicle Structure Stiffness Analysis Model	53
3.1 Description Of Structural Design	53
3.2 Description Of Finite Element Model	57
3.3 Torsional Stiffness Analysis	59
3.4 Vertical Beaming Stiffness Analysis	61
3.5 Lateral Beaming Stiffness Analysis	62
Chapter 4 Results And Discussion	64
4.1 Torsional Analysis Results	64
4.1.1 Deflection Results	64
4.1.2 Stress Results	68
4.2 Vertical Beaming Analysis Results	72
4.2.1 Deflection Results	72
4.2.2 Stress Results	74
4.3 Lateral Beaming Analysis Results	78
4.3.1 Deflection Results	78

4.3.2	Stress Results	80
4.4	Comparison Of Results	84
Chapter 5	Conclusions	89
5.1	Verification Study	89
5.2	Monocoque Analysis	91
5.3	Program Considerations	92
5.4	Further Study	92
5.4.1	Joint Compliance	92
5.4.2	Adhesive Layer Response	93
5.4.3	Physical Testing	93
BIBLIOGRAPHY	94

LIST OF TABLES

TABLE 1	Element Descriptions	11
TABLE 2	Sandwich Material Properties	18
TABLE 3	SHELL-SOLID Hybrid Deflection Results	43
TABLE 4	STIF99 Sandwich Plate Bending Results	44
TABLE 5	Torsion Cylinder Results	49
TABLE 6	Torsional Stiffness Comparison	85
TABLE 7	Austin-Rover Metro Torsion Test	86
TABLE 8	Overall Front End Sheet Metal Stiffness Correlation	87

LIST OF FIGURES

FIGURE 1	Shell4L Element Diagram	13
FIGURE 2	STIF46 Element Diagram	14
FIGURE 3	SHELL4-SOLID Combined Element Diagram	15
FIGURE 4	Cantilever Sandwich Plate Bending Model	19
FIGURE 5	SHELL4L Finite Element Model, Cantilever Plate	22
FIGURE 6	STIF46 Finite Element Model, Cantilever Plate	23
FIGURE 7	SHELL4L Plate Bending Convergence	25
FIGURE 8	SHELL4L Convergence Error	26
FIGURE 9	STIF46 Plate Bending Convergence	27
FIGURE 10	STIF46 Convergence Error	28
FIGURE 11	SHELL4L Finite Element Model, Aspect Ratio	29
FIGURE 12	STIF46 Finite Element Model, Aspect Ratio	31
FIGURE 13	SHELL4L Aspect Ratio Results	32
FIGURE 14	SHELL4L Aspect Ratio Error	33

FIGURE 15	SHELL4L Face Bending Stress	34
FIGURE 16	SHELL4L Face Bending Stress Error	35
FIGURE 17	SHELL4L Core Bending Stress	37
FIGURE 18	SHELL4L Core Bending Stress Error	38
FIGURE 19	STIF46 Aspect Ratio Results	39
FIGURE 20	STIF46 Aspect Ratio Error	40
FIGURE 21	SHELL4-SOLID Finite Element Model	42
FIGURE 22	Cylinder Torsion Model	46
FIGURE 23	Torsion Cylinder Finite Element Model	48
FIGURE 24	SHELL4L Shear Locking Behaviour	50
FIGURE 25	Vehicle Substructures	53
FIGURE 26	Sandwich Monocoque Detail	54
FIGURE 27	Sandwich Panel Corner Joint Detail	56
FIGURE 28	Finite Element Model Of Composite Monocoque	57
FIGURE 29	Element Layer Assignments	58

FIGURE 30	Torsion Boundary Conditions	59
FIGURE 31	Vertical Beaming Boundary Conditions	61
FIGURE 32	Lateral Beaming Boundary Conditions	63
FIGURE 33	Torsional Rotation Of Monocoque	65
FIGURE 34	Structural Deflection Under Torsional Load	66
FIGURE 35	Von-Mises Stress Due To Torsional Load Aluminum Face Layer	69
FIGURE 36	τ_{xy} Stress Due To Torsional Load Aluminum Face Layer	70
FIGURE 37	Von-Mises Stress Due To Torsional Load Polystyrene Core Layer	71
FIGURE 38	τ_{xy} Stress Due To Torsional Load Polystyrene Core Layer	71
FIGURE 39	Vertical Displacement Of Monocoque Floor Pan	72
FIGURE 40	Monocoque Deflection Under Vertical Load Front View	73
FIGURE 41	Von-Mises Stress Due To Vertical Load Aluminum Face Layer	75

FIGURE 42	τ_{xy} Stress Due To Vertical Load Aluminum Face Layer	76
FIGURE 43	Von-Mises Stress Due To Vertical Load Polystyrene Core Layer	77
FIGURE 44	τ_{xy} Stress Due To Vertical Load Polystyrene Core Layer	77
FIGURE 45	Horizontal Displacement Of Monocoque Floor Pan	78
FIGURE 46	Monocoque Deflection Under Lateral Load Front View	79
FIGURE 47	Von-Mises Stress Due To Lateral Load Aluminum Face Layer	81
FIGURE 48	τ_{xy} Stress Due to Lateral Load Aluminum Face Layer	82
FIGURE 49	Von-Mises Stress Due To Lateral Load Polystyrene Core Layer	83
FIGURE 50	τ_{xy} Stress Due To Lateral Load Polystyrene Core Layer	83

LIST OF SYMBOLS

Δ	deflection	f	face thickness
ν	poisson ratio	G_c	shear modulus of core
σ_c	bending stress in core layer	I_p	polar moment
σ_f	bending stress in face layer	k_b	bending deflection constant
τ_c	core shear stress	k_s	shear deflection constant
θ	angular displacement	L	beam length
b	beam width	N	shear stiffness of core
c	core thickness	P	total load
d	beam depth	R_x, R_y, R_z	rotational d.o.f.
D	flexural stiffness of sandwich faces	s	distance between centers of the two faces
E_c	Young's modulus of core	T	applied torque
E_f	Young's modulus of faces	u, v, w	nodal displacements

1.0 INTRODUCTION

1.1 HISTORICAL DEVELOPMENT OF THE AUTOMOBILE CHASSIS

The analysis of automotive structures has been an area of considerable interest since the first 'horseless' carriages were conceived of prior to the turn of the century. The first automotive structures were derived from successful bicycle technology first developed in 1816 by Baron Karl Von Drais de Sauerbron [25]. It is interesting to note that the bicycle remains a more efficient means of locomotion than the automobile and requires only 20% of the energy required for walking.

The first attempts to construct a powered vehicle were met with varying degrees of success. An electric powered tricycle was attempted in 1882 but the structure of the vehicle was not up to the task of carrying the batteries. Steam powered vehicles suffered similar problems as the 'engines' were extremely heavy and required significant support structures. Gottlieb Daimler patented the first lightweight, high speed, gasoline engine in 1885. In the same year, Karl Benz, a significant figure in automobile development, constructed a light weight gasoline powered tricycle having a simple ladder chassis and rack and pinion steering. An English engineer, F.W. Lanchester, designed the first true automobile structure in 1895. The frame consisted of brazed steel tubes which provided support for the engine, drivetrain, suspension and passengers [25].

The concurrent advances of the steel industry, metallurgy, and automobile production in the early 1900's generated the requirement for accurate and timely engineering analysis of the automobile structure. The change from open bodied to closed bodied cars in 1920 further drove the analysis requirements for weight reduction. The need for structural analysis was further enhanced as engine power increased and the dynamic loads due to higher vehicle speeds multiplied.

The energy efficiency requirements of the past two decades have led to lighter automobile structures that require closer, more accurate analysis techniques. The development and use of alternative structural materials such as aluminum and modern composites has also created a need for better automotive structural analysis. Automotive engineers have borrowed heavily from their colleagues in the aerospace industry, especially the finite element techniques used for the analysis of aircraft and spacecraft structures [33].

A salient factor in the development of the automotive structure has been the use of the automobile in competitive endeavours [22, 35, 36, 57]. The conflicting requirements of high structural stiffness and low weight in race car chassis drives the quest for better materials and analysis methods.

1.2 CHASSIS STRUCTURE AND ANALYSIS TECHNIQUES

1.2.1 FRAME AND BODY SHELL STRUCTURES

The first automobile chassis were flat ladder frames and the analysis of such structures was done using elementary beam theory. The finite element analysis of a ladder frame consisted of determining the sectional properties of the members comprising the frame and combining this information with a simple beam element model of the structure.

The early analysis of steel body shells involved the idealization of the structure into either a plane or space frame. The geometric properties of the box sections comprising the body were determined at discrete points and generalized for specific frame rails. A finite element model comprised of beam elements was constructed using a frame representation of the vehicle structure [7, 33, 44]. These models had as few as 100 to 200 degrees of freedom. The results from this class of analysis were varied and errors of 60% in the computed lower natural frequencies were reported [31].

The fundamental problem with these beam models was the assumption of rigid joints between tubular frame members. Lubkin [31] studied the compliance of a welded tubular joint by using a simple H-frame model. Initial results obtained by using a beam finite element model that disregarded joint compliance predicted first and third natural frequencies that were 37% and 60% too high, respectively. A detailed finite element analysis of the tubular joint was subsequently performed using approximately 140 triangle and

quadrilateral plate elements. The joint compliance data thus obtained was applied to the beam model and the errors in the first and third modes dropped to 6.7% and 10.3%, respectively.

More refined analyses were performed as computer capability increased, detailed finite element models consisting of beam and shell elements were constructed [5, 26, 28, 39, 58]. These detailed models often consisted of 1000 to 1500 elements and more closely represented the actual vehicle structure. The results of some of these analyses were considerably better than previous work, Kowalski, [28] lists deflection results for a truck frame that were within 12% of the measured experimental values. Some analyses, notably those presented in [26] and [58], suffered large errors in the deflection results. This was most likely due to the use of a low order CST element to model the body panels in [26] and the over relaxation of the joint compliances in [58]. The use of higher order quadratic and parabolic isoparametric elements in the work presented by Felske [18] and Parekh [39] led to better results with fewer elements.

1.2.2 COMPOSITE SANDWICH STRUCTURES

The finite element analysis of automobile structures employing composite materials in primary load carrying members and panels is not as well represented in the literature. The use of load bearing composite materials in automotive structures is more common in the racing milieu. In the 1950's, the CN7 Bluebird land speed car was designed to use aluminum honeycomb panels as the major load bearing members [35]. The aluminum honeycomb sandwich monocoque of the Cooper is thought to be the first use of modern composites in a Grand Prix car [35]. In 1965 M^cLaren used aluminum skins over end-grain balsa to form a sandwich monocoque chassis. A few years later the M23 was designed and built using a sandwich monocoque comprising aluminum skins over a polystyrene foam core. This car was used by James Hunt to win the World Driving Championship.

The analysis of the early sandwich monocoque structures was accomplished by using empirical relations and the knowledge gained through building and testing. It was not until 1982 that M^cLaren commissioned a finite element analysis for its Formula One carbon fibre sandwich chassis. The analysis was done by Hercules Aerospace and the model consisted of approximately 800 elements [57]. As a result of the use of carbon fibre and advanced analysis methods the chassis was approximately 35% lighter than an equivalent aluminum structure. Ford embarked on a similar venture in 1982 with the design of an IMSA GTP chassis comprised of carbon fibre - Nomex

honeycomb sandwich panels adhesively bonded to one another. A full model finite element analysis of the composite chassis was performed by the Ford aerospace division [23]. Analysis results of chassis stiffness were not published. The finite element analysis did not completely supplant physical testing as the strengths of the most highly stressed, critical components were verified in the lab.

The use of composites for main structural panels in road going vehicles has been slow to develop and as a result the analysis techniques for such materials are not as well developed in the automotive engineering area. Questions of fatigue life, crashworthiness, and production costs remain to be answered by the engineers working in this area [9]. Some vehicles such as the Lotus have been using composite bodies since 1957, but the main structural loads have been taken by a steel "backbone" chassis [1].

The design and analysis of sandwich structures employing foam or end-grain balsa as core material has had wider use in marine [12] and civil engineering structures [13]. The mechanical properties of extruded polystyrene foam were investigated by Bukowski [13] in a series of panel bending tests. The results indicated that measured panel deflections were lower than those predicted by the equation for sandwich panels. The experimentally derived values of G_c and E_c varied depending on the choice of panel skin material. The paper by Olsson [38] discusses the test methods for determining material properties of foam, including tensile, compressive and shear strength and

moduli. Fatigue and fracture toughness testing of foam materials is also discussed. There are indications that the single shear block test predicts shear strengths lower than actual values due to the high stress concentration at the corner of the foam block. The test more correctly predicts the fracture characteristic of the material.

Some analytical equations used in the design of sandwich panel structures are discussed by Teti [54] and Gibson [19]. Teti proposes a modified bending equation to predict the maximum deflection of a sandwich panel. The effects of creep at room temperature were also investigated and the results indicate that a significant reduction in core shear modulus (40%) occurs in a GRP skin - polyurethane foam core sandwich panel subjected to bending. The optimization of sandwich panels for various design objectives is discussed by Gibson.

The finite element analysis of foam cored sandwich structures is discussed in [6, 21, 37, 46, 61]. Backlund, et al [6] review an isoparametric element based on the assumptions of Ahmad, Irons, and Zienkiewicz [2] that uses a reduced integration technique to prevent locking in the thin shell limit. Several applications of this element to the analysis of sandwich structures are given. The static finite element analyses were done by the Department of Aeronautical Structures and Materials, Royal Institute of Technology, Stockholm. The structures studied are a refrigerated truck body, liquid

container tank, and general container constructed of stainless steel - PVC foam - aluminum sandwich panels.

A review of finite element techniques for the analysis of sandwich structures is given by Ha [21]. The importance of shear deformations on the deflection solution is reviewed and a rule of thumb for simple structures is given. The general assumptions made for sandwich plate formulations are reviewed and the displacement field and shear strain relation for a Mindlin based element are discussed. Variations of the sandwich Mindlin element and particularly the treatment of the transverse shear are reviewed. The author indicates that simple C^0 elements are adequate for the analysis of symmetric 3 layer sandwich structures having stiff faces and a flexible core.

An analysis approach for sandwich beams involving the use of quadratic plane elasticity elements to model core behaviour and cubic 2-D beam elements to model face behaviour is given by O'Connor [37]. The beam nodes are offset from the beam neutral axis such that the face-core interface of the combined element occurs at its proper location. The advantage of this approach lies in its ability to model several different classes of sandwich response by using only two types of elements. Several beam bending analyses are presented and the combined elements exhibit reasonable convergence behaviour. This combined element approach is particularly suited to the study of through-the-thickness stresses adjacent to point loads and stress discontinuities near free edges.

Rasmussen [46] discusses an analysis approach for sandwich structures that enables the analyst to keep track of the large permutations of face and core materials available. A review of element formulation is given and the author suggests that variation in the transverse core shear, and core bending stresses be considered. The analysis of a sandwich construction rescue and pilot vessel is given and some emphasis is placed on areas subjected to high local pressure loads.

The effect of transverse discontinuities in foam cores on the fracture strength of sandwich beams is investigated by Zenkert and Groth [61]. Quadratic plane strain elements are used to model the GRP - PVC sandwich beam subjected to 4 point bending; a refined mesh is employed near the material discontinuities. The finite element results correlate well with the experimental work and a reduction of as much as 220% in the load capacity of a beam having a transverse gap in the core is seen.

1.3 SANDWICH MONOCOQUE FINITE ELEMENT ANALYSIS

In the current investigation, the finite element study of an aluminum skin - polystyrene core sandwich chassis involves two parts. The first phase of the investigation is concerned with the selection and verification of an element suitable for the analysis of sandwich panel structures. Elements from two general purpose finite element codes are tested for convergence and accuracy in modelling short panel bending of an aluminum - polystyrene sandwich.

Sensitivity to thickness aspect ratio is also investigated. The best element is chosen based on the results of this study and is used in the analysis of a sandwich monocoque chassis.

The second phase of the investigation involves a large displacement, finite element analysis of an aluminum - polystyrene foam sandwich monocoque chassis. Three typical load cases are considered: torsion, vertical beaming, and horizontal beaming. The finite element model is a complete representation of the chassis and consists of 1446 quadrilateral sandwich shell elements having a total of 8502 degrees of freedom. The current analysis is concerned primarily with structural stiffness and as a consequence a coarse mesh is employed which gives, at best, a preliminary estimate of the stress field. The results of the stiffness analyses are presented and compared with values derived from several classes of automotive chassis.

Both phases of the finite element work were accomplished by using a personal computer. The computer is an IBM compatible machine having an 80386 main processor, an 80387 math coprocessor, 8 megabytes of RAM, and a 300 megabyte storage drive. All model construction was done interactively using a geometric pre-processor, model checking was done visually. Post processing of model results was accomplished using the same programs required for the analysis.

2.0 ELEMENT THEORY AND VERIFICATION

The general theory describing the elements used in this study will be presented as far as is possible, for each element contains proprietary algorithms which the developers claim make their formulation superior to another.

A verification study was undertaken to establish the accuracy of various finite elements in describing the deflection and stress of a sandwich plate subjected to bending as well as the torsion of a sandwich cylinder. The various types of finite elements used in this study have been tabulated in table 1.

Table 1 Element Descriptions

ELEMENT NAME	TYPE OF ELEMENT	PROGRAM NAME
SHELL4L	Quadrilateral Composite Layered Shell	COSMOS/M
SHELL4-SOLID Combined	Quadrilateral Thin Shell 8-Node Isoparametric Solid	COSMOS/M
STIF46	8-Node Isoparametric Layered Solid	ANSYS
STIF99	8-Node Isoparametric Layered Shell	ANSYS

2.1 ELEMENT THEORY

2.1.1 COMPOSITE QUADRILATERAL SHELL ELEMENT, SHELL4L

The element formulation used in the SHELL4L element is described in Belytschko [11] and Allman [4]. This shell element is constructed by combining the stiffness expressions of a C^0 triangular plate bending element of the Mindlin type [Belytschko] and a plane elasticity element with vertex rotations [Allman].

The triangular plate bending element uses linear displacement fields for both rotations and transverse deflections. Previous Mindlin formulations have had problems with shear locking in the thin plate limit which reduced integration schemes had not wholly solved. Belytschko et. al. propose a scheme whereby the displacements are decomposed into a bending mode, associated with bending strain energy, and a shear mode, associated with the shear strain energy. If the nodal rotations and displacements describe pure bending then the element bending mode coincides with the Kirchhoff configuration and the shear strain energy vanishes, thereby alleviating the shear locking problem.

The in-plane displacements of the SHELL4L element are described by the plane elasticity element discussed in [Allman]. This element uses compatible quadratic displacement fields which give rise to a linear stress distribution across the element.

The flat shell element, then, is assembled by combining the plate bending triangle element stiffness with the plane elasticity triangle element stiffness.

The quadrilateral shell element is constructed using four triangular elements, in the sandwich formulation the nodes lie on the midplane of the sandwich. An illustration of this element is shown in figure 1

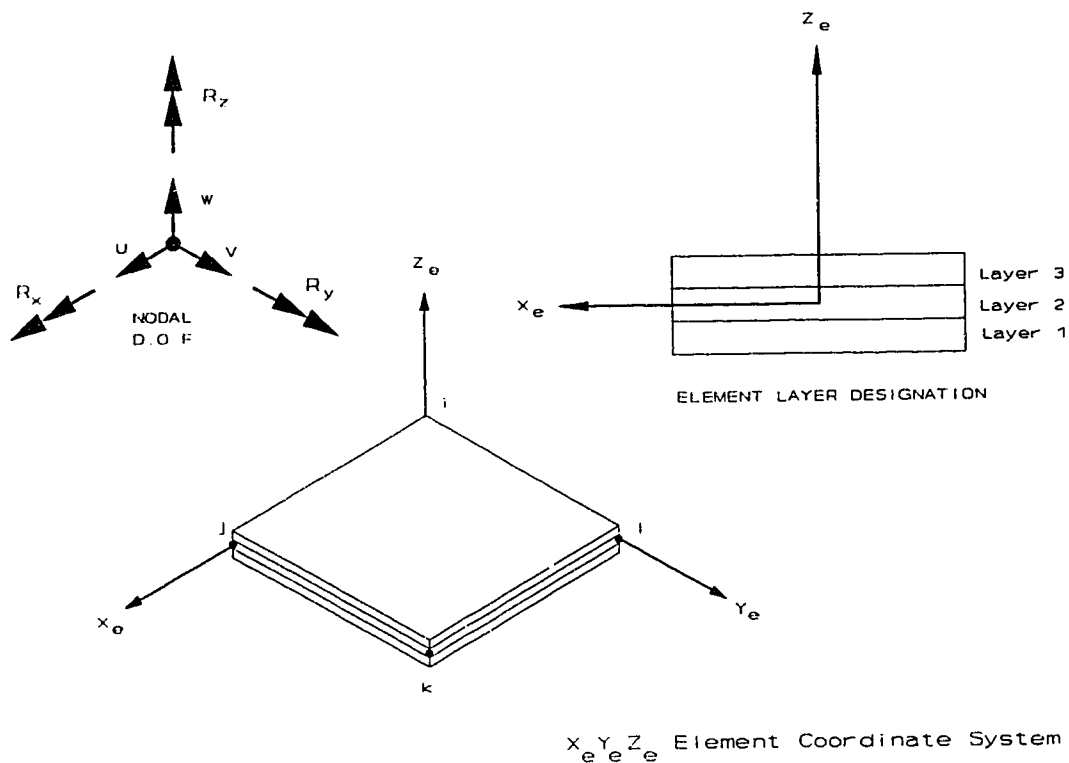


Figure 1 SHELL4L Element Diagram

2.1.2 8-NODE LAYERED SOLID ELEMENT, STIF46

The theoretical basis for this layered solid element is discussed in the ANSYS Theoretical Manual and in Taylor [53] and Wilson [60]. This element

is based on a non-conforming element called the QM6 [Taylor] which is in turn a variation of the Q6 element discussed in [Wilson]. The element is an 8 node isoparametric brick having modified extra quadratic shape functions and a total of 24 d.o.f. (3 translations per node). An illustration of this element may be seen in figure 2.

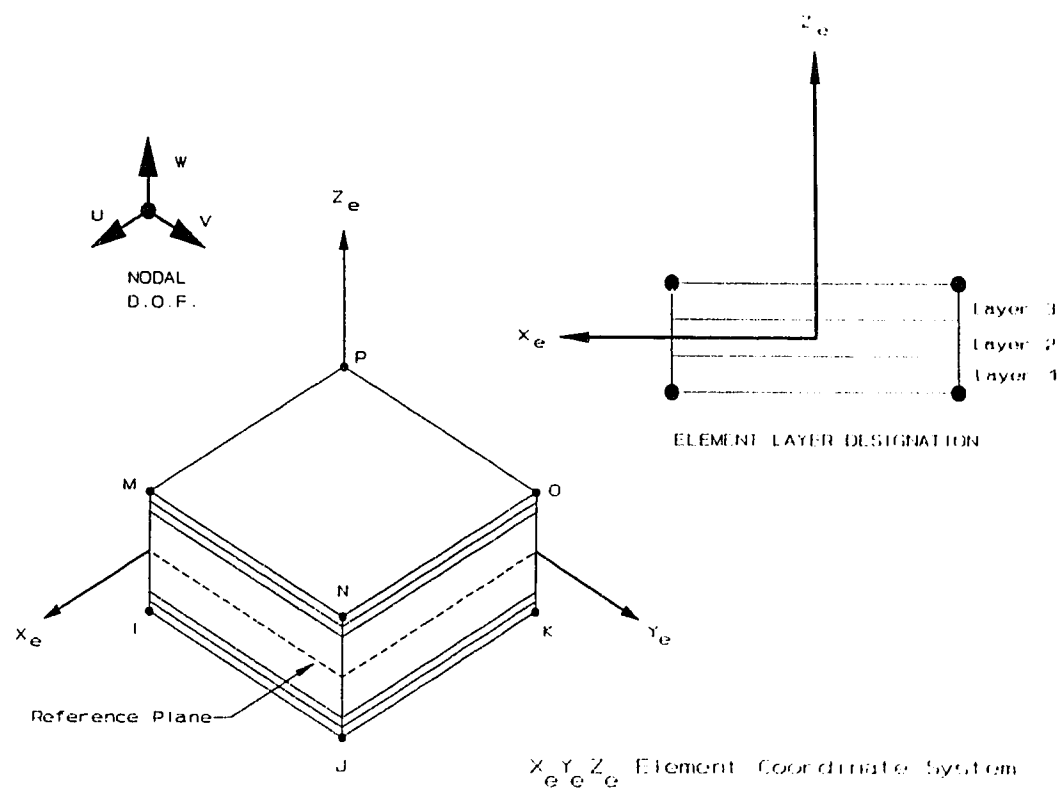


Figure 2. STIF46 Element Diagram

2.1.3 SHELL-SOLID COMBINED ELEMENT, SHELL4-SOLID

This combined element was formed by using a quadrilateral thin shell element to represent the face layers of a sandwich panel and an 8 node isoparametric brick to represent the core. The resulting combined "sandwich" element has a total of 48 d.o.f.. An illustration of this combined "sandwich" element is shown in figure 3.

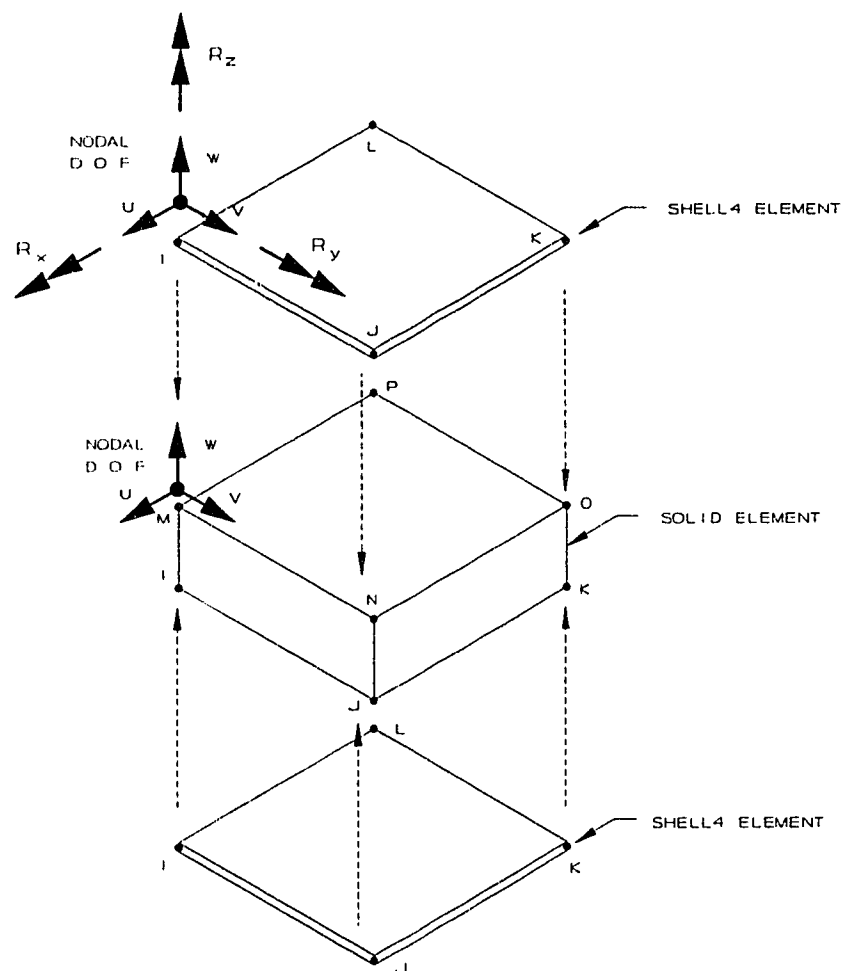


Figure 3 SHELL4-SOLID Combined Element Diagram

The quadrilateral thin shell element is described in Lashkari [30] and lists the papers by Batoz [8] and Allman [4] as its theoretical basis. This element is formed by combining the bending stiffness of a Discrete Kirchhoff Theory (DKT) plate element with the stiffness matrix of the plane elasticity element described by [Allman].

The DKT element is derived from the small displacement theory of plates with transverse shear deflections (Mindlin theory) which is used primarily to describe the kinematics of the deformed plate. The energy function is modified to reflect the fact that under Kirchhoff theory the transverse shear strains are negligible, therefore the term containing the shear strain energy is discarded. By discarding the shear strain energy term convergence to the Kirchhoff solution for a thin plate is assured. The Kirchhoff plate theory assumptions are imposed at discrete points along the element, i.e. the corner nodes of a triangular element.

2.1.4 LAYERED SHELL ELEMENT, STIF99

The theoretical basis of the layered shell element is discussed in both the ANSYS theoretical and user manuals [17], [27] as well as the paper by Ahmad, Irons, and Zienkiewicz, [2]. The element formulation is based on three dimensional elasticity and assumes that midplane normals in the undeformed state remain straight but not necessarily normal to the midplane in the deformed state. The strain energy associated with stresses perpendicular to

the midplane is discarded. The elasticity matrix [D] is derived for each layer in the sandwich and the element stiffness matrix [k] involves the summation of the individual layer elasticity matrices through the thickness of the element. Provision is made in the elasticity matrix [D] to reduce or avoid shear locking. This is done by dividing the transverse shear moduli by a shear factor (f), where (f) is given by:

$$f = \begin{bmatrix} 1.2 \\ 1.0 + 0.2 \left(\frac{Area}{25t^2} \right) \end{bmatrix}$$

(whichever term is greater)

As subsequent testing showed, this method of avoiding shear locking does not seem to work when large differences exist between face and core shear moduli of a sandwich panel. Indeed the likelihood is that the face shear moduli, which are very large in comparison to those of the core, will dominate the expression.

2.2 PLATE BENDING VERIFICATION

The sensitivity of the finite element solution to mesh density was investigated for the SHELL4L and STIF46 elements. A similar study was done to establish the solution accuracy of the SHELL4L and STIF46 elements for various element thickness aspect ratios, (t/L).

2.2.1 ANALYTICAL MODEL

2.2.1.1 DESCRIPTION OF MODEL

A cantilevered sandwich plate measuring 250 mm x 250 mm x 15 mm was used as the model for the plate bending verification. The sandwich plate is comprised of three layers; the two outer layers will be referred to as the "faces" while the inner layer will be referred to as the "core".

The aluminum facings are of a 6061-T6 aluminum alloy 0.635mm in thickness. The core is a 15 mm thick, high density, extruded polystyrene foam manufactured by DOW Chemical. The physical properties of these materials are described in table 2.

Table 2 Sandwich Material Properties

MATERIAL PROPERTY	MATERIAL	
	6061-T6	POLYSTYRENE (HI-100)
E (MPa)	70,000	25.5
G (MPa)	26316	13.8
Poisson Ratio	0.33	0.2
Density (kg/m ³)	2700	40.8

The length and width dimensions were chosen to represent a short panel in which shear deflections would be significant. The panel core thickness of 15mm results in the total tip deflection being divided almost equally between the bending deflection component and the shear deflection component. The requirement that the element be capable of representing both shear deflection and bending deflection is an important one, especially when sandwich structures comprising stiff outer skins and a comparatively flexible core are being modelled.

An illustration of the cantilevered plate is shown in figure 4.

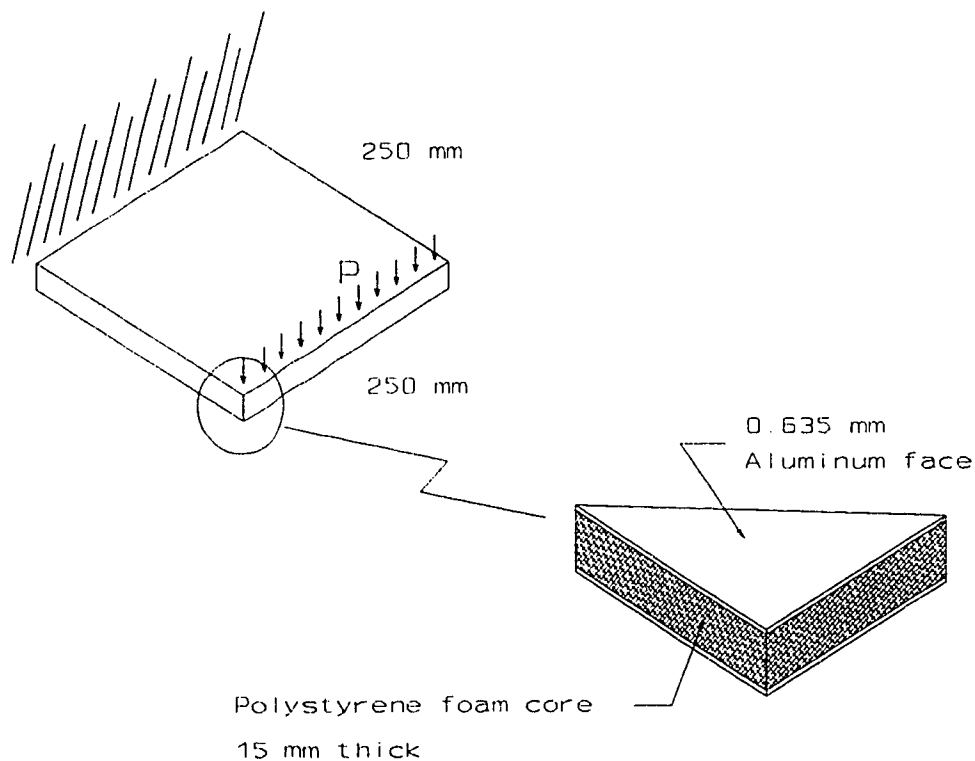


Figure 4 Cantilever Sandwich Plate Bending Model

2.2.1.2 ANALYTICAL SOLUTION

The analytic solution used to describe the deflection and stress is taken from Nichols [34]. The relevant equations are reproduced below:

The deflection at the tip is described by equation (1).

$$\Delta = \frac{k_b PL^3}{D} + \frac{k_s PL}{N} \quad (1)$$

The flexural stiffness of the sandwich panel is described by equation (2).

$$D = E_f \frac{bf^3}{6} + E_f \frac{bfs^2}{2} + E_c \frac{bc^3}{12} \quad (2)$$

The shear stiffness of the core is described by equation (3).

$$N = \frac{G_c bs^2}{c} \quad (3)$$

The bending stress in the facing is described by equation (4).

$$\sigma_f = \frac{M}{D} E_f \left(\frac{c+f}{2} \right) \quad (4)$$

The maximum bending stress in the core is described by equation (5).

$$\sigma_c = \frac{M}{D} E_c \left[\frac{c}{2} \right] \quad (5)$$

The maximum core shear stress is described by equation (6).

$$\tau_c = \frac{V}{D} \left(E_f \frac{f_s}{2} + E_c \frac{c^2}{8} \right) \quad (6)$$

These equations have been used to plot the theoretical curves in the graphs comparing the analytical solution to the finite element solution.

2.2.2 MESH SENSITIVITY FINITE ELEMENT MODEL

2.2.2.1 SHELL4L MODEL

The finite element model of the 250 mm x 250 mm x 15 mm plate is illustrated in figure 5. Because the SHELL4L element is an area element physical thickness is not required in the model. Each layer of the sandwich is assigned to a corresponding layer in the element. The top aluminum face is assigned to element layer 1 and is given a thickness of 0.635 mm. The core is assigned to element layer 2 and is given a thickness of 15 mm. The bottom aluminum face is assigned to element layer 3 and given the same thickness as the top face. The result is a three layered sandwich element representation of the physical model.

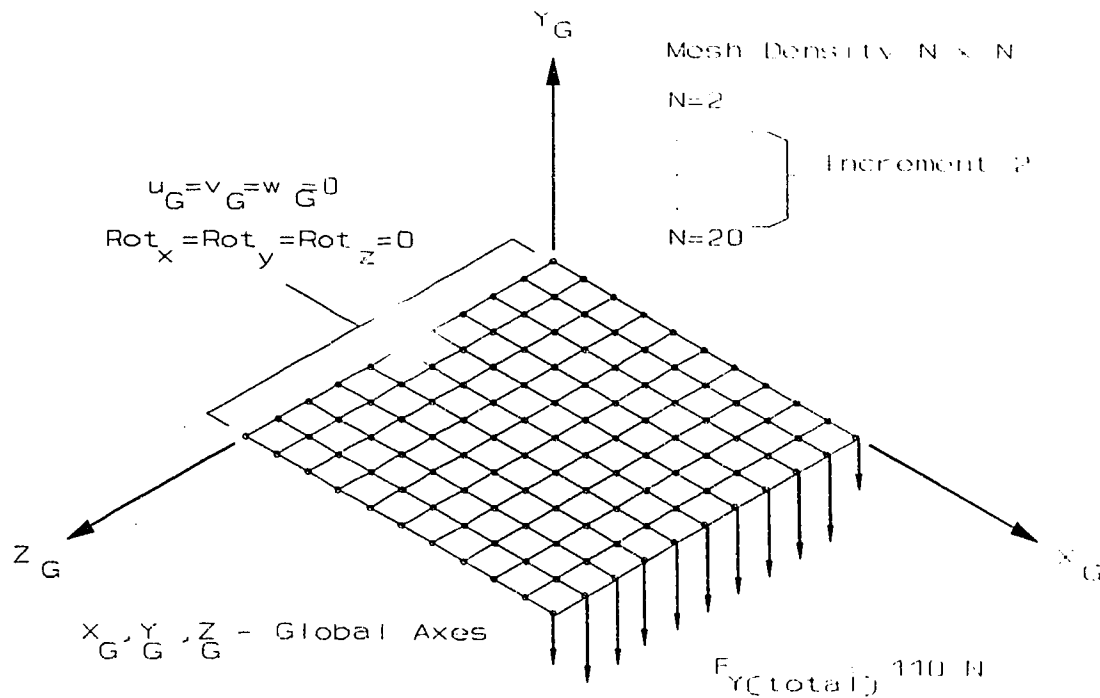


Figure 5 SHELL4L Finite Element Model, Cantilever Plate

A 110 N load was applied to the nodes along the free edge of the cantilevered panel. Displacement boundary conditions corresponding to the cantilever support condition were applied to the edge opposite the loaded side. The element mesh was varied from 2 elements to 20 elements per side in increments of 2, a mesh density of 40 x 40 was also investigated. The deflection of the free edge of the panel is determined.

2.2.2.2 STIF46 MODEL

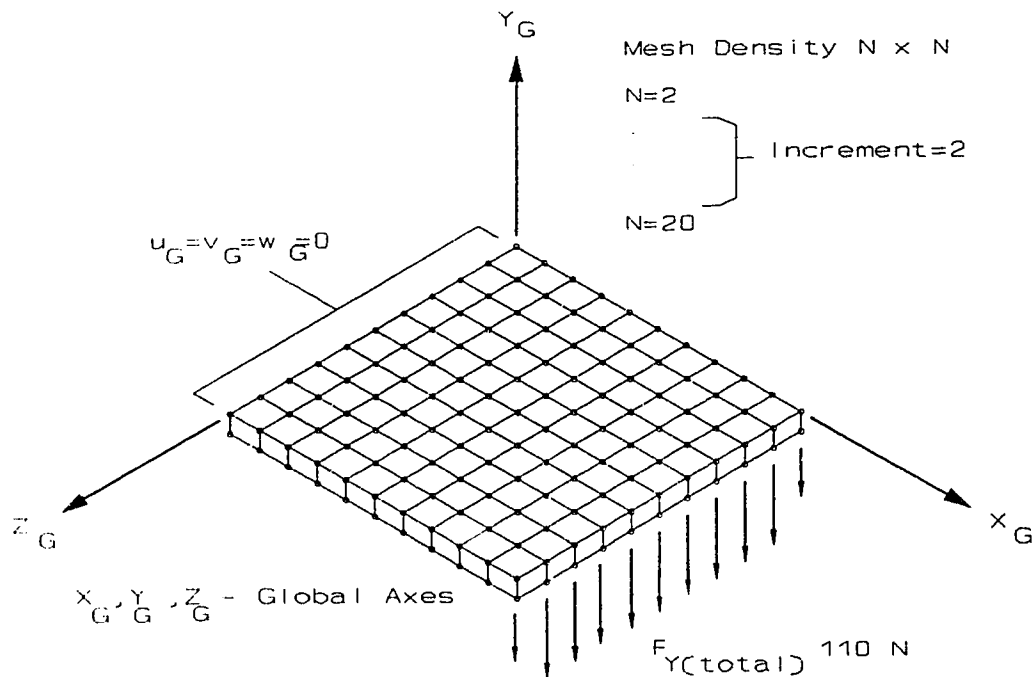


Figure 6 STIF46 Finite Element Model, Cantilever Plate

The STIF46 finite element model of the 250 mm x 250 mm x 15 mm sandwich plate is illustrated in figure 6. Because the STIF46 element is a volume element the model must represent the plate thickness. A single element is used to model the panel thickness, while the layer assignments are identical to those described in 2.2.2.1. The load condition applied to the model is identical to that used for the SHELL4L model. The boundary conditions corresponding to the cantilever boundary are different from those of the shell

model in that no rotational constraints are required as the solid element does not have rotational degrees of freedom.

The element mesh was varied from 2 elements to 20 elements per side in increments of 2. The deflection of the free edge of the panel was determined.

It should be noted that if detailed through the thickness stress information is required the STIF46 element may be stacked and several elements may be used to model the sandwich plate thickness dimension.

2.2.3 MESH SENSITIVITY RESULTS

2.2.3.1 SHELL4L RESULTS

The results of the mesh density analysis for the SHELL4L composite shell element may be seen in figure 7. The graph indicates a free edge deflection asymptote of approximately 0.87 mm at a mesh density of 40 x 40. The solution has an asymptote approximately 4.3 percent lower than the value of 0.91 mm predicted by equation (1). The solution error is less than + 5 percent at a mesh density of 6 and the finite element solution crosses the theoretical solution at a mesh density of 8 and asymptotes to a solution less than - 5 percent in error. The deflection error as a function of mesh density may be seen in figure 8.

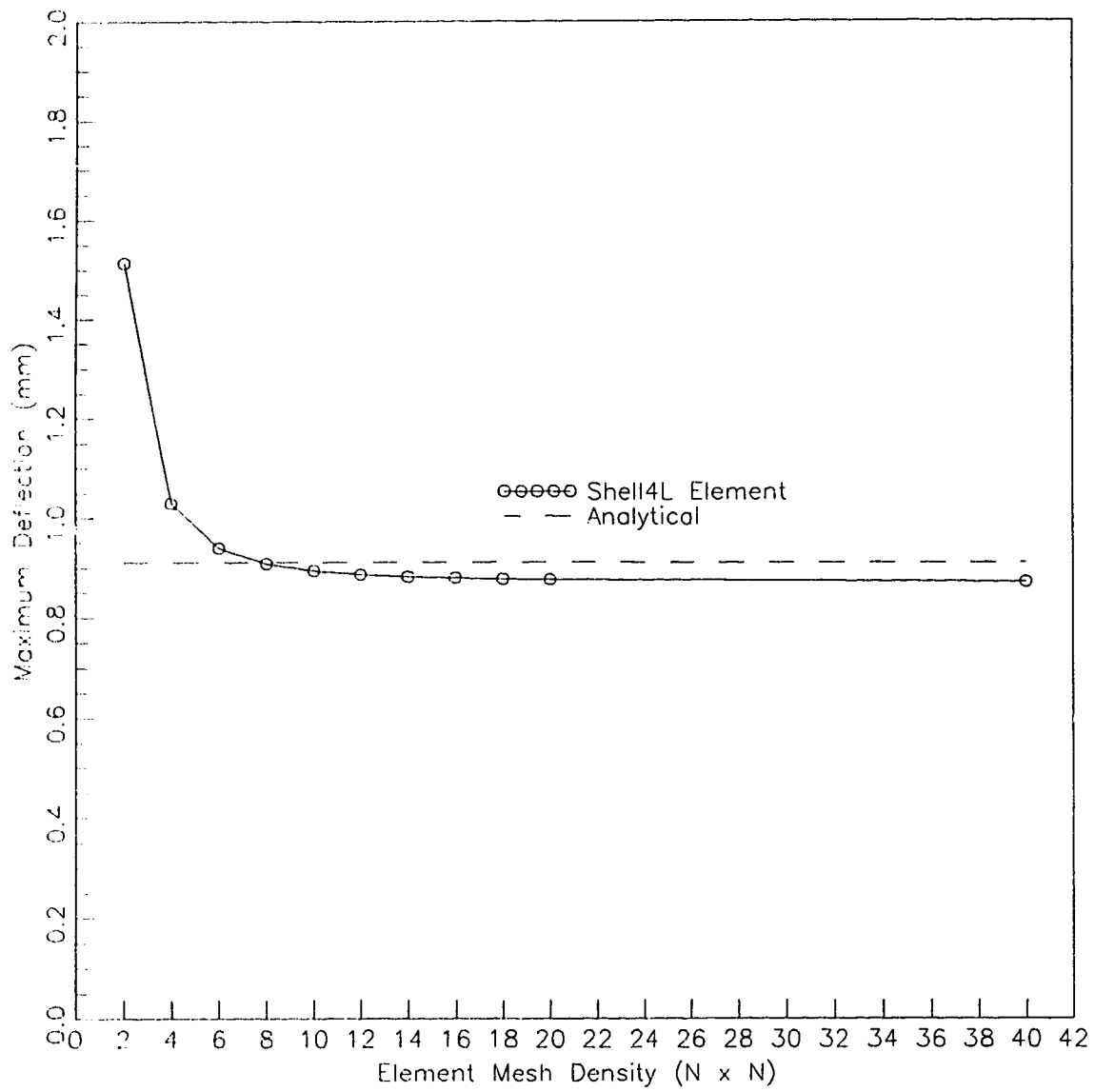


Figure 7 SHELL4L Plate Bending Convergence

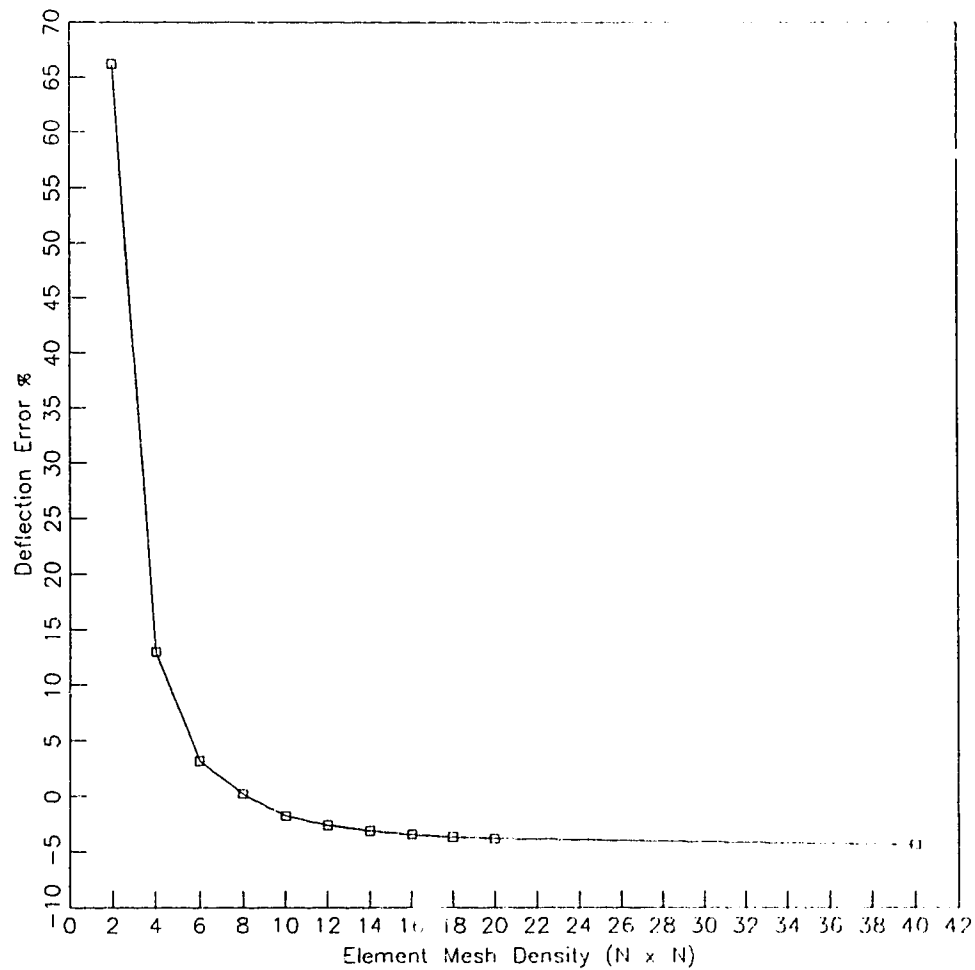


Figure 8 SHELL4L Convergence Error

The results of the mesh density analysis indicate that the SHELL4L quadrilateral composite shell element exhibits acceptable engineering accuracy for plate bending models at mesh densities greater than 6. The element is able to accurately represent the bending and shear deflection components of the total displacement.

2.2.3.2 STIF46 RESULTS

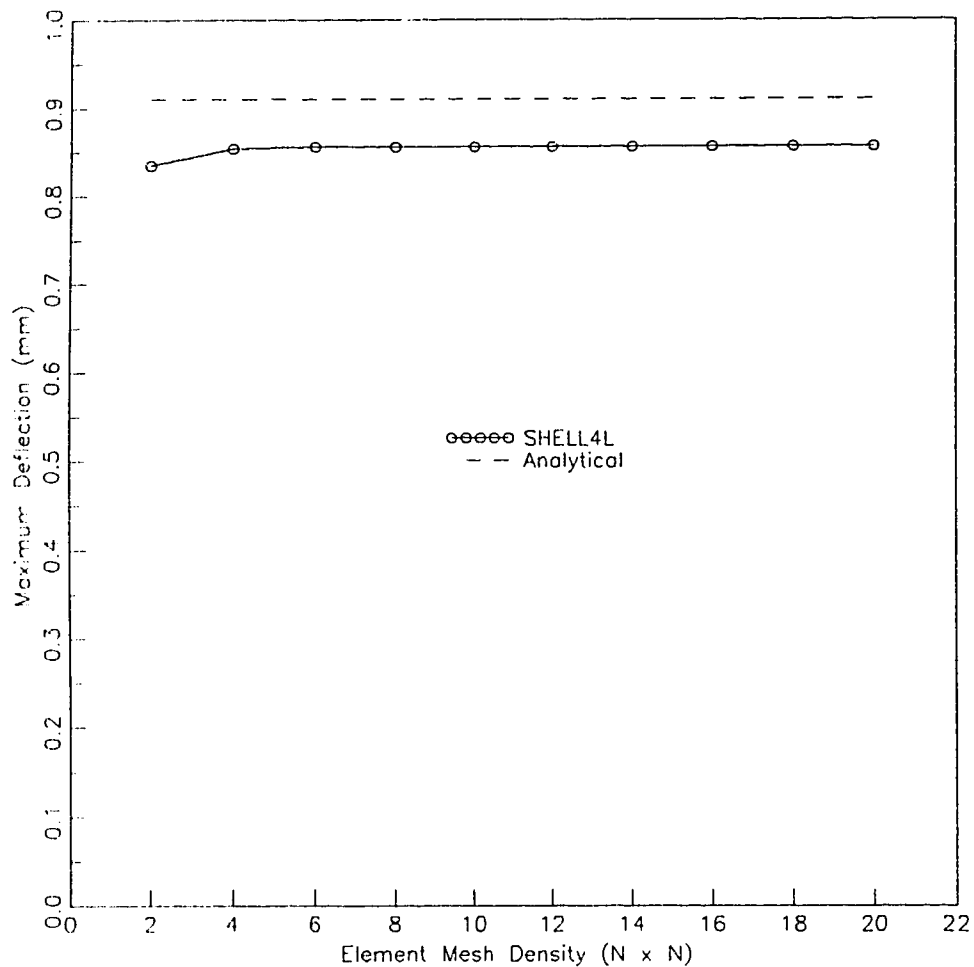


Figure 9 STIF46 Plate Bending Convergence

The results of the mesh density analysis for the STIF46 composite solid element may be seen in figure 9. The results show a very rapid convergence from below to a solution asymptote of 0.85 mm at a mesh density of 6. The solution asymptote is approximately 5.9 percent less than the solution

predicted by equation (1). The deflection error as a function of mesh density may be seen in figure 10.

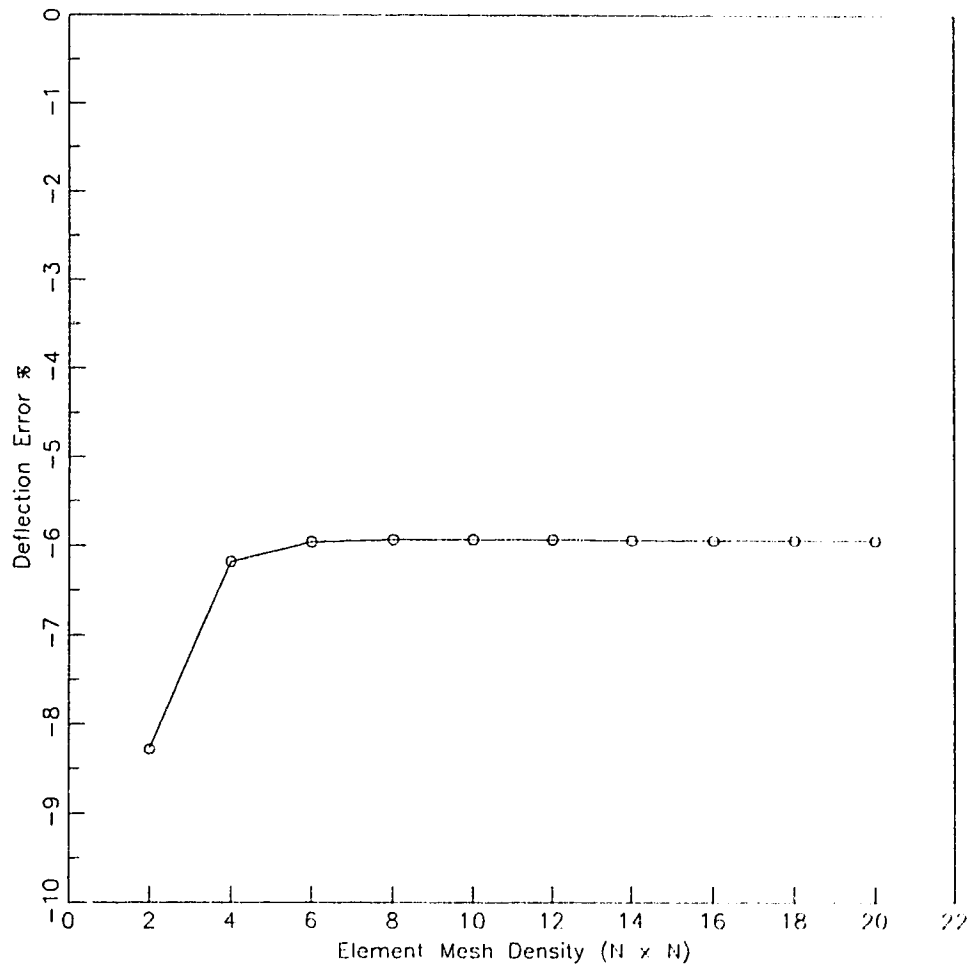


Figure 10 STIF46 Convergence Error

The results of the mesh density analysis indicate that the STIF46 composite solid element converges rapidly to a solution having a slightly larger error than that of the SHELL4L composite shell element. The element is capable of representing the shear and bending deflection components.

2.2.4 ASPECT RATIO (t/L) SENSITIVITY FINITE ELEMENT MODEL

The purpose of this investigation is to determine the effect of varying the element thickness aspect ratio (t/L) on the deflection solution of the cantilever sandwich plate described in 2.2.1. The SHELL4L and STIF46 elements are used to model the problem.

2.2.4.1 SHELL4L MODEL

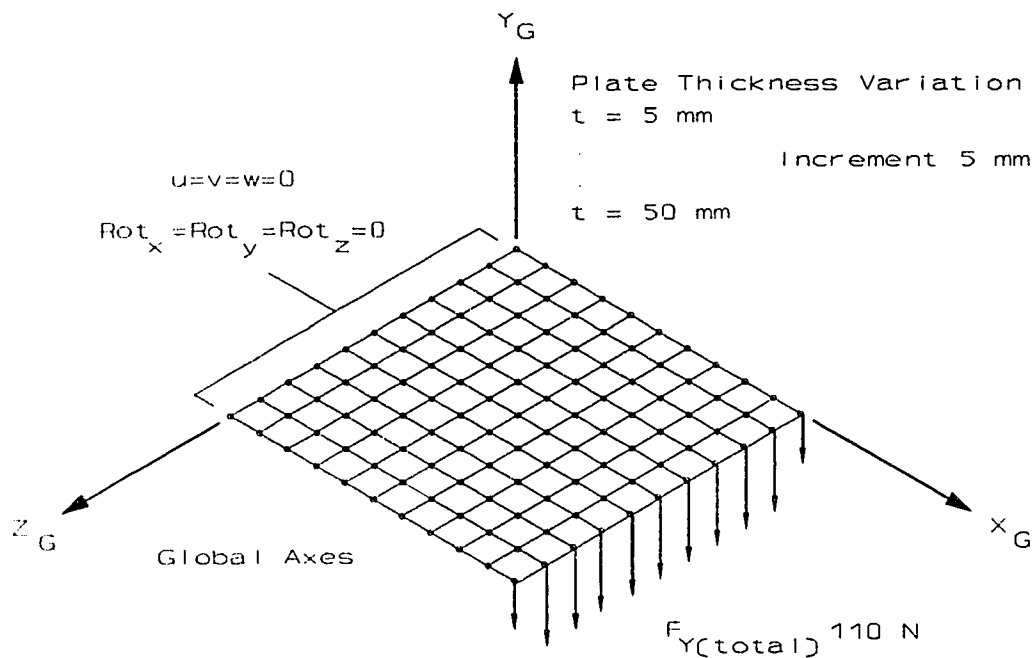


Figure 11 SHELL4L Finite Element Model, Aspect Ratio

The finite element model is similar to that described in 2.2.2.1 and is illustrated in figure 11. As with the mesh density analysis each layer of the sandwich is assigned to a corresponding layer in the element. The top and

bottom aluminum faces are assigned to element layer 1 and 2 respectively and are given thickness of 0.635 mm. The core is assigned to element layer 2 and its thickness is incremented by 5 mm over a range of 5 mm to 50 mm. The corresponding range in the thickness aspect ratio is 0.20 to 2.0. This range of aspect ratios was chosen as it represents the practical limits of the panel thickness expected in the vehicle structure design.

A mesh density of 20 elements per side was chosen based on the results of the sensitivity analysis performed previously. A 110 N load was applied to the nodes along the free edge of the cantilevered panel. Displacement boundary conditions corresponding to the cantilever support condition were applied to the edge opposite the loaded side. The deflection of the free edge of the panel is determined for each of the t/L ratios. The face and core nodal bending stresses at the constrained edge of the panel are determined as well for each of the t/L ratios.

2.2.4.2 STIF46 MODEL

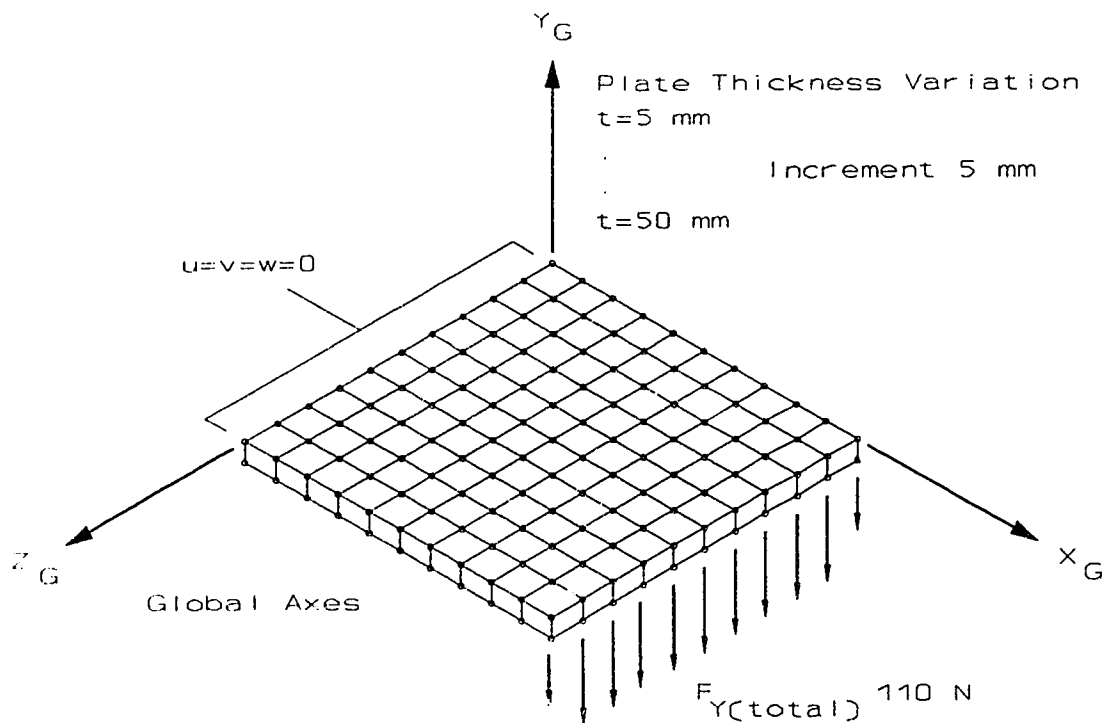


Figure 12 STIF46 Finite Element Model, Aspect Ratio

The model comprised of STIF46 elements is similar to that described in 2.2.4.1. An illustration of this finite element model may be seen in figure 12. As in the mesh density model a single element is used to model the sandwich plate thickness. The t/L ratio is varied in an identical manner and the load and displacement boundary conditions are as before.

2.2.5 ASPECT RATIO (t/L) SENSITIVITY RESULTS

2.2.5.1 SHELL4L RESULTS

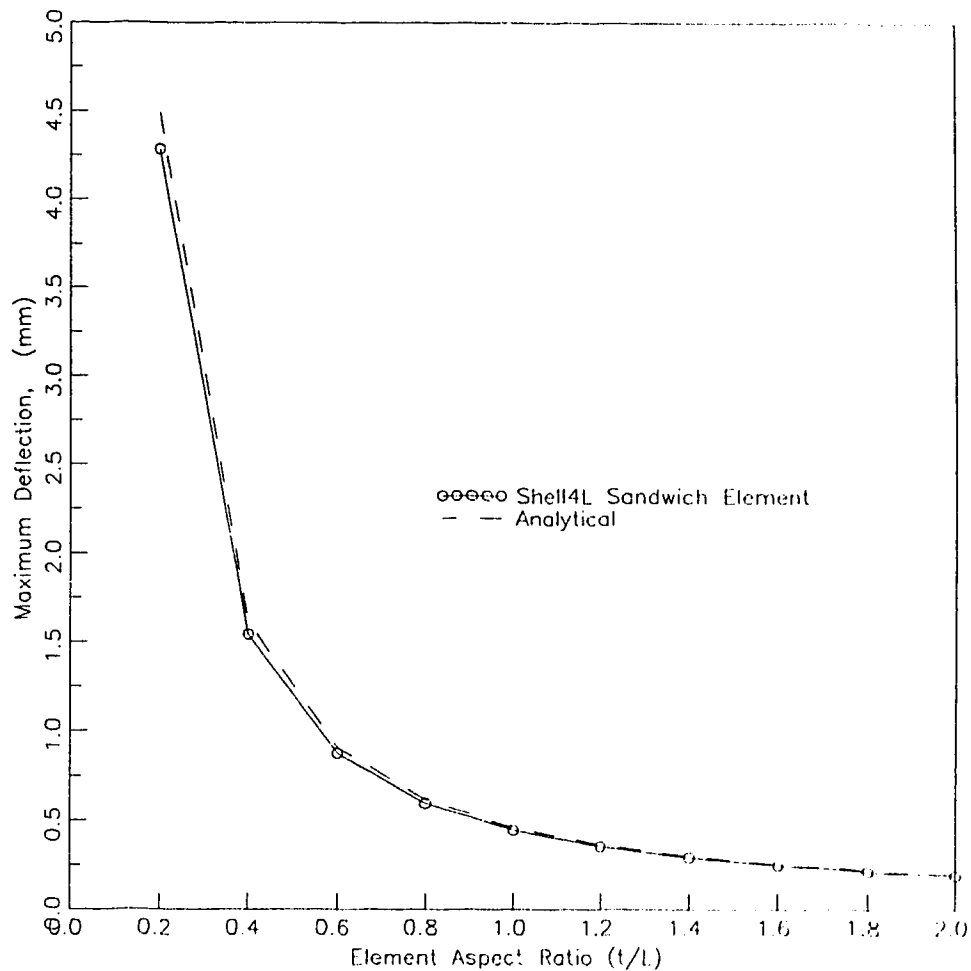


Figure 13 SHELL4L Aspect Ratio Results

The free edge deflection graph illustrated in figure 13 indicates a good correlation between the finite element solution and the analytical solution. The maximum error in the free edge deflection is 4.5 percent at an aspect ratio of 0.20, figure 14. This is due to the dominant influence of the face bending

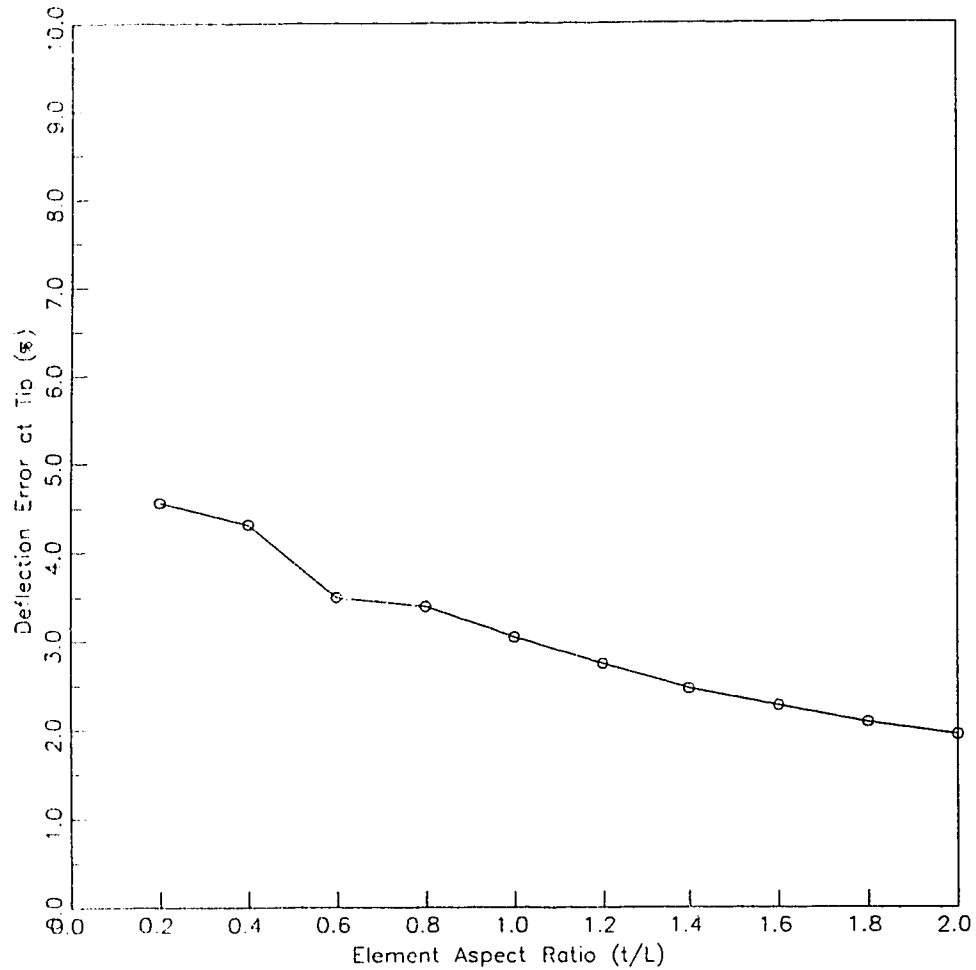


Figure 14 SHELL4L Aspect Ratio Error

stiffness on the aggregate sandwich plate stiffness. The solution error decreases as the aspect ratio increases and reaches a minimum value of just under 2 percent at a ratio of 2.0. At this aspect ratio the shear deflection component of the total free edge deflection dominates the analytical solution. The effect of the face bending stiffness is reduced and the shear stiffness of

the core dictates the deflection solution. The SHELL4L element is capable of representing the shear deflections that occur in sandwich structures.

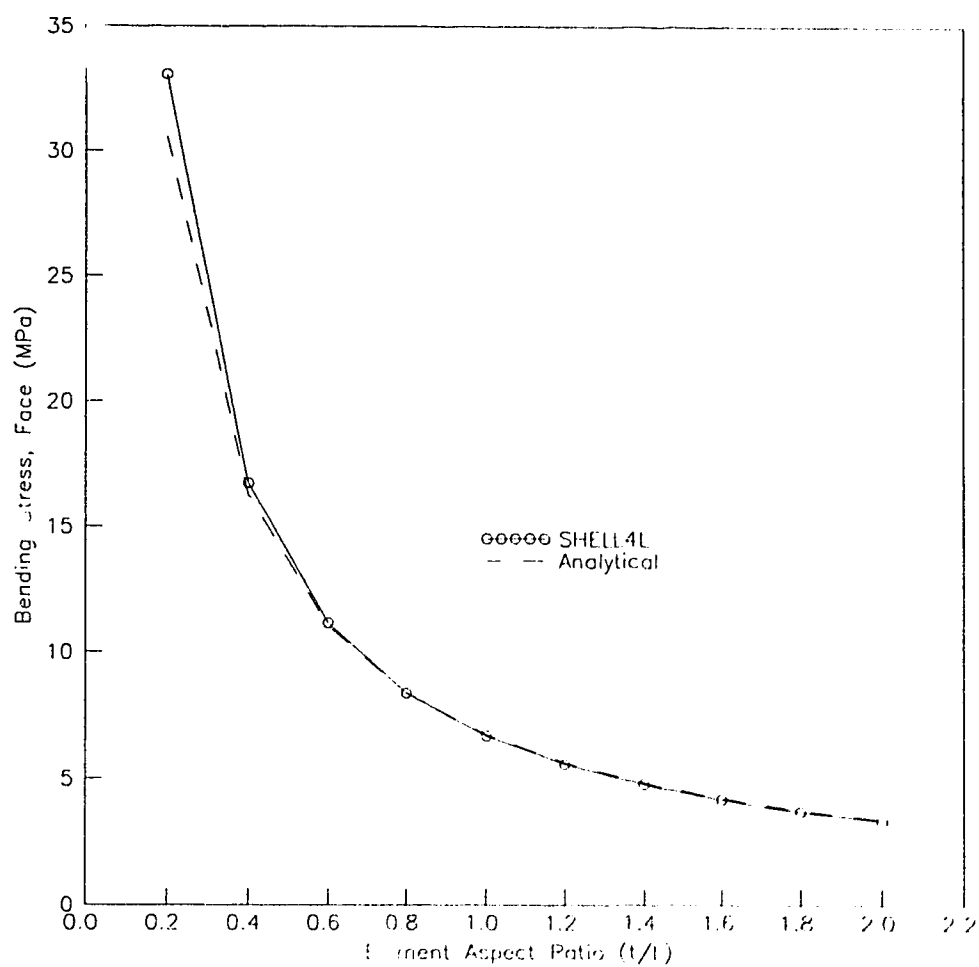


Figure 15 SHELL4L Face Bending Stress

The maximum nodal bending stresses occurring in the aluminum face layer are presented in figure 15. At an aspect ratio of 0.2 the finite element

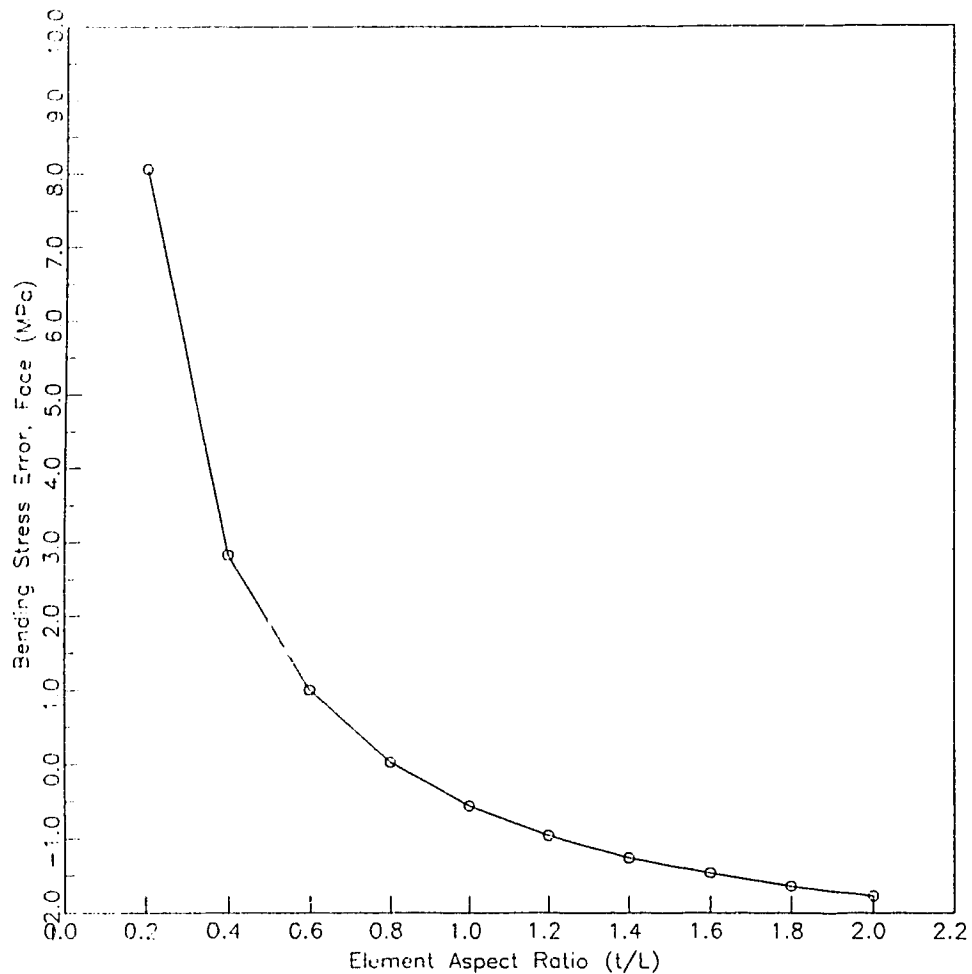


Figure 16 SHELL4L Face Bending Stress Error

model predicts a greater bending stress than that predicted by the analytical solution. The finite element deflection curve crosses the analytic solution at an aspect ratio of 0.8, this corresponds to the change from bending dominance to shear dominance in the solution. The deflection curve terminates beneath the analytical curve at an aspect ratio of 2.0. The error in the bending stress

solution is illustrated in figure 16 and shows the maximum error (8.0 percent) occurring at an aspect ratio of 0.2. The solution error plot appears to have the same shape as the bending stress plot indicating a similar functionality. Minimum solution error is attained at 0.8 aspect ratio reflecting the change in the dominance of face bending over core shear.

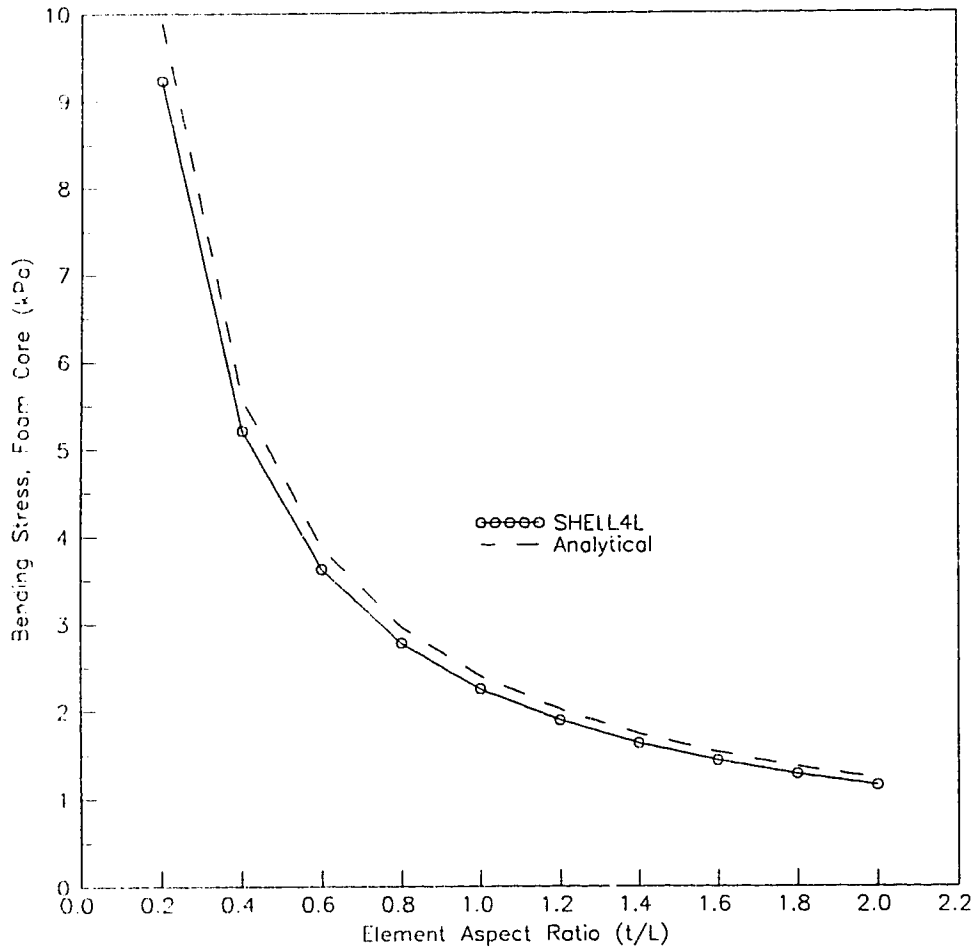


Figure 17 SHELL4L Core Bending Stress

The nodal bending stress in the foam core layer is shown in figure 17. The finite element solution is consistently lower than the analytical solution for all aspect ratios. The bending stress error plot, figure 18, illustrates the consistent solution error of 6.2 percent. The results are consistent with the analytical solution in that core bending has little influence on the response of the sandwich plate as a whole.

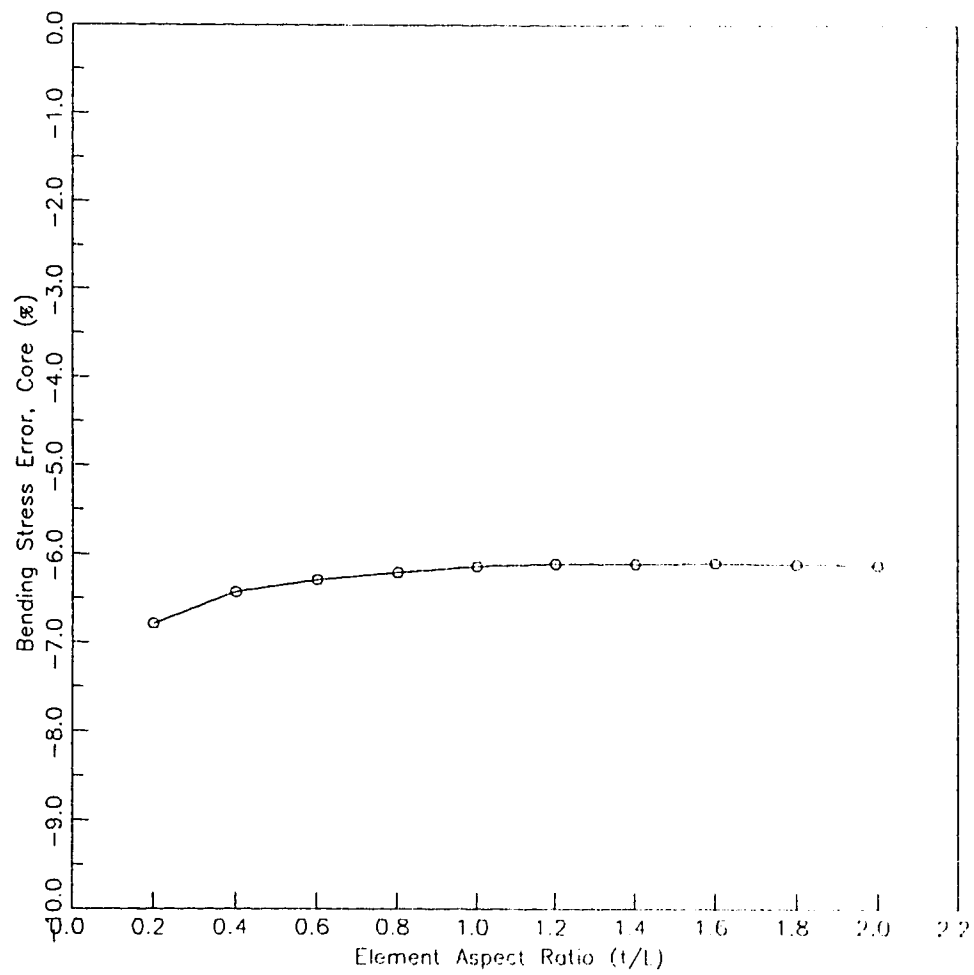


Figure 18 SHELL4L Core Bending Stress Error

2.2.5.2 STIF46 RESULTS

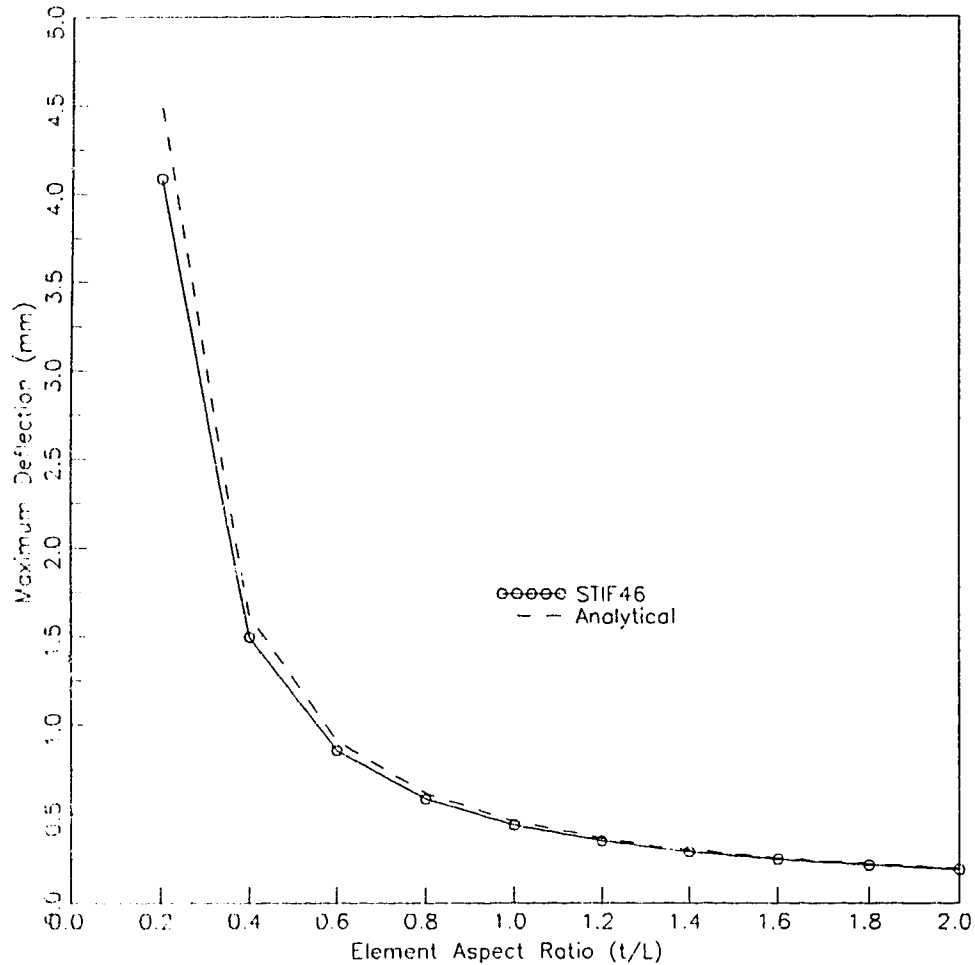


Figure 19 STIF46 Aspect Ratio Results

The free edge deflection results for the STIF46 finite element model are presented in figure 19 and show a good correlation to the analytical results. The finite element solution remains under the curve describing the analytical solution for all aspect ratios. The deflection error for this element is illustrated

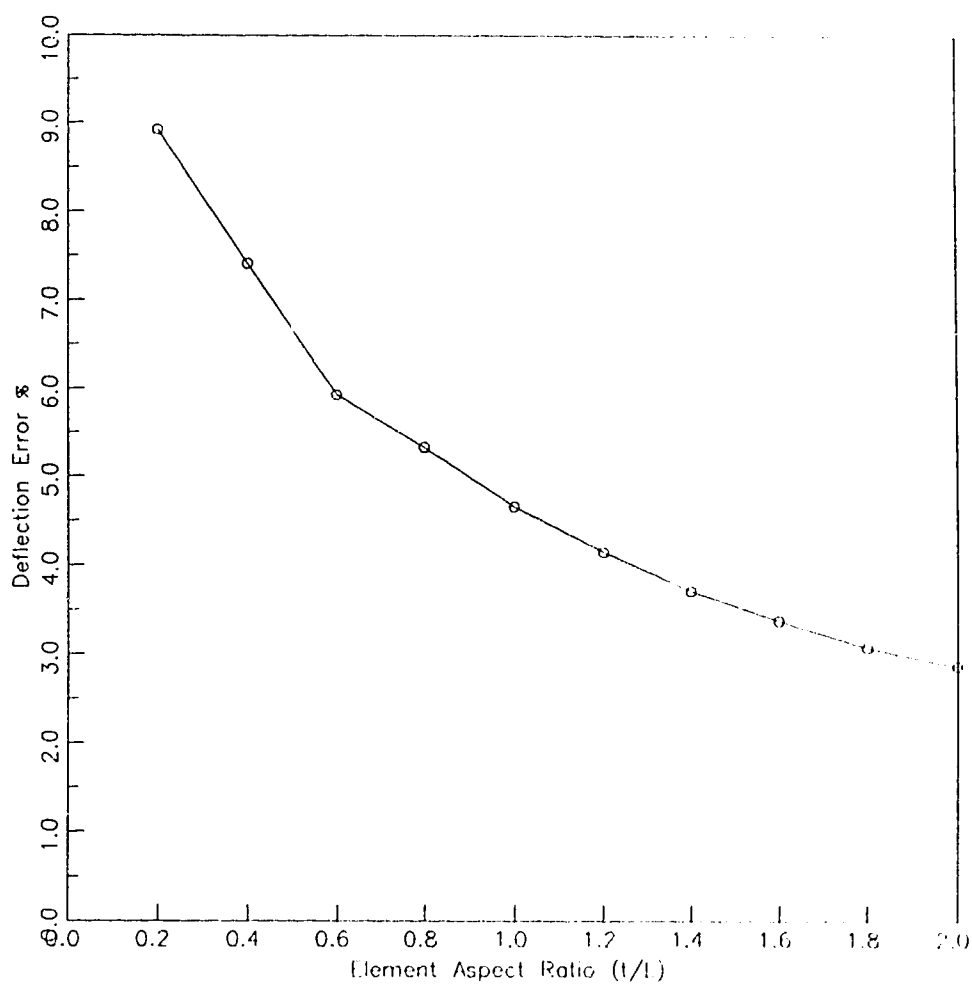


Figure 20 STIF46 Aspect Ratio Error

in figure 20 and exhibits a consistent decline from 8.9 percent to 2.9 percent over the full range of aspect ratios.

2.2.5.3 COMPARISON

A comparison of the results from the two element types indicates that the SHELL4L element has better accuracy than the STIF46 element. The free edge deflection error is consistently lower for the SHELL4L element over the entire range of aspect ratios.

2.2.6 SHELL4-SOLID HYBRID ANALYSIS

A preliminary investigation was done using a shell-solid hybrid to model a plate subjected to 3 point bending. The model geometry and mesh density are different than the preceding cases, however it is instructive to review the results of this work to gain some insight on the behaviour of this hybrid model.

2.2.6.1 FINITE ELEMENT MODEL

The finite element model shown in figure 21 consists of a sandwich of elements comprising the three material layers previously discussed. The difference being that each material layer is represented by its own element. The top and bottom aluminum faces are modelled using the SHELL4 shell element while the core layer is modelled using four 8-node isoparametric SOLID elements through the thickness.

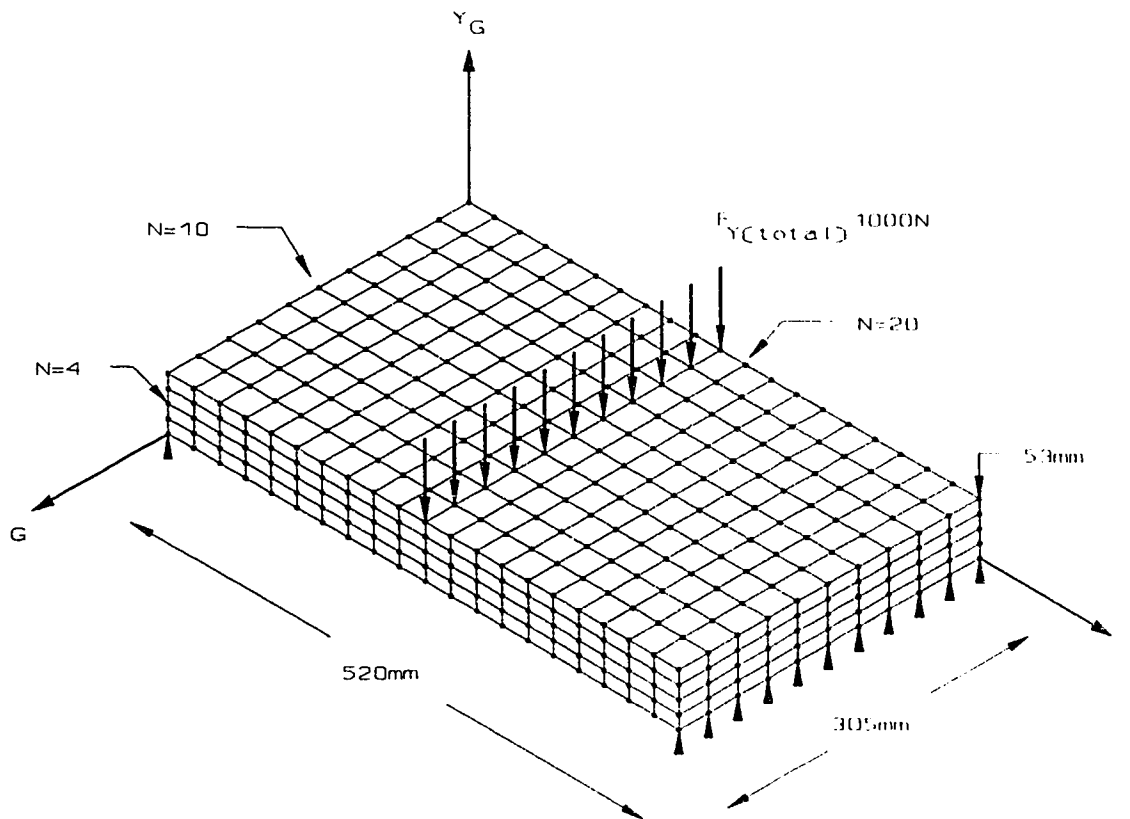


Figure 21 SHELL4-SOLID Finite Element Model

The resulting hybrid is expensive in finite element terms in that it contains a total of 84 d.o.f per element. In contrast the quadrilateral layered shell element and the 8-node isoparametric layered solid element contain 24 d.o.f. per single element.

2.2.6.2 SHELL4-SOLID RESULTS

The results of this analysis have been tabulated in table 3.

Table 3 Shell-Solid Hybrid Deflection Results

Load (N)	Analytical Deflection (mm)	Finite Element Deflection (mm)	Deflection Error (%)
1000	0.74	0.84	13.5

As indicated the hybrid model over-predicts the plate deflection by 13.5 percent and is not a very efficient finite element method for analyzing sandwich structures. The advantage that this model may have lies in its ability to represent through the thickness stress fields in the core layer. This advantage is offset by the existence of the more efficient layered solid element which has a smaller wavefront. More extensive testing was not performed on this shell-solid hybrid because of its large wavefront and the inherent limitations this imposes on practical model size.

2.2.7 STIF99 ANALYSIS

An abbreviated cantilever plate bending test similar to the one described in 2.2.1 was performed using the STIF99 8-node isoparametric layered shell element.

2.2.7.1 FINITE ELEMENT MODEL

The finite element model used for this investigation is identical to that described in section 2.2.2 and figure 3. The layer assignments, material properties, load and boundary conditions are, likewise, identical to those described previously.

A second analysis was done to investigate the apparent shear locking effect that was seen to be occurring in the first analysis described above. The only change made to the model in this second analysis was to set the shear moduli, G_{xz} and G_{yz} of the face layers to a number close to zero.

2.2.7.2 RESULTS

The results of this analysis have been tabulated in table 4.

Table 4 STIF99 Sandwich Plate Bending Deflection Results

Free Edge Deflection Results	Model #1 $G_{xz} = G_{yz} = 26316$	Model #2 $G_{xz} = G_{yz} = 0.001$
Finite Element Results	0.398 mm	1.057 mm
Analytical Prediction	0.910 mm	0.910 mm
Deflection Error	- 0.512 mm	+ 0.147 mm
Analytic Bending Component	0.421 mm	0.421 mm
Analytic Shear Component	0.489 mm	0.489 mm

The finite element prediction of the bending deflection for model #1 is inaccurate, however the model does predict the bending component of the total deflection rather closely. This result would seem to indicate that the element is exhibiting shear locking behaviour. The results of model #2 for which the transverse shear moduli of the face layers have modified show an improved prediction (approximately 16 % error) of the free edge bending deflection. This result would seem to confirm the shear locking hypothesis. Further study of the mesh and aspect ratio sensitivity for this element was not pursued because of the more favourable results being obtained with the SHELL4L and STIF46 elements.

2.3 CYLINDER TORSION ANALYSIS

2.3.1 DESCRIPTION OF PHYSICAL MODEL

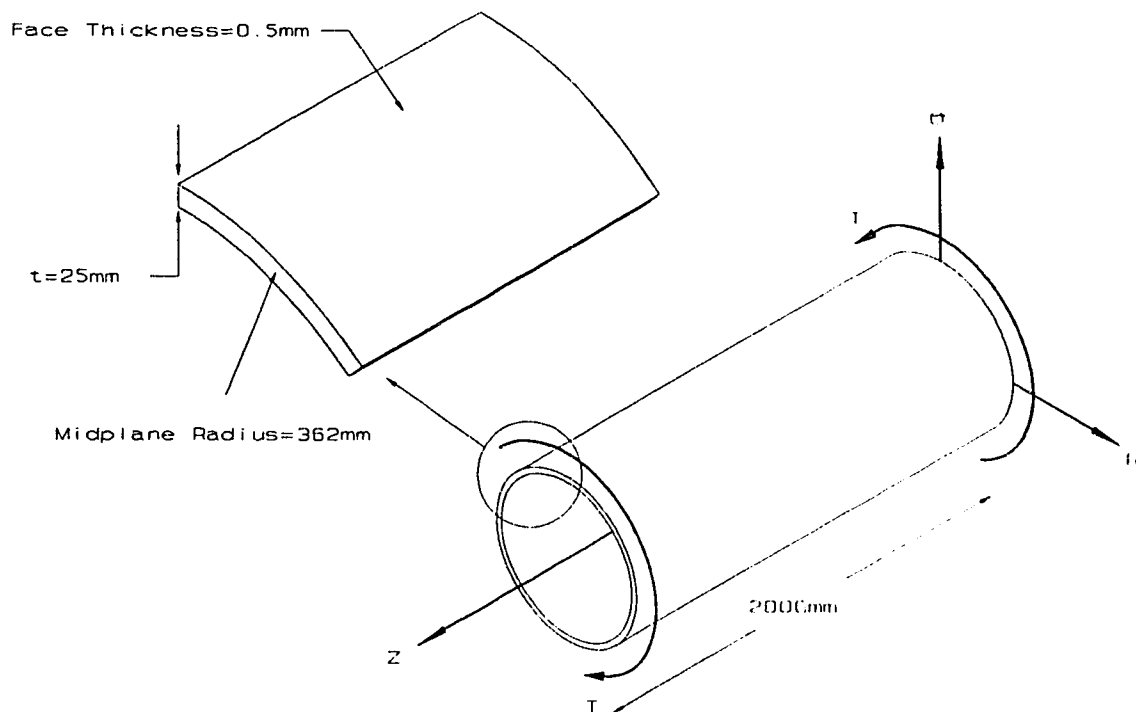


Figure 22 Cylinder Torsion Model

An illustration of the sandwich composite cylinder used for this study is shown in figure 22. The cylinder is constructed of the same materials used for the sandwich plate bending analyses. The cylinder has a mean radius of 362 mm and a length of 2000 mm. The sandwich comprises two aluminum face layers each 0.5 mm thick and a polystyrene foam core 25 mm thick. A torque of 1.305×10^6 Nm is applied about the centroidal axis.

2.3.2 DESCRIPTION OF ANALYTICAL SOLUTION

The analytical solution assumes that the face layers resist the torque while the core layer contributes little to the torsional stiffness. The equation used to determine the angle of twist is described by equation (7).

$$\theta = \frac{T L}{I_p G} \quad (7)$$

The shear stress in the face layer is described by equation (8)

$$\tau_{\max} = \frac{T c}{I_p} \quad (8)$$

2.3.3 FINITE ELEMENT MODEL

The finite element model is illustrated in figure 23. SHELL4L elements are used to model the cylinder and as before element layers 1 and 2 are assigned to the aluminum faces while element layer 2 is assigned to the foam core. The model is comprised of a total of 480 layered composite shell elements, 20 elements being used along the length of the cylinder while 24 elements are used around the circumference.

The theta displacement d.o.f. are constrained at one end of the cylinder while a force equivalent to the assumed torque is distributed along the

circumferential nodes at the free end of the cylinder. A single axial d.o.f. is constrained to prevent rigid body translation.

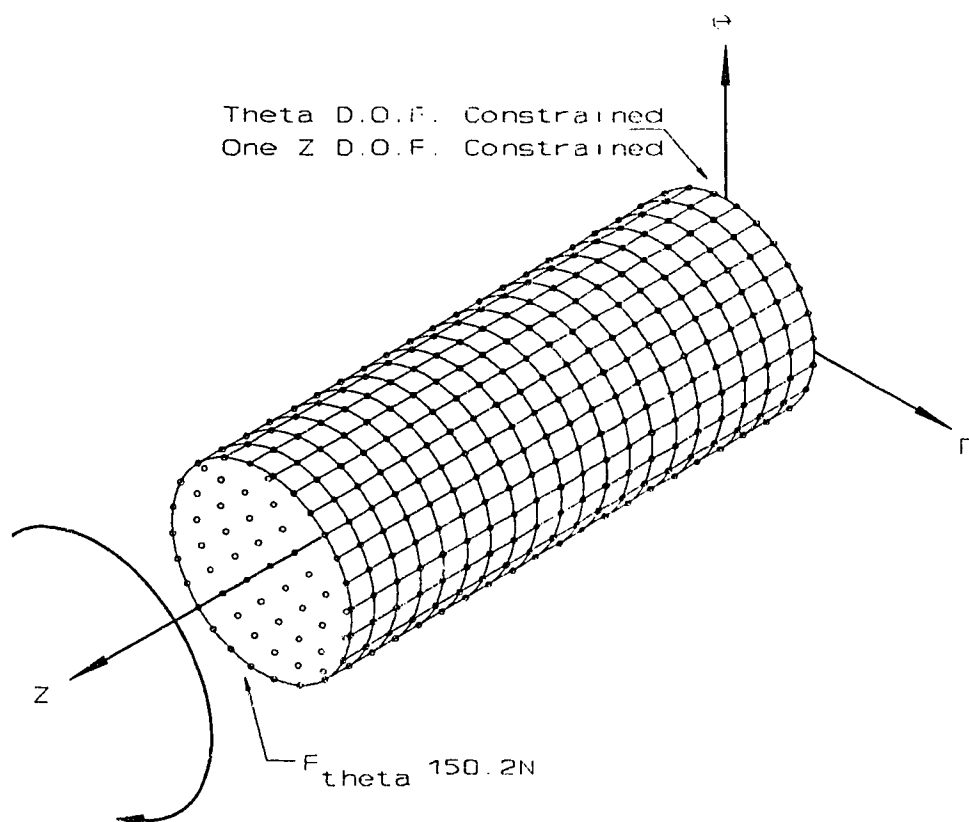


Figure 23 Torsion Cylinder Finite Element Model

2.3.4 FINITE ELEMENT RESULTS

The results of this investigation have been tabulated and are presented in table 5.

Table 5 Torsion Cylinder Results

	θ (rads)	T_{\max} (MPa)
Analytical Prediction	3.315×10^{-4}	1.64
Finite Element Result	3.326×10^{-4}	1.61
Error	0.33 %	1.8 %

A comparison of the analytic and finite element results shows an excellent correlation between the two for both the displacement and the shear stress results. In both cases the solution error is well within acceptable values and indicates the suitability of the SHELL4L element for modelling a structure subjected to a torsional load.

2.4 COMMENTS ON ELEMENT/PROGRAM ANOMALIES

2.4.1 SHELL4L SHEAR LOCKING

During the course of the verification program the SHELL4L element exhibited signs of shear locking for particular element layer configurations. The problem manifested itself in deflection solutions which were very much smaller

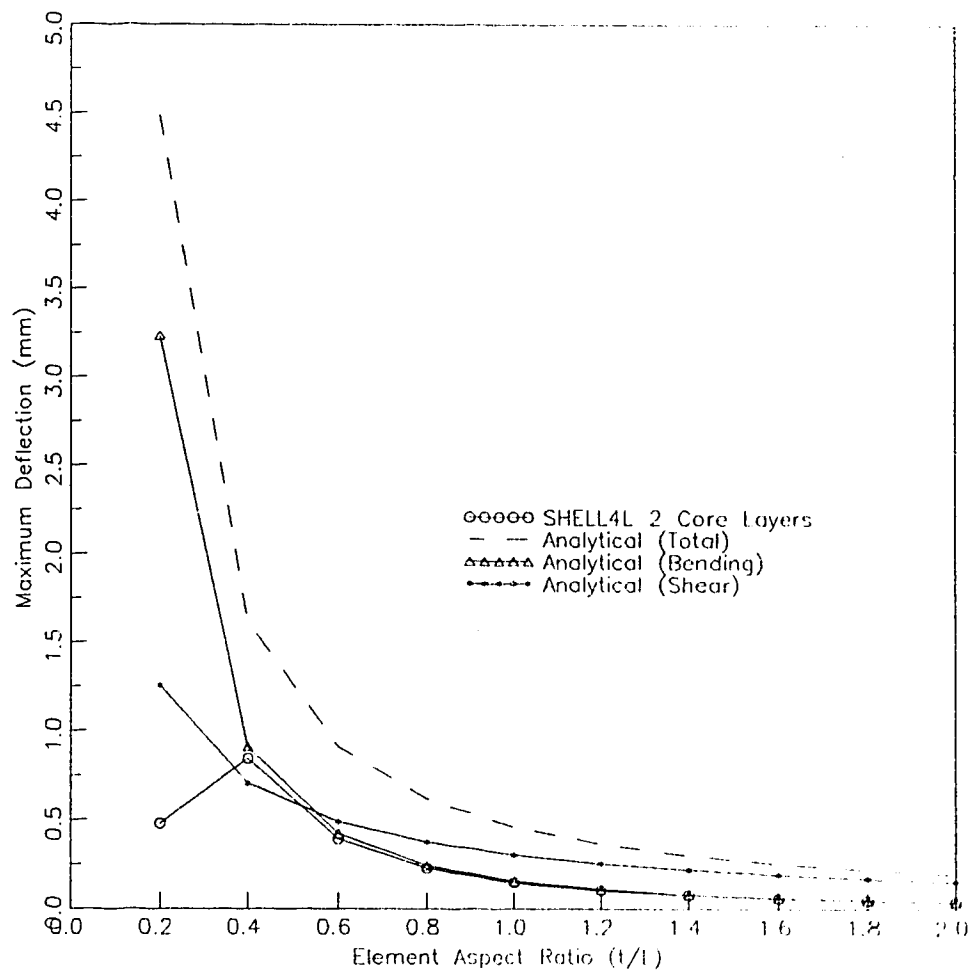


Figure 24 SHELL4L Shear Locking Behaviour

than those anticipated and seemed to correspond very closely with the bending component of the total deflection. An example of this can be seen in figure 24 which shows the deflection solution for a cantilevered sandwich plate laying well below the analytic solution. The shear locking occurred when more than one element layer was assigned to the core. The reasons for the shear locking have already been discussed in the theory section.

When queried the element developer indicated that the shear locking under these circumstances could be alleviated by setting the transverse shear moduli G_{xz} and G_{yz} of the face layers to a number approaching zero. When this was done the finite element deflection solution did indeed approach the analytic but was not as accurate as the model in which a single element layer was assigned to the core layer. The developer indicated that when the sandwich or three layer option was selected an internal flag was set which caused the transverse shear moduli of the face layers to be set to a small number. This explanation was subsequently tested by setting the transverse shear moduli of the face layers to a small number in a model containing three layer elements. This test resulted in extremely large deflection values which were orders of magnitude larger than the analytic solution. The test indicates that the layered shell element is being modified in other ways to allow it to accurately represent sandwich plate bending.

2.4.2 COORDINATE SYSTEM ERRORS

During the course of the investigation an error in the local coordinate system definition was observed in the COSMOS/M software. Forces and displacements defined in a local cylindrical coordinate system were not being translated correctly into the global cartesian system. As a result of this error the forces and displacements so defined assumed directions corresponding to the global cartesian coordinate directions (i.e. F_r became F_x and F_θ became F_y).

To compound the problem there was no indication in the input data that an error had occurred, the only indication of error manifested itself in the solution, particularly the deflection results.

This program error emphasizes the requirement of continually evaluating finite element results for correctness and running unique verification problems, a methodology for such checking is given in Akin [3]. An extensive quality assurance program and rigorous error reporting is an essential requirement for commercial finite element programs.

3.0 VEHICLE STRUCTURE STIFFNESS ANALYSIS MODEL

The structural design of the sandwich chassis had its genesis in the author's home in the form of a cardboard mock-up constructed to ensure that compatibility existed between man and structure. What follows is a description of the philosophy governing the structural design, the materials used in the design and a review of the design goals. The finite element model representing the vehicle structure is outlined as are the three load cases used to determine the structural stiffness in torsion and lateral and horizontal beaming.

3.1 DESCRIPTION OF STRUCTURAL DESIGN

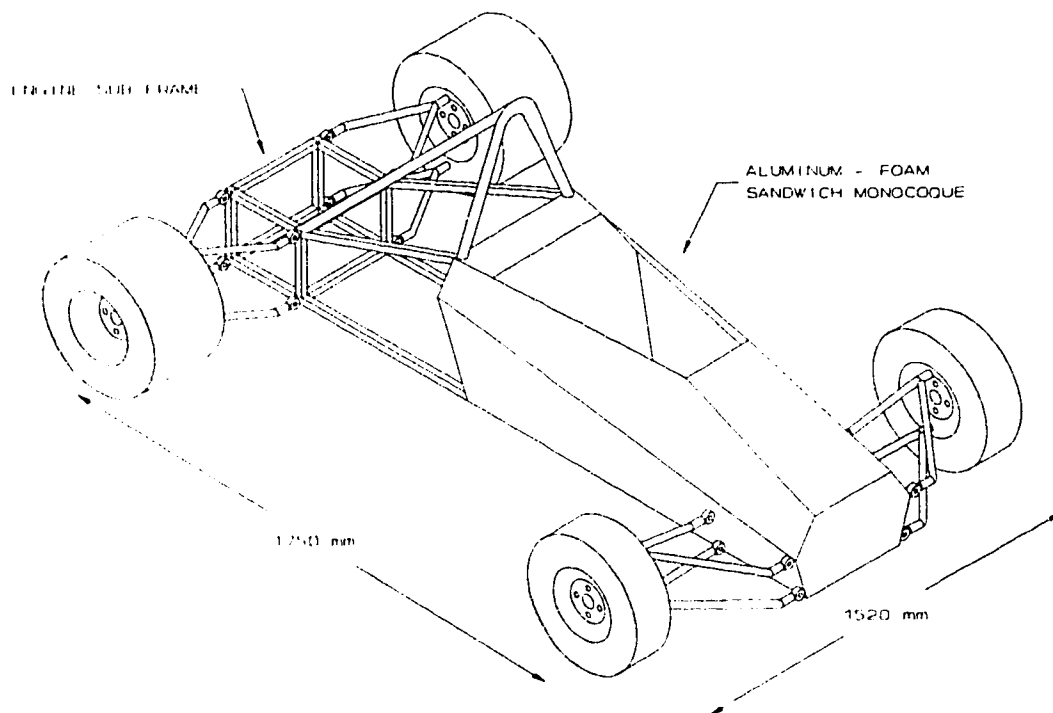


Figure 25 Vehicle Substructures

The vehicle structure consists of an aluminum-foam sandwich monocoque encompassing the driver and a tubular space frame containing the engine, transmission and rear suspension attachment points. The major substructures comprising the single seat vehicle are shown in figure 25. The monocoque structure, ("monocoque" is a French word meaning "shell only") is the focus of the structural stiffness evaluation.

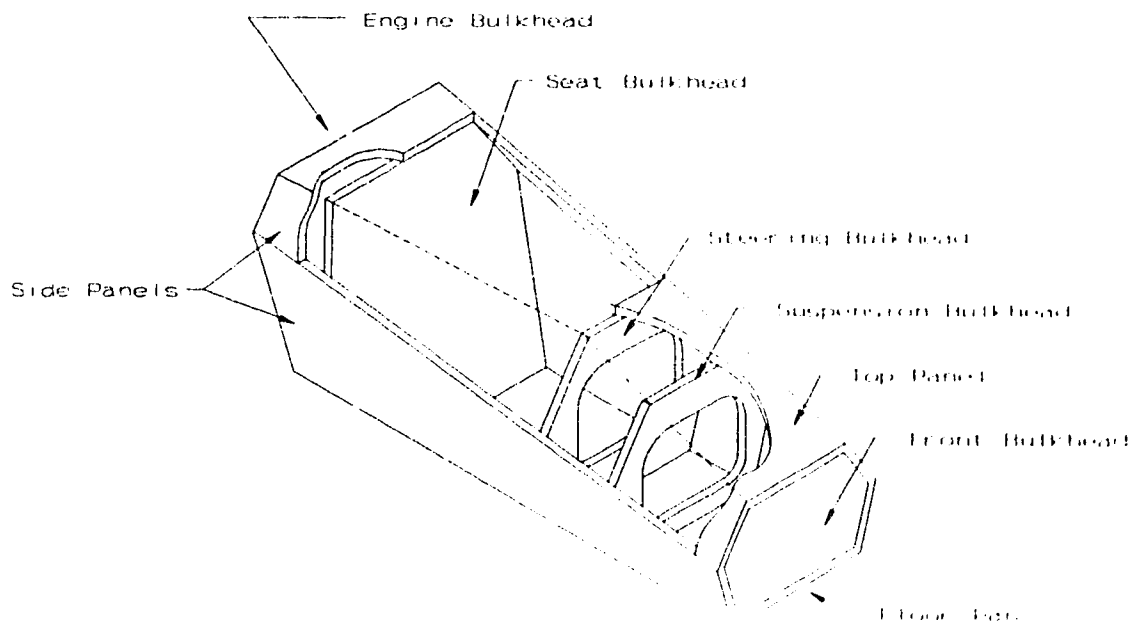


Figure 26 Sandwich Monocoque Detail

The sandwich monocoque design, shown in detail in figure 26, is a slab sided structure comprised of an aluminum-foam composite of a type similar to that described earlier in the verification section. The design calls for the monocoque to be constructed of 25.4 mm thick aluminum-foam sandwich plate which is scored and folded around 5 internal bulkheads of the same plate. The

monocoque structure is 1465 mm long and 658 mm wide at its largest dimension. The design approach is similar to that used in the Ferrari 126C2 and the McLaren M23 Formula One chassis described in Henry [22].

Emphasis was placed on the geometry of the cockpit opening as this represents the section through which the greatest torsional rigidity loss occurs. The cockpit structure has high sides which rise above the shoulders while the size of the opening is minimized. The seat-back slopes forward to "box in" as much of the cockpit as is possible; the panel supporting the legs has a similar function. These design features are intended to minimize the loss of torsional rigidity through this section of the structure.

The design calls for what is known as the "cut and fold" method of sandwich panel construction. A feature of this method which has effect on the analysis of the structure is the corner joint formed between panel sections after the fold is made. An illustration of this corner joint is shown in figure 27. The compliance of these panel joints will influence the stiffness of the overall structure. As seen in the illustration the joints are reinforced to improve the stiffness.

The philosophy governing the structural design then is one of maximum rigidity at all sections of the sandwich monocoque. The design is stiffness based rather than stress based as is the case for most racing vehicle structures. Such stiffness based chassis designs are typically over designed in terms of stress and fatigue [28].

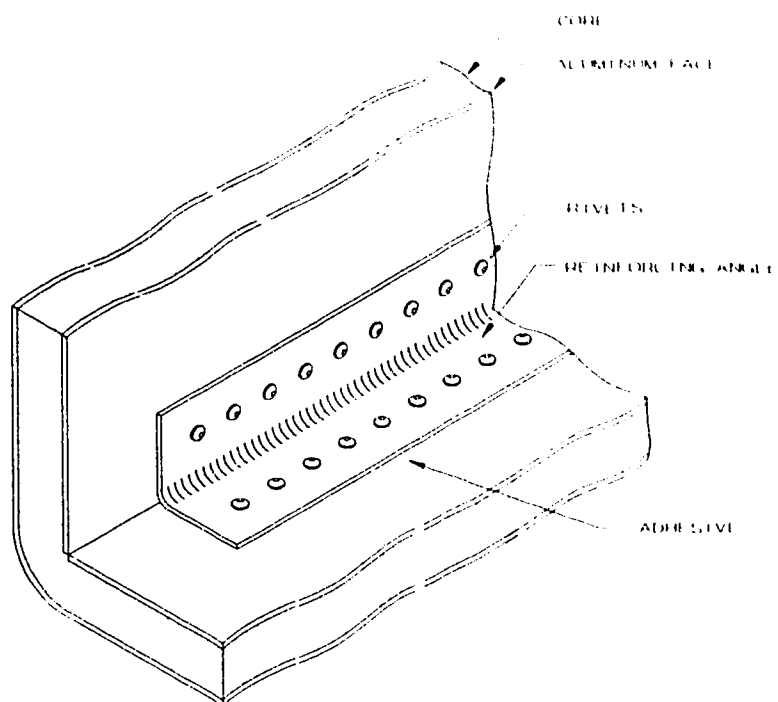


Figure 27 Sandwich Panel Corner Joint Detail

3.2 DESCRIPTION OF FINITE ELEMENT MODEL

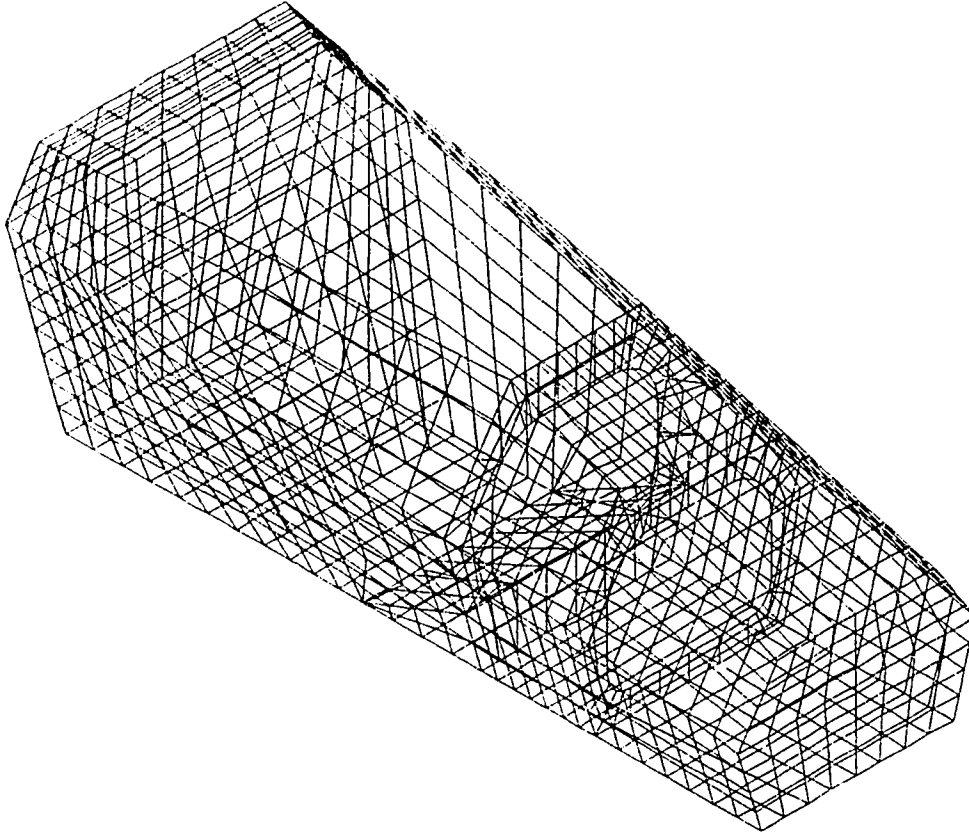


Figure 28 Finite Element Model of Composite Monocoque

The finite element model of the sandwich monocoque is shown in figure 28. The entire monocoque structure is modelled and consists of 1446 SHELL4L composite shell elements, 1417 nodes and a total of 8502 degrees of freedom. The element layer assignment, shown in figure 29, is similar to that described in the verification section. The top and bottom aluminum faces are 0.508 mm (0.020 in.) thick and are assigned to element layers 1 and 3. The extruded polystyrene core is 24.384 mm thick and is assigned to element layer 2. The resulting sandwich panel is 25.4 mm (1 in.) thick and is used for

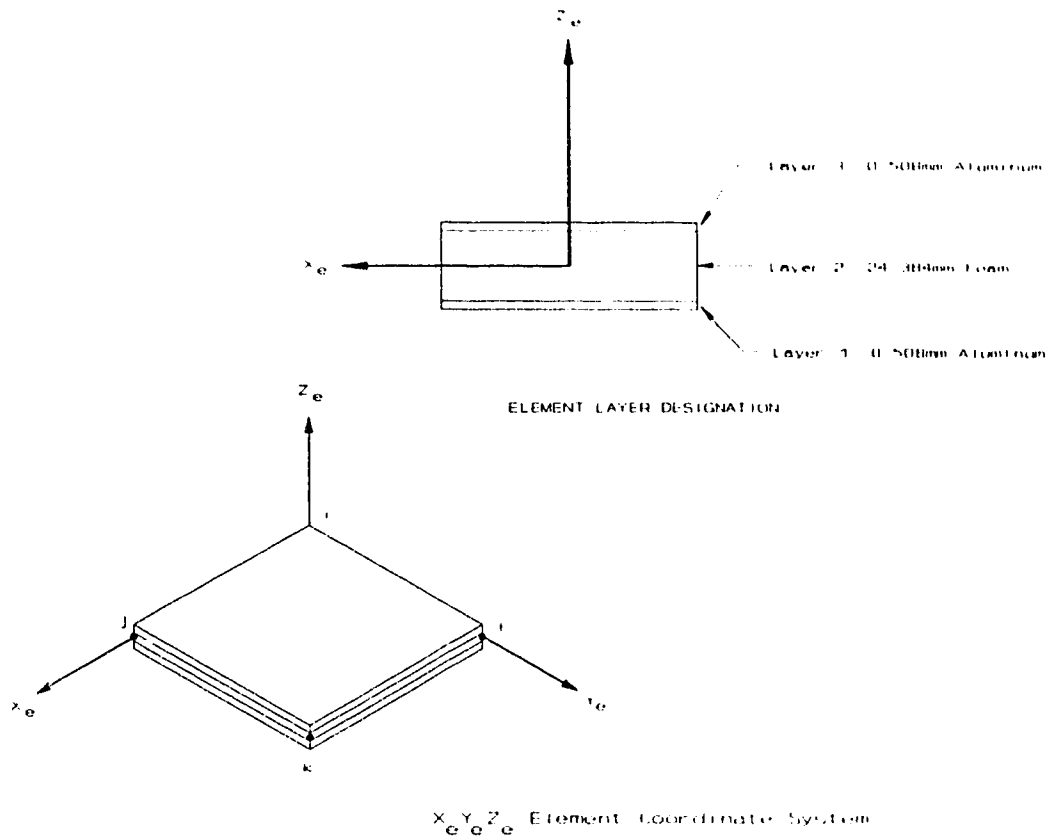


Figure 29 Element Layer Assignments

all of the panels comprising the monocoque structure.

Area aspect ratios (W/L) are within the 1:5 limit recommended for the SHELL4L element. Thickness aspect ratios (t/L) range from 0.268 to 1.52 and fall within the range of aspect ratios investigated in the verification study. An assumption inherent in the element formulation is that no slippage occurs between element layers, this implies that adhesive layer effects are not considered. It is assumed that the panel joints are completely efficient and therefore joint compliance is not considered.

3.3 TORSIONAL STIFFNESS ANALYSIS

Torsional stiffness analysis is the basic method by which chassis performance is determined. The requirement for a torsionally rigid structure is determined by suspension design which depends on small chassis deflections to allow predictable suspension response. A torsionally rigid structure is required for the attachment of suspension components in order that the suspension kinematics and dynamics be predictable. The effects of changes to suspension parameters are then relatively independent of chassis compliance.

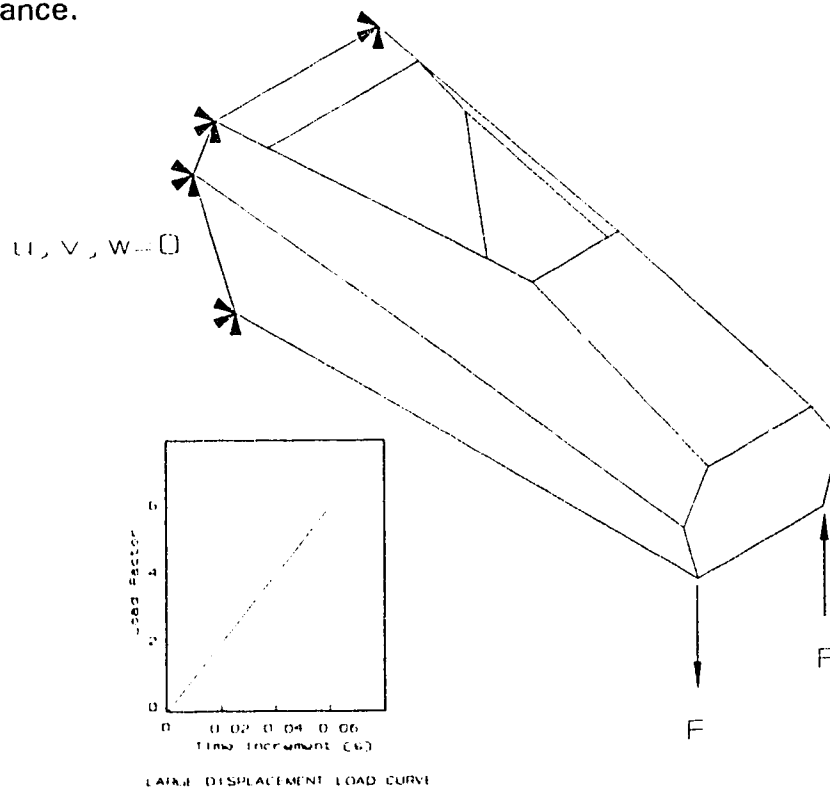


Figure 30 Torsion Boundary Conditions

A diagram illustrating the boundary conditions applied to the finite element model used to determine the torsional stiffness is shown in figure 30.

$\{u, v, w\}$ displacement constraints are applied to 6 nodes of the rearmost bulkhead, these constraints represent the simplest boundary condition to recreate in a physical test. Equal but opposite forces of 3332 N are applied at two nodes on the foremost bulkhead thereby creating a force couple of 1.3568×10^6 N-mm.

The load curve used to increment the applied forces during the non-linear analysis is shown in figure 30. A large displacement analysis is performed using a full Newton-Raphson solution technique which requires that the system stiffness matrix be re-formed after each iteration. A displacement solution tolerance of 0.001 mm is specified and convergence is attained at each load step when the maximum displacement residual is less than the solution tolerance. The solution does not proceed to the next load step until convergence is achieved or a pre-set iteration limit is reached.

The stress results for the faces and core are plotted on contour plots and checked to ensure that component stresses remain below their respective failure values. A graph showing chassis rotation as a function of longitudinal position is prepared.

3.4 VERTICAL BEAMING STIFFNESS ANALYSIS

Vertical beaming is a term used to describe the deflection of a vehicle chassis structure when loaded in a vertical plane aligned with the longitudinal axis. Such a load condition occurs when the vehicle is subjected to bumps and dips in the road surface.

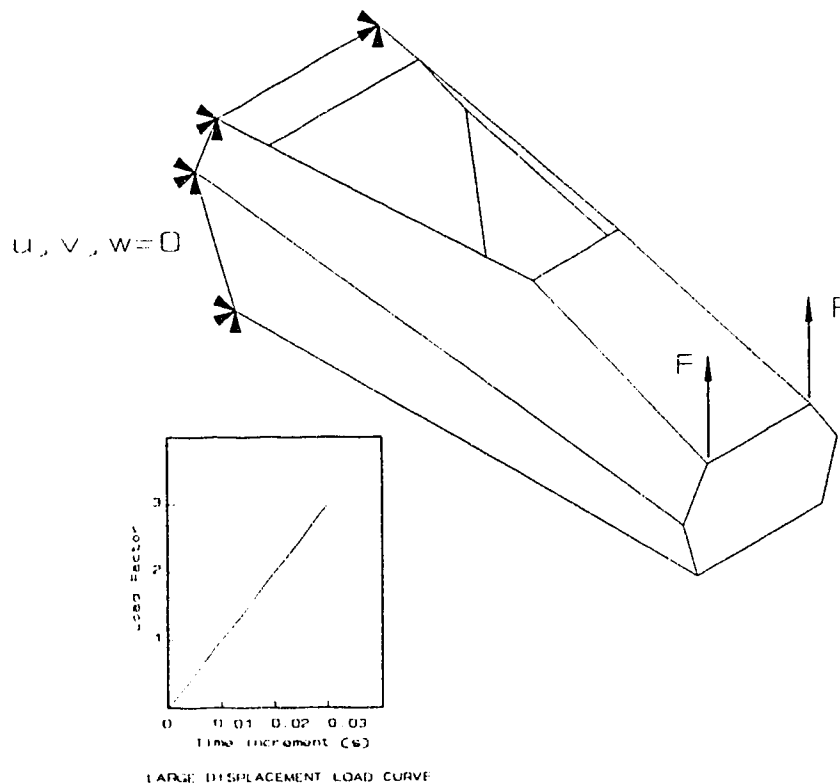


Figure 31 Vertical Beaming Boundary Conditions

An illustration of the boundary conditions applied to the finite element model used to determine the vertical beaming stiffness may be seen in figure 31. Displacement constraints identical to those described in the torsional stiffness analysis are applied to the finite element model. A vertical force of

1000 N is applied to each of two nodes on the uppermost corners of the front bulkhead. This load corresponds to the expected static vehicle load.

The load curve used to increment the static load is also shown in figure 31 and represents a design acceleration load recommended by Howell and Chang [24]. A large displacement analysis using a full Newton-Raphson solution technique is performed and a convergence tolerance of 0.001 mm is defined.

Component stress results are plotted and checked for failure values. The vertical displacement of the floor pan is plotted as a function of longitudinal chassis position.

3.5 LATERAL BEAMING STIFFNESS ANALYSIS

Lateral beaming describes the deflection of a vehicle structure when it is loaded in a horizontal plane. This load condition occurs in the structure when it is subjected to cornering forces.

The boundary conditions applied to the model used to investigate the lateral beaming stiffness are shown in figure 32. Displacement boundary conditions remain unchanged from the two previous analyses. A lateral force of 1000 N is applied to each of two nodes on the corners of one side of the front bulkhead.

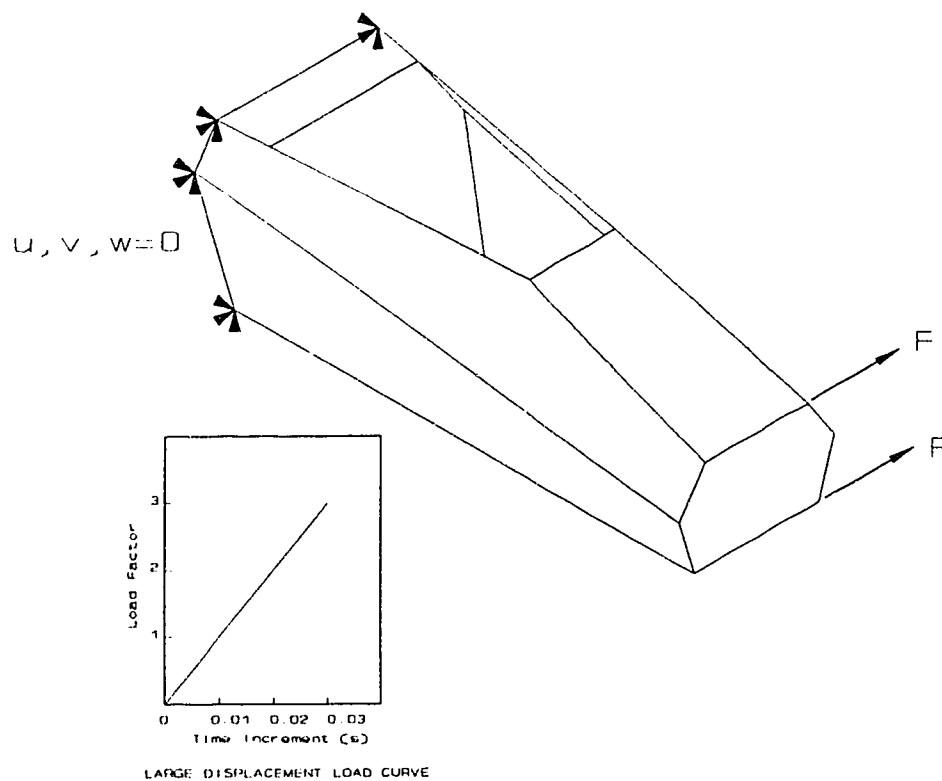


Figure 32 Lateral Beaming Boundary Conditions

The lateral load is incremented using the same load curve as was used for the vertical case, this graph is shown in figure 32. A large displacement analysis is performed and the solution technique and displacement tolerance are as before. Stress results are plotted and a global lateral beaming stiffness value is determined from the finite element displacement results.

4.0 RESULTS AND DISCUSSION

The finite element analysis results for the composite monocoque are presented in three sections, each corresponding to a specific load case. The deflection and stress results are reviewed for each case. The stress results are presented as preliminary values only, a more detailed finite element mesh in the areas of interest is required for greater accuracy. A comparison of chassis stiffness values is made between the finite element model and various production and high performance vehicle structures.

4.1 TORSIONAL ANALYSIS RESULTS

4.1.1 DEFLECTION RESULTS

The rotation of the floor pan about a longitudinal axis along the length of the monocoque is defined by determining the angle of a line drawn between opposite element nodes laying on the perimeter of the floor. The term "chassis station" refers to a coordinate position measured from the front bulkhead along the longitudinal (global-X) axis of the structure. The abbreviation "CS" in conjunction with a coordinate value is used to identify a specific chassis coordinate position.

In figure 33, a graph of the floor pan rotation angle at various chassis stations is presented along with a plot of the displaced geometry of the finite element model. Additional views of the deflected structure are seen in figure 34.

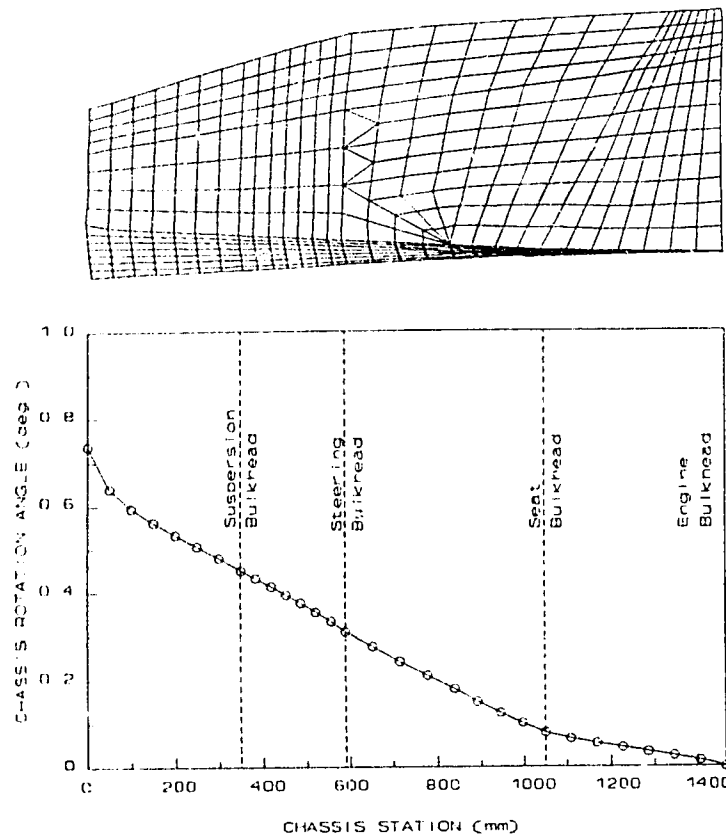


Figure 33 Torsional Rotation of Monocoque

The abrupt change in the slope of the graph at CS-50 is attributable to a local effect due to the application of the point loads comprising the force couple. The slope of the curve has a relatively constant value of 572×10^{-6} degree/mm between CS-100 and the suspension bulkhead. A slight change in slope occurs at the suspension bulkhead where the angular rotation becomes 587×10^{-6} degree/mm. These results are expected through the forward section of the monocoque where the structure is enclosed. The cutouts in the suspension and steering bulkheads allow increased deformation thereby reducing the aggregate section stiffness.

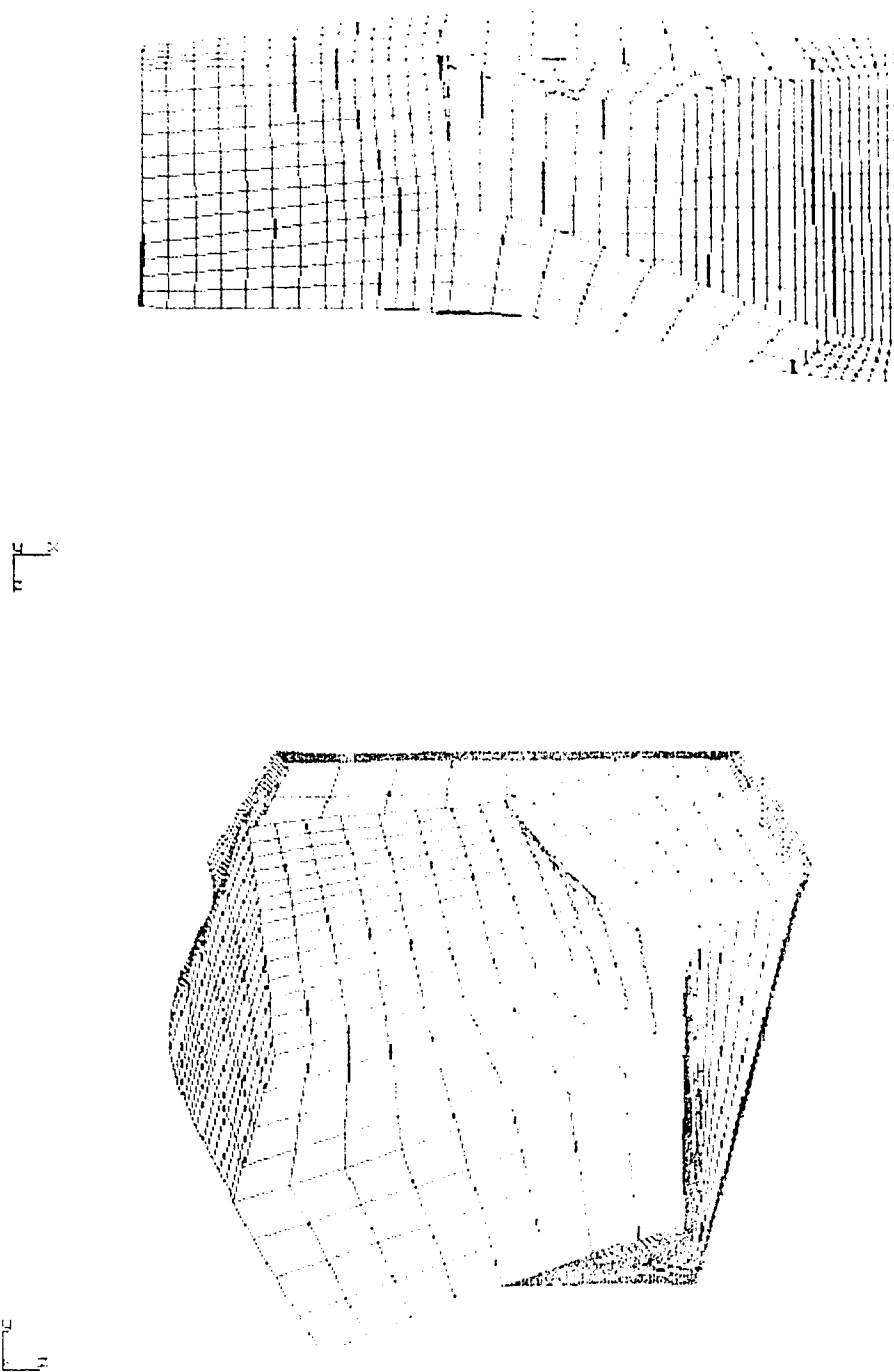


Figure 34 Structural Deflection Under Torsional Load

With an angular rotation coefficient of 504×10^{-6} degree/mm the open cockpit section between the steering bulkhead (CS-590) and the start of the seat bulkhead (CS-1050) is stiffer than the two forward sections. The high cockpit sides, the presence of the box section formed by the thigh panel and steering bulkhead and the intrusion of the seat bulkhead into the cockpit result in the higher coefficient. The stiffest section (188×10^{-6} degree/mm) of the monocoque is the completely enclosed box between the seat and the engine bulkheads.

Torsional stiffness for vehicle structures is commonly expressed as the quotient of the applied torque divided by the resulting maximum global rotation angle. The torsional stiffness value derived from the finite element analysis is 11,046 Nm/deg. The specific torsional stiffness is a measure of how efficiently the material in the structure is used and is derived by dividing the torsional stiffness value by the weight of the bare structure. The estimated weight of the monocoque is 196 N therefore the specific torsional stiffness is $56.3 \text{ Nm/deg/N}_{(\text{chassis weight})}$. A comparison of these values with those of other vehicle structures is given in section 4.4.

4.1.2 STRESS RESULTS

The results of the stress analysis are to be considered as preliminary values as the focus of the finite element study was the structural deflection, a more accurate stress evaluation would require additional analysis. The stress results then, are presented in this light.

The Von-Mises stress in the aluminum facing (element layer 3) may be seen in figure 35. The stress values range from 0 to 165 MPa and are well below the yield stress of 240 MPa defined for the 6061-T6 alloy. As expected the maximum stress occurs at the point of load application on the front bulkhead.

The shear stress τ_{xy} is expressed in the element coordinate system and values for the aluminum face layer are shown in figure 36. Values are well below allowable levels and do not present a design problem.

The Von-Mises stress and τ_{xy} in the polystyrene core were examined and found to be well below the allowable values for this material. The contoured stress plots for the core layer may be seen in figures 37 and 38.

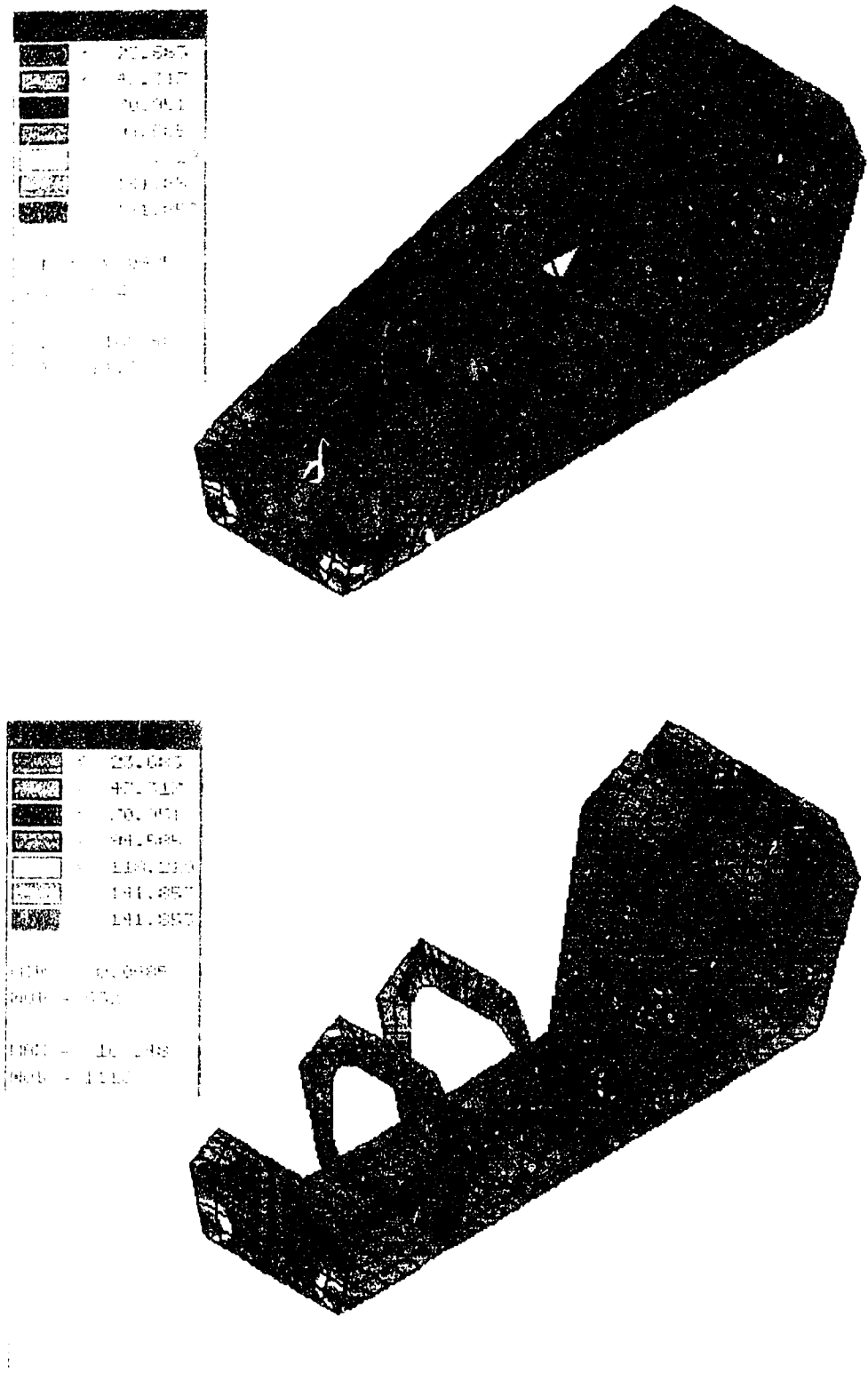


Figure 35 Von-Mises Stress Due To Torsional Load, Aluminum Face Layer

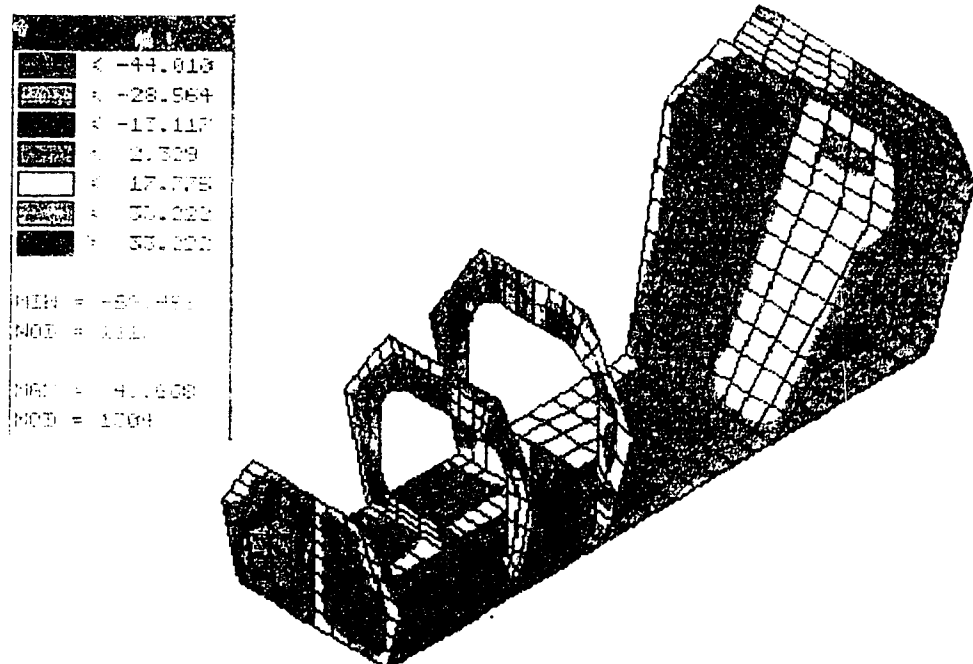
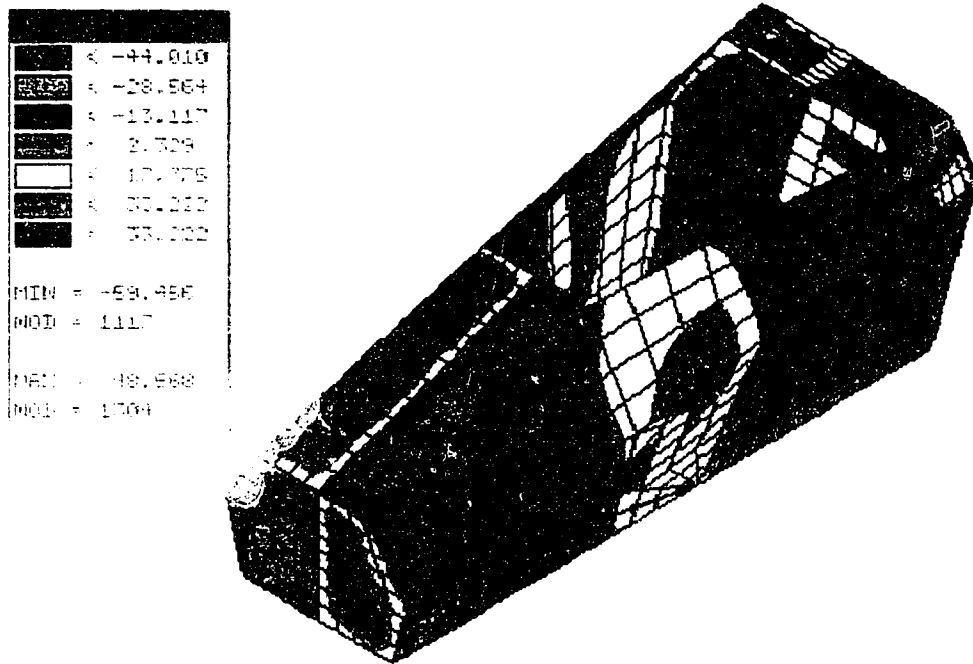


Figure 36 τ_{xy} Stress Due To Torsional Load, Aluminum Face Layer

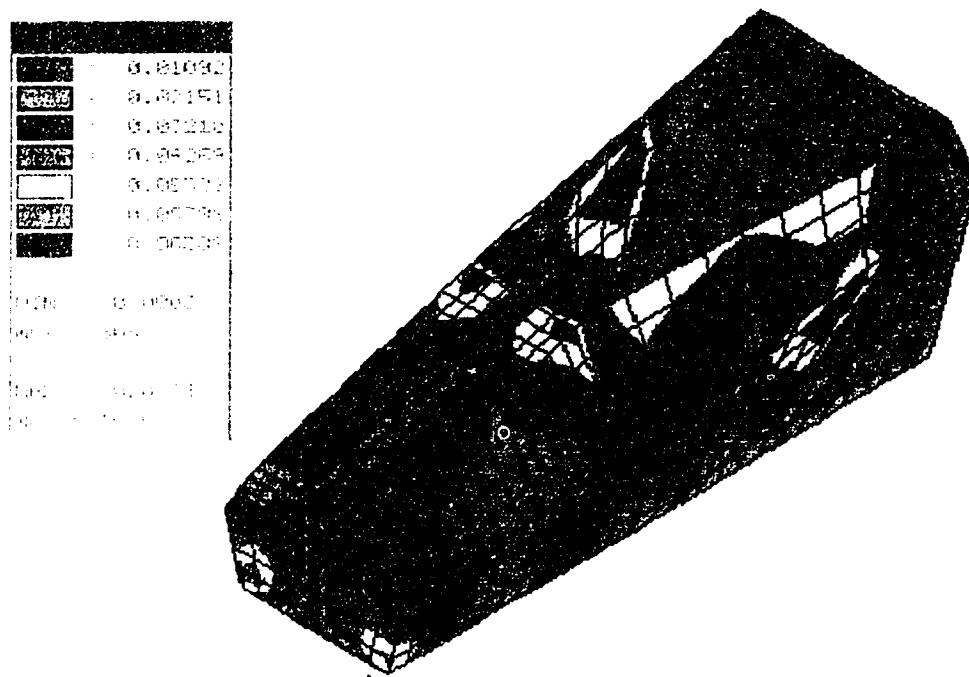


Figure 37 Von-Mises Stress Due To Torsional Load, Polystyrene Core Layer

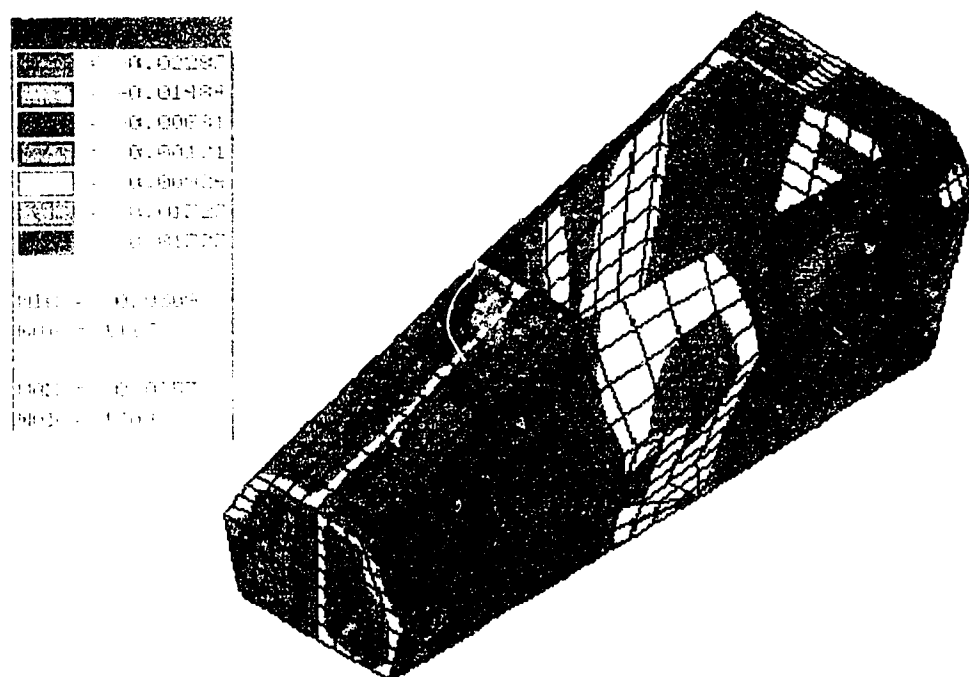


Figure 38 τ_{xy} Stress Due To Torsional Load, Polystyrene Core Layer

4.2 VERTICAL BEAMING ANALYSIS RESULTS

4.2.1 DEFLECTION RESULTS

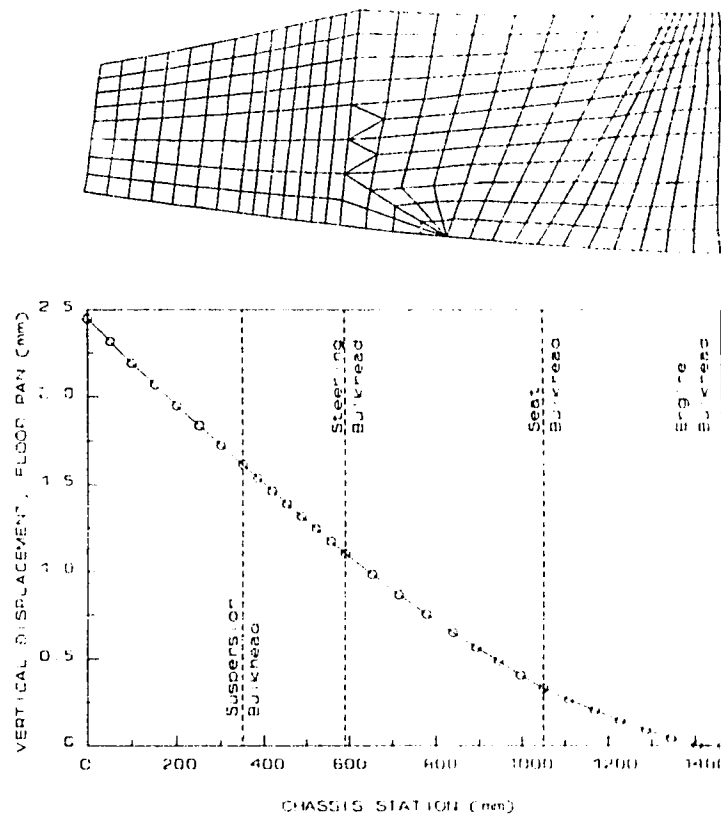


Figure 39 Vertical Displacement of Monocoque Floor Pan

The vertical displacement of the floor pan is graphed and presented in figure 39. An additional view of the deflected structure is presented in figure 40. The structure is acting like a cantilevered beam having a section modulus that varies with length. The basic deflection relation for a cantilevered beam is a cubic function, in this case the moment of inertia is also a function of position. The function describing the moment of inertia is not continuous along the length of the structure. Discontinuities occur at the steering bulkhead

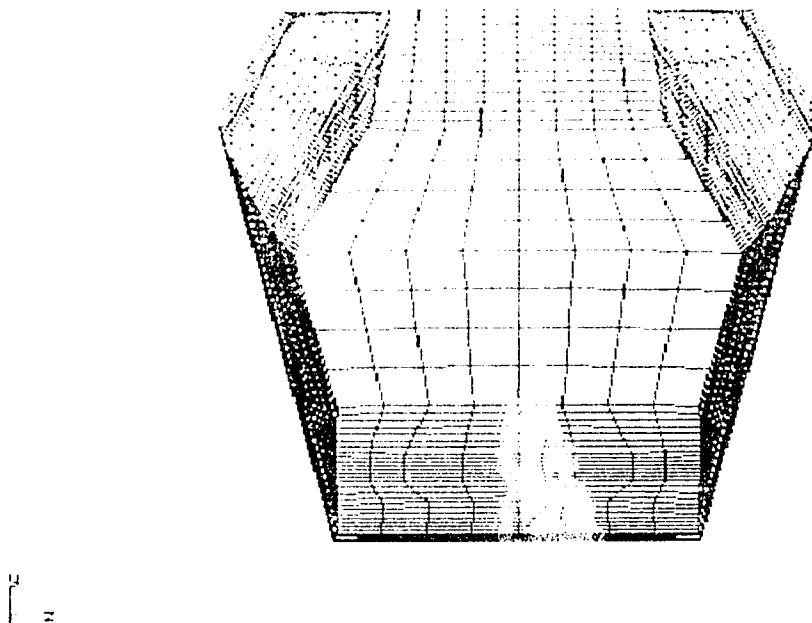


Figure 40 Monocoque Deflection Under Vertical Load, Front View

(CS-590), where the top panel ends, and at the seat bulkhead (CS-1050), where the seat back begins to slope toward the engine bulkhead. Because the shear center of each section lies on the vertical plane of symmetry containing the section centroids, vertical beaming and twisting are uncoupled.

Vertical beaming stiffness is defined as the quotient of the applied force divided by the maximum vertical deflection. The results of the finite element analysis indicate a vertical beaming stiffness of 2448 N/mm. The specific vertical beaming stiffness is $12.5 \text{ N/mm/N}_{(\text{chassis weight})}$.

4.2.2 STRESS RESULTS

The stresses in the monocoque subjected to vertical beaming loads are quite small, not surprising as the design is deflection limited. The Von-Mises stresses in the most highly stressed aluminum face are shown in figure 41. A maximum stress of 61 MPa occurs at a support and is well below the yield value for the aluminum alloy. A word of caution, however, a refined mesh and a more detailed model of the support connection is required to accurately predict the stress field in this region. The stresses in the main part of the structure are considerably less than 61 MPa. Likewise, the shear stresses τ_{xy} in the aluminum facing are very small, the stress contours may be seen in figure 42.

The Von-Mises and τ_{xy} core stress contour plots are shown in figure 43, and in figure 44, respectively. The maximum stress values in the core are considerably lower than the allowable values for the polystyrene material.

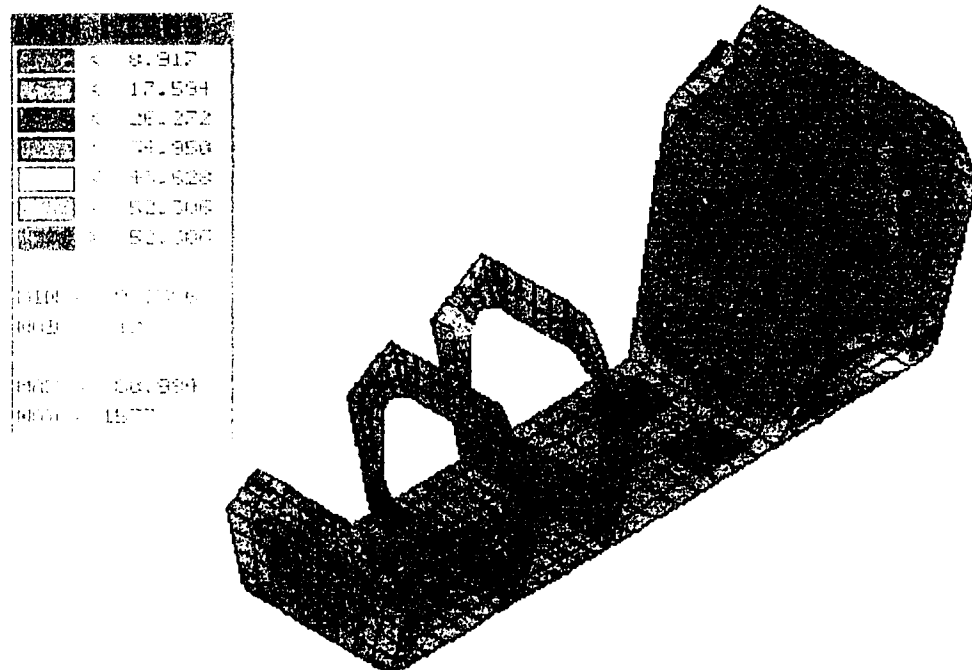
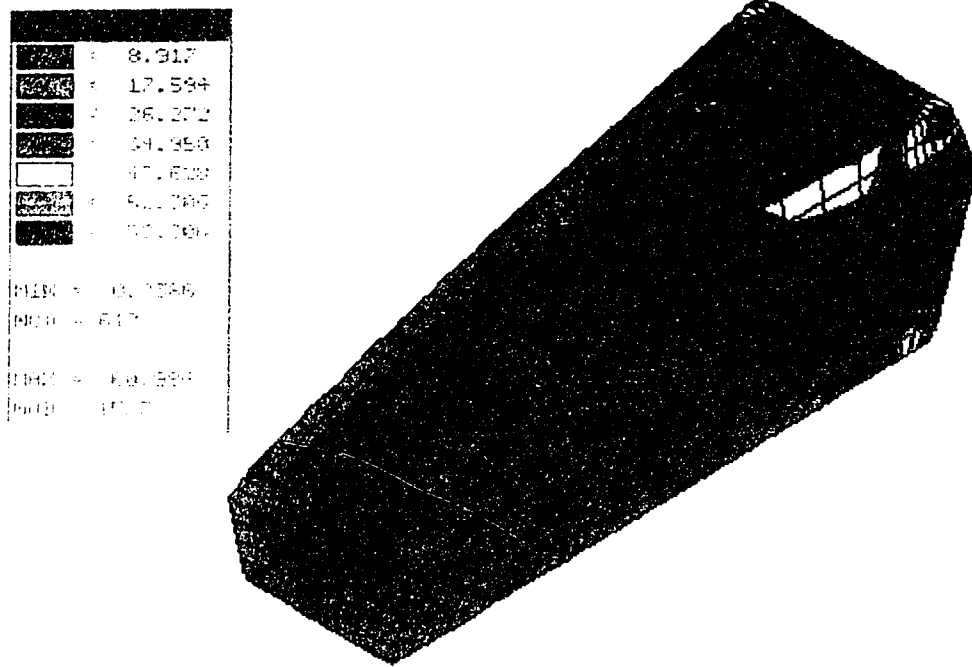


Figure 41 Von-Mises Stress Due To Vertical Load, Aluminum Face Layer

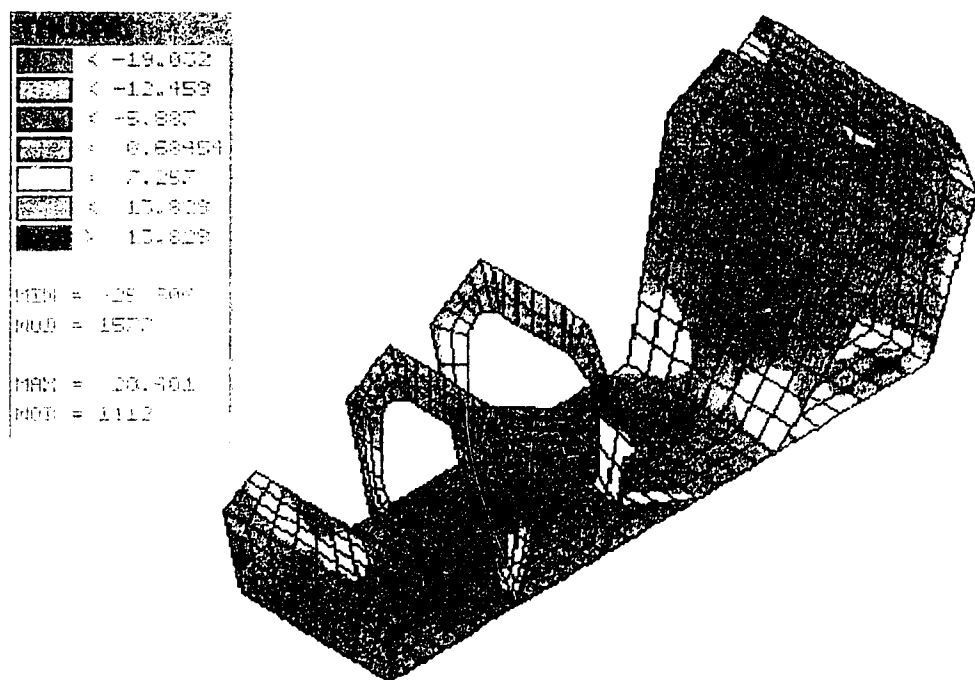
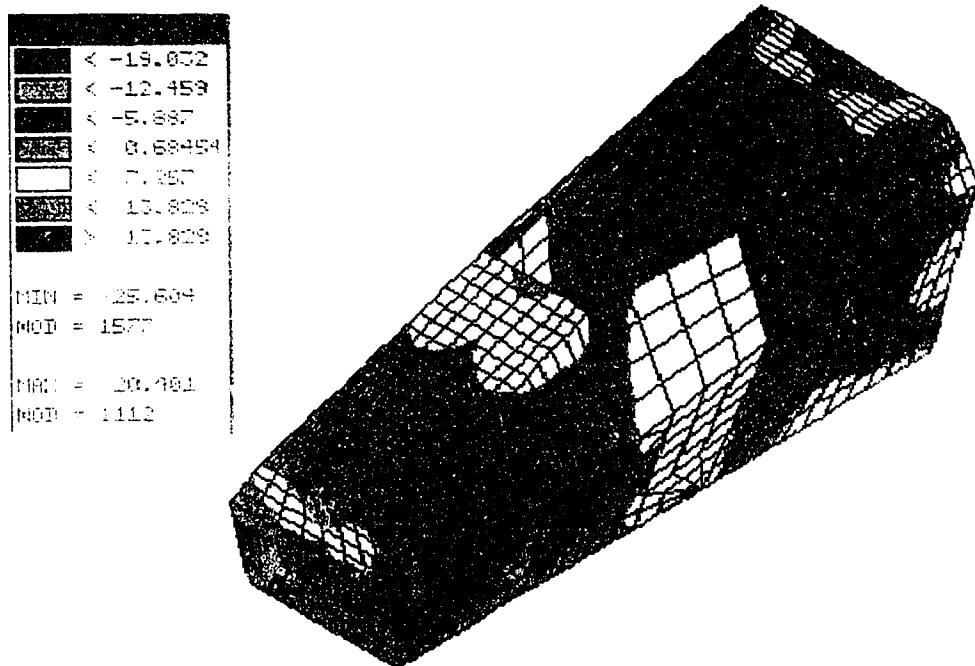


Figure 42 τ_{xy} Stress Due To Vertical Load, Aluminum Face Layer

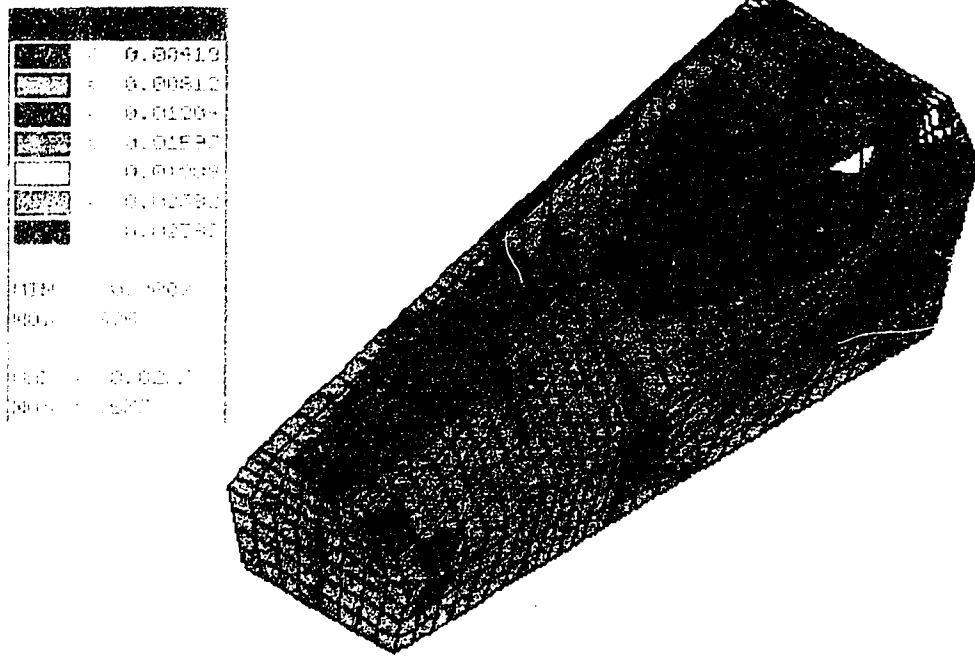


Figure 43 Von-Mises Stress Due To Vertical Load, Polystyrene Core Layer

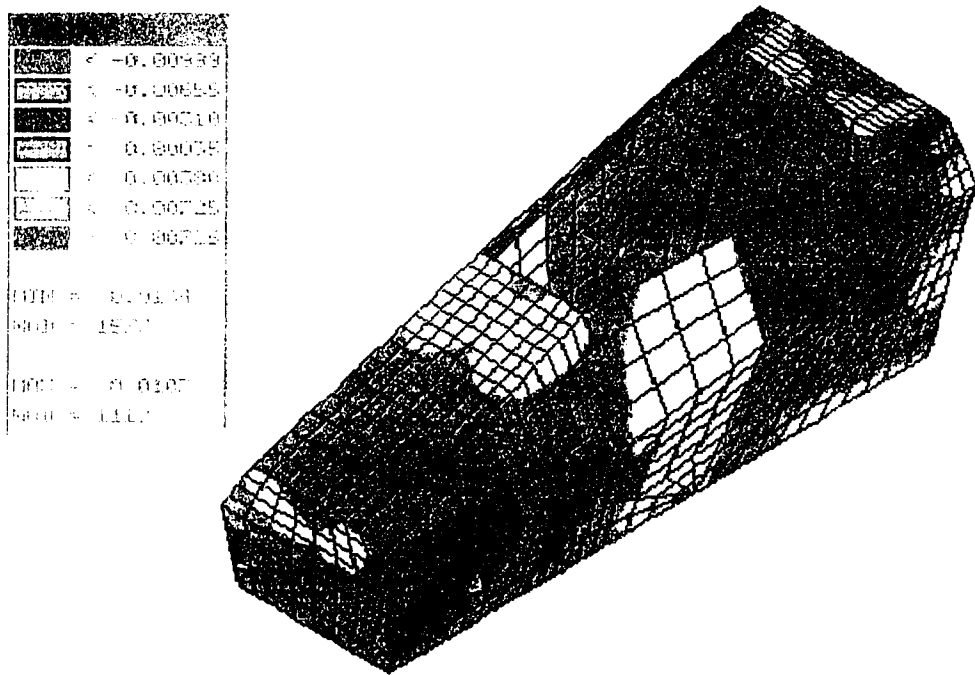


Figure 44 T_{xy} Stress Due To Vertical Load, Polystyrene Core Layer

4.3 LATERAL BEAMING ANALYSIS RESULTS

4.3.1 DEFLECTION RESULTS

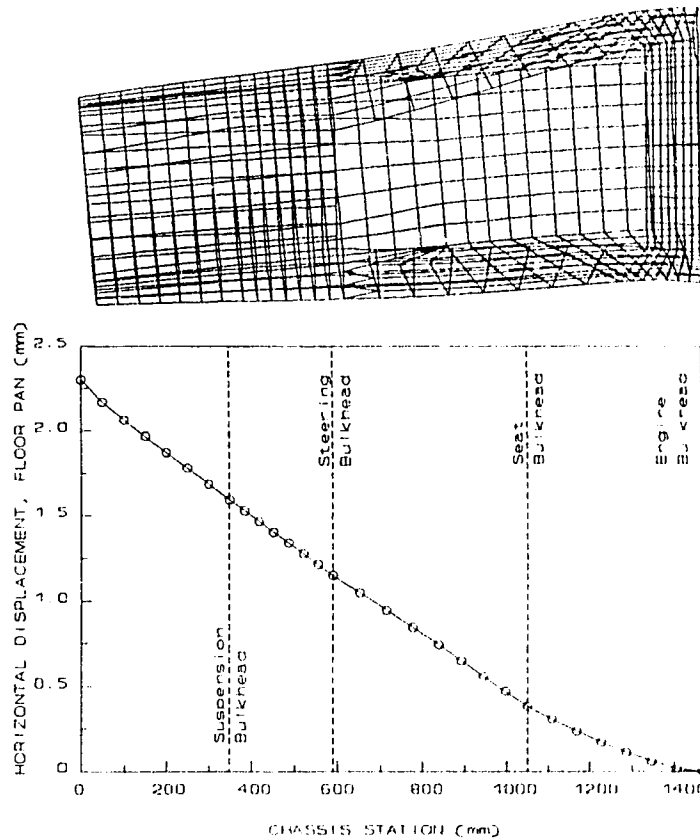


Figure 45 Horizontal Displacement of Monocoque Floor Pan

A graph of the horizontal displacement of the monocoque floor pan plotted against chassis station is shown in figure 45. Slope changes occur at chassis station coordinates corresponding to bulkhead positions and reflect the discontinuities in the function describing the moment of inertia I_{yy} . The function governing the lateral deflection of the monocoque is very nearly linear at each section laying between CS-0 to CS-1050. The maximum lateral deflection of the monocoque is 2.3 mm.

Because the shear center at each section of the monocoque does not lie in a horizontal plane containing the section centroid and the structure is not loaded through the shear center, twisting of the monocoque accompanies lateral bending deflection. The twisting about a longitudinal axis can be seen in the front view of the deflected shape plot shown in figure 46.

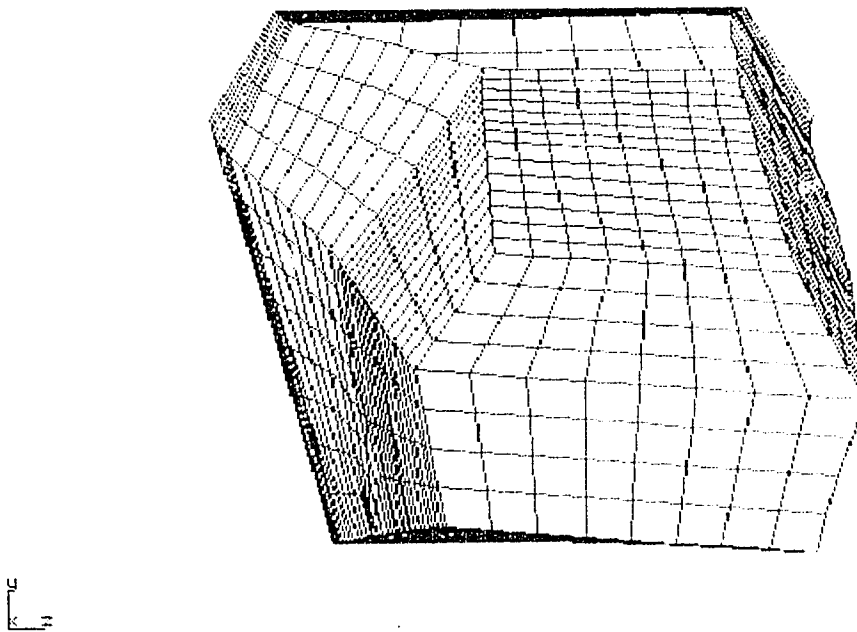


Figure 46 Monocoque Deflection Under Lateral Load, Front View

The lateral beaming stiffness of the structure predicted by the finite element analysis is 2606 N/mm, while the specific stiffness is 13.3 N/mm/N_(chassis weight). The monocoque structure then, is slightly stiffer about the y-axis than it is about the z-axis.

4.3.2 STRESS RESULTS

The stresses arising from the lateral deflection of the monocoque are predictably small and of the same magnitude as those found in the vertical load case. The maximum Von-Mises stress in the aluminum face, seen in figure 47, is 71 MPa and occurs adjacent to a fixed support on the rear bulkhead. A yield failure of an aluminum facing is not expected. The τ_{xy} shear stress contours of the same face may be seen in figure 48. These preliminary findings indicate that the structure has sufficient strength in the face layers.

Similar observations can be made for the polystyrene core layer. The Von-Mises stress results seen in figure 49 and the τ_{xy} stress results, figure 50, indicate very low values. Core failure at these load levels is not anticipated.

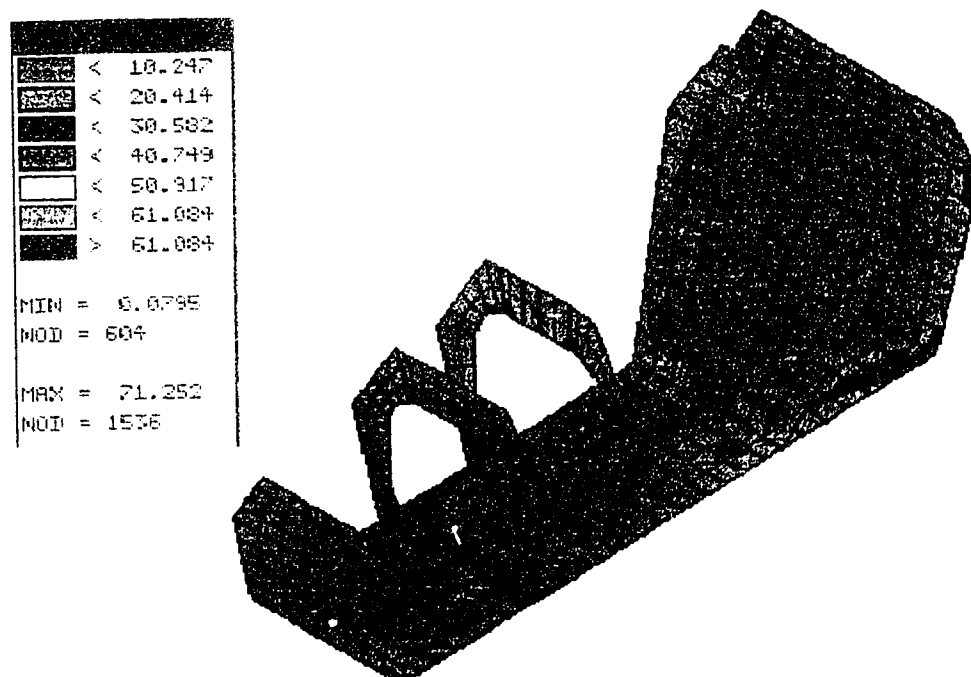
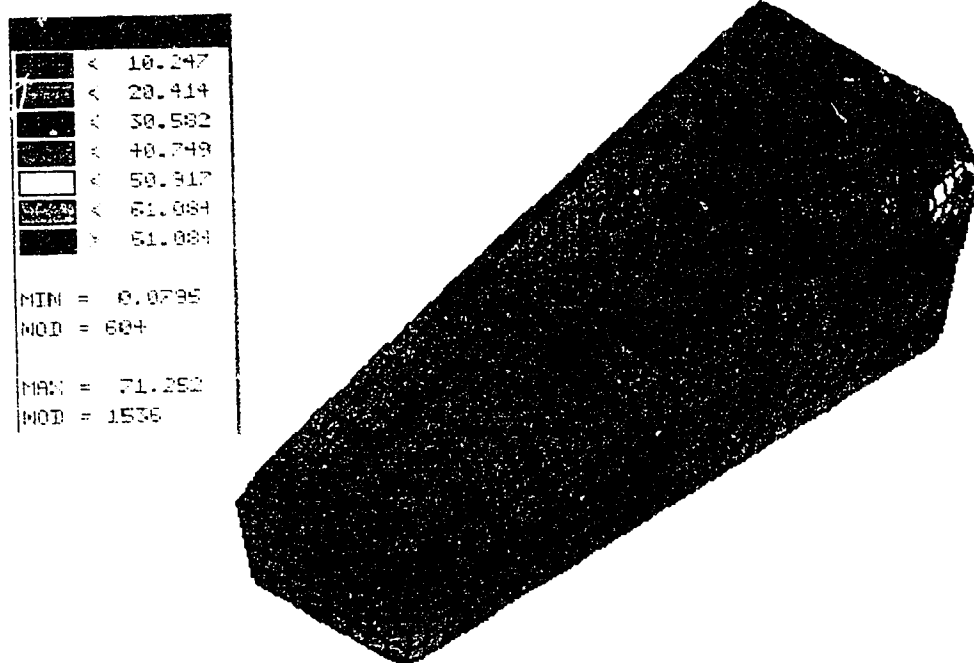


Figure 47 Von-Mises Stress Due To Lateral Load, Aluminum Face Layer

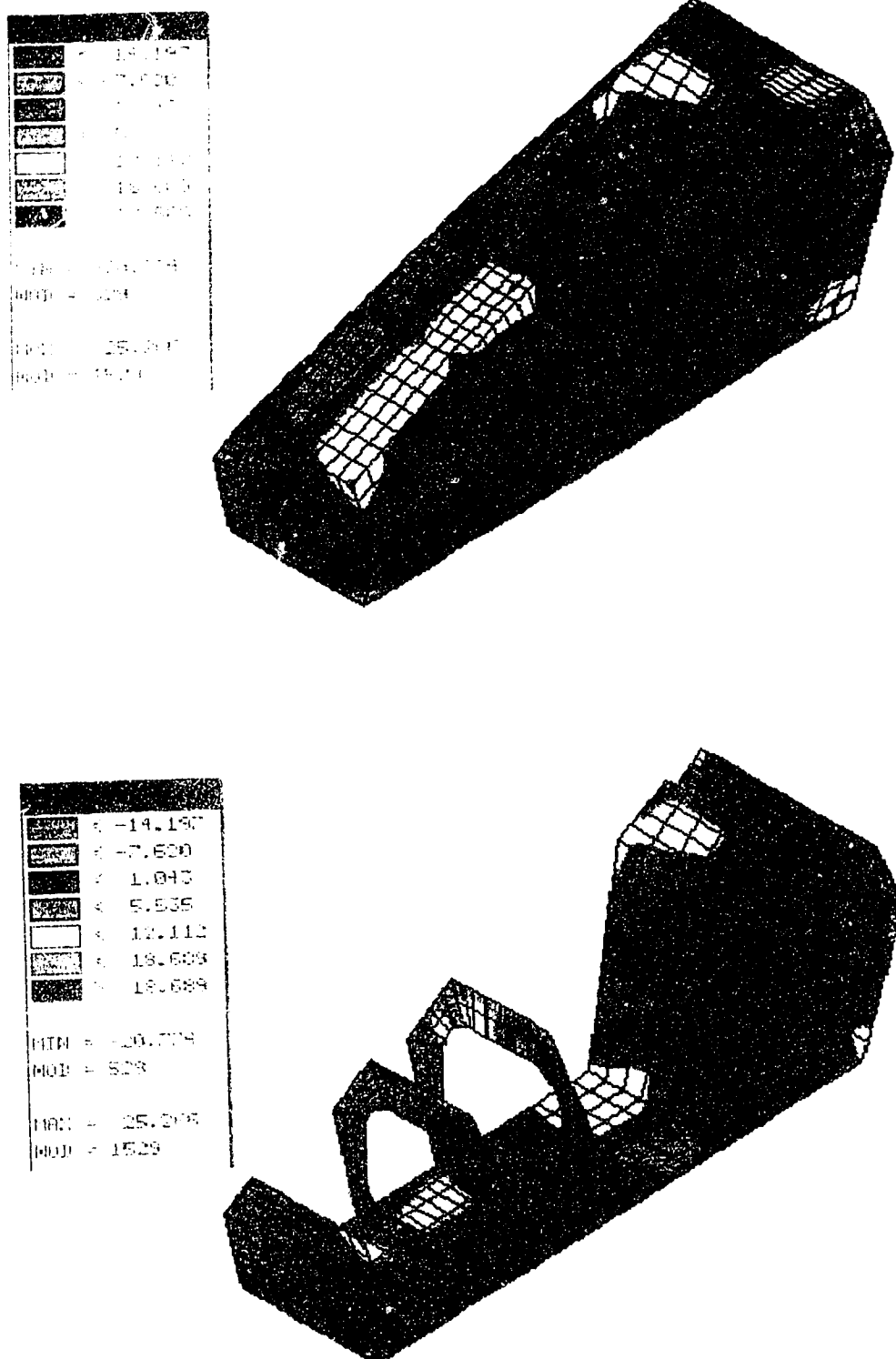


Figure 48 T_{xy} Stress Due To Lateral Load, Aluminum Face Layer

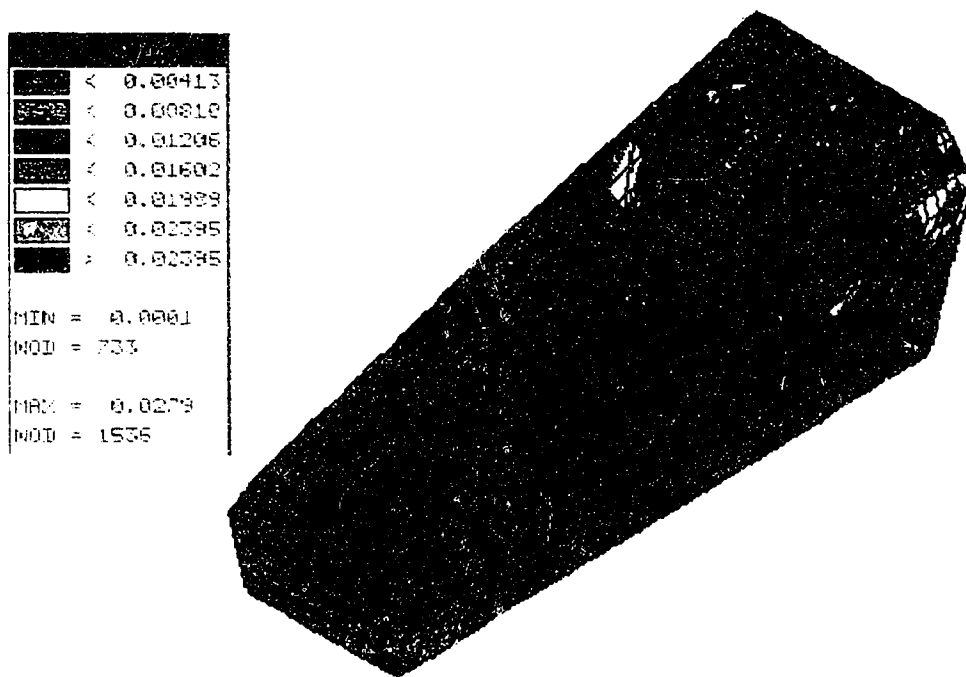


Figure 49 Von-Mises Stress Due To Lateral Load, Polystyrene Core Layer

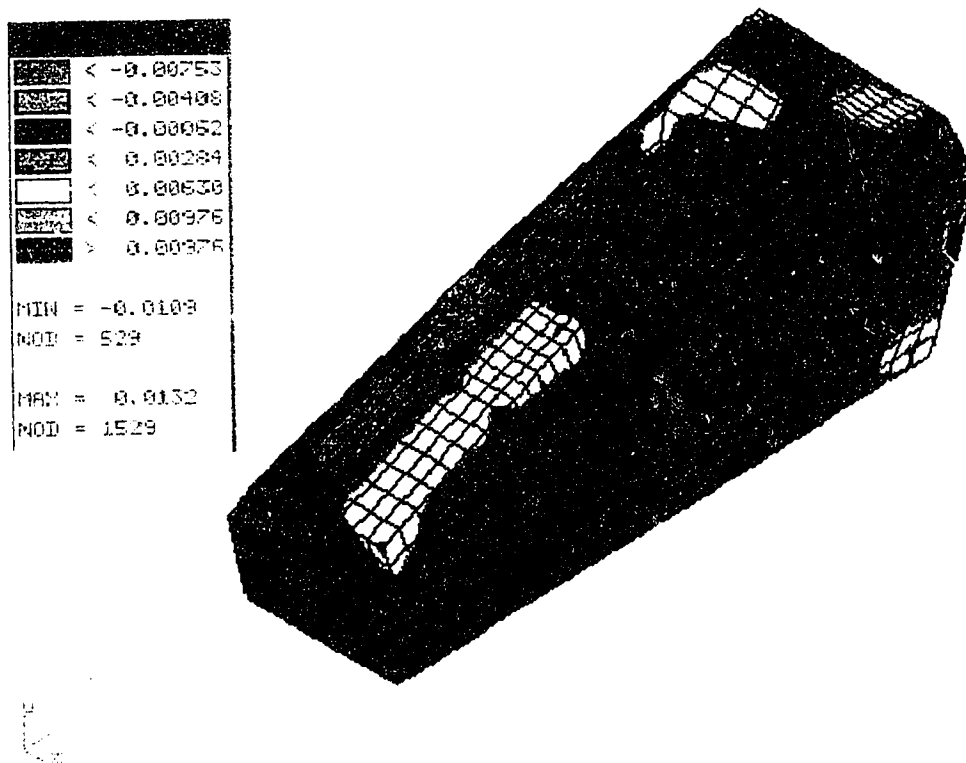


Figure 50 τ_{xy} Stress Due To Lateral Load, Polystyrene Core Layer

4.4 COMPARISON OF RESULTS

Torsional stiffness is an excellent basis of comparison for various types of vehicle chassis constructions. Vertical and horizontal beaming values are less so due to the differences in testing methods. The chassis construction type, chassis weight, and torsional stiffness values for several production and high performance vehicles are tabulated and presented in table 6.

The physical geometry of the chassis will obviously have a large influence on its torsional stiffness, however a comparison of similar classes of structure will indicate whether the finite element model developed in this study is producing realistic results. It is expected that a high sided, enclosed sandwich monocoque chassis would perform better than a typical road sedan chassis. This expectation is borne out by a comparison of the stiffness values between the Austin-Rover Metro and the finite element results of this investigation. The torsional stiffness of the finite element model is twice that of the aluminum Metro and 56 percent greater than the steel Metro.

A comparison of the finite element model with various racing car chassis indicates that the model stiffness falls within realistic values. The finite element torsional stiffness of 11,046 Nm/degree lies between the 4,070 Nm/degree single skin monocoque of the Lotus 79 and the 20,351 Nm/degree carbon fibre, sandwich monocoque of the McLaren MP4.

Table 6 Torsional Stiffness Comparison

Vehicle Name	Chassis Type	Chassis Weight (N)	Torsional Stiffness (Nm/deg)	Specific Torsional Stiffness Nm/deg/N
Stout F.E Model	Monocoque 25mm Aluminum-Foam Sandwich	196	11,046	56.3
Ford GT40	Single Skin Monocoque 0.028" Steel Sheet Spot Welded	1,335	16,959	12.7
Ford Test Prototype	Unibody, Semi-Monocoque Steel Stamping Spot Welded	N/A	6,349	N/A
Formula One Lotus 79	Single Skin Monocoque Aluminum Sheet Riveted	423	4,070	9.6
Formula One Lotus 80	Sandwich Monocoque Alum. Skin - Alum. Honeycomb Adhesive Bonded, Riveted	378	6,784	17.9
Formula One 1984 Lotus	Sandwich Monocoque Carbon Fibre, Kevlar, Honeycomb Adhesive Bonded	311	13,567	43.6
Formula One McLaren MP4	Sandwich Monocoque Carbon Fibre, Alum. Honeycomb Adhesive Bonded	311	20,351	65.4
Austin-Rover Metro	Unibody, Semi-Monocoque Aluminum Stamped Panels Adhesive Bonded, Spot Welded	726	5,400	7.4
Austin-Rover Metro	Unibody, Semi-Monocoque Steel Stamped Panels Spot Welded	1,344	7,078	5.3

Because of the assumptions made in the numerical analysis of the aluminum-foam sandwich monocoque it is possible that the predicted structural stiffness are too high. A review of the finite element and physical test results obtained in an investigation of the Austin-Rover Metro done by Selwood, et.al. [50] gives some indication of the accuracy of the numerical method.

Table 7, from Selwood, gives a comparison of the torsional stiffness and aperture deflection values obtained with a finite element model and through physical testing of an aluminum chassis Austin Metro.

Table 7 Austin-Rover Metro Torsion Test ^[50]

Properties		Aluminum Metro Finite Element Prediction	Aluminum Metro Test Results
Torsional Stiffness (Nm/deg)		4533	5400
Aperture Distortion at 4080 Nm Torsion Load (mm)	Windshield A	6.21	4.06
	Windshield B	6.00	3.14
	Tailgate C	6.80	7.36
	Tailgate D	6.80	7.14
	Door E	1.33	1.36
	Door H	2.20	2.00
	Quarter R	1.10	1.26
	Light S	0.81	1.28

The finite element model was comprised of 1200 parabolic shell elements and consisted of a half body model. Local reductions in body shell panel thickness due to stamping were taken into account. It appears as though the finite element model was less stiff than the actual structure and under-predicted the torsional rigidity. Selwood, et.al., point to an adhesive effect as a possible reason for the 16% error in the torsional stiffness prediction.

A similar finite element investigation and physical test of front end sheet metal (FESM) is given by Kowalski [28]. The results of this comparison are reproduced in table 8.

Table 8 Overall Front End Sheet Metal Stiffness Correlation ^[28]

Overall Sheet Metal Stiffness	Finite Element Model	Laboratory Test	Corrected Test
Vertical Beaming (N/cm)	6190	4860	5040
Lateral Beaming (N/cm)	630	700	700
Torsion (Nm/deg)	6070	4340	5340
Fore-Aft (N/cm)	7540	6310	6350

In most cases the finite element model over-predicts the stiffness of the FESM, the exception being the lateral beaming test. The corrected test results reflect the effect that the testing apparatus stiffness has on the measured FESM stiffness. The original laboratory results did not account for the test apparatus

compliance thereby causing the finite element values to appear grossly in error. The error in the torsional stiffness finite element value when based on the corrected test results is 13.7 percent. The corrected error in the vertical beaming value is 22.8 percent and 10 percent for the lateral beaming result.

It would appear then that the finite element model, developed in this investigation, of the aluminum-foam sandwich monocoque is producing stiffness values which are reasonable. It is likely that the assumption of perfect bonding between the aluminum skins and foam core, as well as the assumption of 100 percent panel joint efficiency, would cause the finite element model to over-predict the chassis stiffness. The maximum expected error in the torsional stiffness value is estimated at between 20 to 30 percent. A detailed finite element model of a panel joint would yield some insight into the expected joint compliance under various load conditions. With an estimate of the joint compliance further refinement of the overall model stiffness would be possible.

5.0 CONCLUSIONS

A study was performed to investigate the characteristics of four finite elements to determine their suitability for the evaluation of sandwich composite structures. A verification analysis was done to determine the convergence characteristic as well as sensitivity to changes in the element thickness aspect ratio. A torsion case was studied to determine element accuracy in representing shear deflection and stress.

An element type was chosen based on the results of the verification study and was used to investigate the structural stiffness of an aluminum-foam sandwich monocoque chassis. An evaluation of structural deflection was made for each of three load cases: torsion, vertical beaming, and lateral beaming.

5.1 VERIFICATION STUDY

Based on the results of the verification study the SHELL4L element was chosen as the best element for use in the analysis of the monocoque chassis stiffness. The element is efficient and performed well in the verification tests. It is well suited for the global stiffness evaluation of this sandwich monocoque. If more detailed through-the-thickness stress information is required then the layered solid, STIF46 element can be stacked in the thickness direction and used for the analysis of sandwich structures.

The SHELL4L quadrilateral layered composite shell element exhibited acceptable convergence behaviour for the plate bending test. The element

converged monotonically from above to a deflection solution 4.3 percent lower than that predicted by the analytic solution. Acceptable solution accuracy is achieved at a mesh grid of 6 by 6.

The SHELL4L element, in its 3 layer "sandwich" configuration, performed well in the thickness aspect ratio test, exhibiting a maximum deflection error of 4.5 percent at an aspect ratio of 0.2. The deflection error decreased to 2 percent at an aspect ratio of 2.0. The element is capable of representing both shear and bending deflection components over a range of thickness aspect ratios of 0.2 to 2.0.

The SHELL4L and STIF99 shell elements exhibited shear locking behaviour under certain element configurations. Shear locking occurs in the SHELL4L element when 4 or more material layers are assigned to the element. The STIF99 isoparametric shell element exhibits shear locking for all element layer configurations. In both cases the element deflection solution seems to converge to the bending component predicted by the analytic solution. When the shear moduli of the face are several orders of magnitude larger than those of the core, the face transverse shear moduli appear to dominate the elasticity matrix [D] and lead to the shear locking.

The SHELL4L element performed well on the analysis of a cylinder subjected to a torsion load. The element predicted both the angular deflection and the resulting shear stress to within 2 percent accuracy. The element is capable of representing in-plane shear deflections and stresses.

The SHELL4-SOLID combined sandwich element was not able to accurately predict the deflection of a beam subjected to 3 point bending. Shear stress is discontinuous across the facing - core interface thereby reducing the effective element stiffness which leads to excessive deflection values. The combined element consisting of shell - solid - shell elements stacked together is too flexible and over-predicts the deflection by 13.5 percent.

5.2 MONOCOQUE ANALYSIS

The SHELL4L finite element model of the aluminum-foam sandwich monocoque predicts a torsional stiffness of 11,046 Nm/deg. Loss of torsional rigidity through the cockpit opening is minimized by the use of high side panels, a small cockpit opening and an angled seat bulkhead. Preliminary torsional stress values are well below failure values for the aluminum face layers and the polystyrene core. Comparison of the torsional stiffness results for this model with the values of other vehicle structures indicates that the finite element model is producing results which fall within realistic upper and lower bounds.

A high torsional stiffness is concomitant with large vertical and lateral beaming stiffness values. The finite element model predicts a vertical beaming stiffness of 2448 N/mm and a lateral beaming stiffness of 2606 N/mm. The torsional stiffness requirements therefore direct the design targets.

5.3 PROGRAM CONSIDERATIONS

The discovery of a number of errors in the commercial finite element programs used during this study indicates the necessity of user defined verification procedures. Procedures such as coordinate transformations should be checked to ensure correctness. Simple verification problems in addition to those recommended by the software developer should be used to test element and program accuracy. Input data must be reviewed to ensure that the intended element and material properties have been correctly represented. Assumptions and restrictions made during the geometric modelling must be clearly defined. The results of a finite element analysis must be reviewed in light of the modelling assumptions and element capability.

5.4 FURTHER STUDY

5.4.1 JOINT COMPLIANCE

A detailed finite element study of a sandwich panel joint under various load conditions is required to establish joint compliance values. The study would consist of a three dimensional model that used several layered solid elements to represent the panel thickness. A simple physical test to verify the finite element derived joint compliance value is required. Such compliance values could then be introduced into the vehicle chassis model to further refine the analysis.

5.4.2 ADHESIVE LAYER RESPONSE

A study of the adhesive layer response and its influence on the structural stiffness is required to further refine the finite element model of the sandwich monocoque chassis. A simple finite element model could be constructed by assigning additional adhesive layers to the layered shell element. Adhesive material properties would have to be established through physical testing. A more complex model may be required to adequately represent the adhesive layer response.

5.4.3 PHYSICAL TESTING

A full scale physical test of the aluminum-foam sandwich monocoque is required to verify the global response of the finite element model. Deflection of the chassis under load conditions corresponding to torsion, lateral and vertical beaming would be measured at specific chassis coordinates. A strain gauge study of the physical model would establish element accuracy in predicting the strain or stress field at various model locations. Provision should be made to account for testing apparatus compliance in the measurement of chassis deflection.

BIBLIOGRAPHY

- [1] Adams, A.A., "Composite Structure For Automobiles - Lotus Experience", Lotus Cars Norwich England.
- [2] Ahmad, S., Irons, B.M., and Zienkiewicz, O.C., "Analysis of Thick and Thin Shell Structures by Curved Finite Elements", *Int. Jour. Num. Meth. Eng'rg*, Vol. 2, pp.419-451, 1970.
- [3] Akin, E., "Detecting and Avoiding Numerical Difficulties", *Finite Element Analysis of Thin Wall Structures*, (John Bull, Editor), Elsevier Applied Science, London, 1988.
- [4] Allman, D.J., "A Compatible Triangular Element Including Vertex Rotations For Plane Elasticity Analysis", *Computers and Structures*, Vol. 19, No. 12, 1984, pp. 1-8.
- [5] Augustitus, J.A., Kamal, M.M., and Howell, L.J., "Design Through Analysis Of An Experimental Automobile Structure", *SAE Paper No. 770597*, 1977.
- [6] Backlund, J., Olsson, K.A., and Maartmann, F., "Computerized Analysis and Design of Sandwich Constructions", *Proc. Of The First Int. Conf. On Sandwich Constructions*, Stockholm, Sweden, 1989, pp.87-105.
- [7] Barone, M.R., and Chang, D.C., "Finite Element Modelling Of Automotive Structures", *Modern Automotive Structural Analysis*, (M.M. Kamal and J.A. Wolf, Editors), Van Nostrand Reinhold Co., Toronto, 1982, pp.116-158.
- [3] Batoz, J., Bathe, K.J., and Ho, L.W., "A Study of Three Node Triangular Plate Bending Elements", *Int. Jour. Num. Meth. Eng'rg*, Vol.15, No.12, 1980, pp.1771-1812.

- [9] Beardmore, P., Johnson, C.F., and Strosberg, G.G., "Composite Intensive Automobiles-An Industry Scenario", *Composite Structures 5*, (Editor: I.H. Marshall), Elsevier Applied Science, London, 1989, pp. 39-87.
- [10] Beaudry, D., Watson, G., and Hertz, P.B., "Crash Simulation Using FEA", *C/C&R*, October 1989.
- [11] Belytschko, T., Stolarski, H., and Carpenter, N., "A C^0 Triangular Plate Element With One-Point Quadrature", *Int. Jour. Num. Meth. Eng'rg*, Vol.20, 1984, pp.787-802.
- [12] Brinken, F., and Reif, G., "Meeting Future Design Challenges With Advanced Core Materials", *Proc. Of The First Int. Conf. On Sandwich Constructions*, Stockholm, Sweden, 1989, pp.215-233.
- [13] Bukowski, K., and Conway, P., "The Application Of Extruded Polystyrene Foam As An Insulating Core Material In Sandwich Constructions", *Proc. Of The First Int. Conf. On Sandwich Constructions*, Stockholm, Sweden, 1989, pp.529-554.
- [14] Carpenter, W.C., "Stresses in Bonded Connections Using Finite Elements", *Int. Jour. Num. Meth. Eng'rg*, Vol.15, 1980, pp.1659-1680.
- [15] Cook, R.D., *Concepts and Applications of Finite Element Analysis*, John Wiley and Sons, Toronto, 1981.
- [17] DeSalvo, G.J., and Gorman, R.W., *ANSYS Engineering Analysis System User's Manual Revision 4.4*, Vol. I & II, Swanson Analysis Systems Inc., Houston, 1989.
- [18] Felske, W.L., "Cast Steering Knuckle Finite Element And Laboratory Strain Analysis", Second International Conference On Vehicle Structural Mechanics, *SAE Paper No. 770613*, 1977.

- [19] Gibson, L.J., "The Use Of Models For Foam Core Behaviour In The Design Of Sandwich Panels", *Proc. Of The First Int. Conf. On Sandwich Constructions*, Stockholm, Sweden, 1989, pp.165-185.
- [20] Glance, P.M., and Daroczy, G., "Computer-Aided Design, Analysis, And Testing Of Automotive Bumpers", *SAE Paper No. 880462*, 1988.
- [21] Ha, K.H., "Finite Element Analysis of Sandwich Construction: A Critical Review", *Proc. Of The First Int. Conf. On Sandwich Constructions*, Stockholm, Sweden, 1989, pp.69-85.
- [22] Henry, A., *Grand Prix Car Design and Technology in the 1980's*, Hazelton Publishing, Richmond Surrey, 1988.
- [23] Hillesland, H., "Aerospace Materials And Processes Utilized In A Race Car", Ford Aerospace And Communications Corp., Palo Alto, 1983.
- [24] Howell, L.J., "Establishing Automotive Structural Design Criteria", *Modern Automotive Structural Analysis*, (M.M. Kamal and J.A. Wolf, Editors), Van Nostrand Reinhold Co., Toronto, 1982.
- [25] Kamal, M.M., and Wolf, J.A., "The Automobile And Its Structure-A Historical Review", *Modern Automotive Structural Analysis*, (M.M. Kamal and J.A. Wolf, Editors), Van Nostrand Reinhold Co., Toronto, 1982, pp.1-34.
- [26] Kirioka, K., Ohkubo, Y., and Hotta, Y., "An Analysis Of Body Structures-Part II", *SAE Paper No. 710157*, 1971.
- [27] Kohnke, P. (Ed.), *ANSYS Engineering Analysis System Theoretical Manual Revision 4.4*, Vol. I & II, Swanson Analysis Systems Inc., Houston, 1989.

- [28] Kowalski, M.F., "Design Analysis for Stiffness and Deflection", *Modern Automotive Structural Analysis*, (M.M. Kamal and J.A. Wolf, Editors), Van Nostrand Reinhold Co., Toronto, 1982, pp.255-279.
- [29] Lakshminarayana, H.V., and Murty, S.S., "A Shear-Flexible Triangular Finite Element Model For Laminated Composite Plates", *Int. Jour. Num. Meth. Eng'rg*, Vol.20, 1984, pp.591-623.
- [30] Lashkari, M., *COSMOS/M User Guide Release Version 1.6*, Structural Research and Analysis Corporation, Santa Monica, 1990.
- [31] Lubkin, J.L., "The Flexibility Of A Tubular Welded Joint In A Vehicle Frame", *SAE Paper No. 740340*, 1974.
- [32] McLay, R.W., Buckley, J., Floyd, T., and Viens, D., "A Minimum Energy Composite Automobile", *Composite Structures*, (Editor: I.H. Marshall), Applied Science Publishers, London, 1981, pp.475-483.
- [33] Melosh, R.J., "Finite Element Analysis Of Automobile Structures", *SAE Paper No. 740319*, 1974.
- [34] Nichols, R., *Composite Construction Materials Handbook*, Prentice-Hall, New Jersey, 1976.
- [35] Noakes, K., *Build To Win*, Osprey Publishing Ltd., London, 1988.
- [36] Noakes, K., *Successful Composite Techniques*, Osprey Publishing Ltd., London, 1989.
- [37] O'Connor, D.J., "A Finite Element Package For The Analysis Of Sandwich Constructions", *Composite Structures*, Vol.8, 1987, pp.143-161.

- [38] Olsson, K.A., and Lönng, A., "Test Procedures For Foam Core Materials", *Proc. Of The First Int. Conf. On Sandwich Constructions*, Stockholm, Sweden, 1989, pp.293-318.
- [39] Parekh, C.J., Basas, J.E., and Kothawala, K.S., "Application Of isoparametric Elements In Vehicle Structural Mechanics", *SAE Paper No. 770606*, 1977.
- [40] Park, S.W., and DuVall, F.W., "Finite Element Structural Analysis As Applied To An Automotive Door Structure", *SAE Paper No. 740320*, 1974.
- [41] Pawlowski, J., *Vehicle Body Engineering*, Business Books Ltd., London, 1969.
- [42] Peery, D.J., and Azar, J.J., *Aircraft Structures, 2nd Edition*, McGraw-Hill, Toronto, 1982.
- [43] Peffley, T.R., McClelland, B.G., and Woods, M.W., "Automotive Component Finite Element Analysis Applying Material Characteristics Of 40% Glass-Reinforced Polyphenylene Sulfide", *SAE Paper No. 880035*, 1988.
- [44] Petersen, W., "Application Of Finite Element Method To Predict Static Response Of Automotive Body Structures", *SAE Paper No. 710263*, 1971.
- [45] Prabhakaran, R., "Photoelastic Techniques For The Complete Determination Of Stresses In Composite Structures", *Composite Structures*, (Editor: I.H. Marshall), Applied Science Publishers, London, 1981, pp.235-246.
- [46] Rasmussen, J., and Baatrup, J., "Rational Design Of Large Sandwich Structures", *Proc. Of The First Int. Conf. On Sandwich Constructions*, Stockholm, Sweden, 1989, pp.485-509.

- [47] Reichard, R.P., "The Design Of FRP Sandwich Panels For Ship And Boat Hulls", *Proc. Of The First Int. Conf. On Sandwich Constructions*, Stockholm, Sweden, 1989, pp.349-361.
- [48] Saarela, O.J., "Microcomputer Software For Dimensioning Composite Sandwich Structures", *Proc. Of The First Int. Conf. On Sandwich Constructions*, Stockholm, Sweden, 1989, pp.187-194.
- [49] Seeds, A., and Sheasby, P.G., "Evaluation Of Adhesive Joining Systems In Aluminum Box Beams", *SAE Paper No. 870152*, 1987.
- [50] Selwood, P.G., Law, F.J., Sheasby, P.G., and Wheeler, M.J., "The Evaluation of an Adhesively Bonded Aluminum Structure in an Austin-Rover Metro Vehicle", *SAE Paper No. 870149*, 1987.
- [51] Stanforth, A., *Race And Rally Car Source Book*, Haynes Publishing Group, Newbury Park, 1987.
- [52] Strøbech, C., "One And Two Component Polyurethane Adhesives For Bonding Sandwich Elements", *Proc. Of The First Int. Conf. On Sandwich Constructions*, Stockholm, Sweden, 1989, pp.261-277.
- [53] Taylor, R.L., Beresford, P.J., and Wilson, E.L., "A Non-Conforming Element For Stress Analysis", *Int. Jour. Num. Meth. Eng'rg*, Vol.10, 1976, pp.1211-1219.
- [54] Teti, R., and Caprino, G., "Mechanical Behaviour of Structural Sandwiches", *Proc. Of The First Int. Conf. On Sandwich Constructions*, Stockholm, Sweden, 1989, pp.53-67.
- [55] Tsai, P.J., "Design Analysis For Stress And Fatigue", *Modern Automotive Structural Analysis*, (M.M. Kamal and J.A. Wolf, Editors), Van Nostrand Reinhold Co., Toronto, 1982, pp.280-315.

- [56] Ugural, A.C., *Stresses in Plates and Shells*, McGraw-Hill, Toronto, 1981
- [57] Van Valkenburgh, P., *Race Car Engineering And Mechanics, 2nd Edition*, Van Valkenburgh, Seal Beach, 1986.
- [58] Wadleigh, K.H., "Application Of Finite Element Methods To Complete Automobile Structural Design Evaluation", *SAE Paper No. 740322*, 1974.
- [59] Wheeler, M.J., Sheasby, P.G., and Kewley, D., "Aluminum Structured Vehicle Technology-A Comprehensive Approach To Vehicle Design And Manufacturing In Aluminum", *SAE Paper No. 870146*, 1987.
- [60] Wilson, E.L., Taylor, R.L., Doherty, W.P., and Ghaboussi, J., "Incompatible Displacement Models", *Numerical and Computer Methods in Structural Mechanics*, (Ed. S.J. Fenves, et al), Academic Press, New York, 1973, p.43.
- [61] Zenkert, D., and Groth, H.L., "The Influence Of Flawed Butt-Joints In Foam Core Sandwich Beams", *Proc. Of The First Int. Conf. On Sandwich Constructions*, Stockholm, Sweden, 1989, pp.363-381.